

THE NICHE FOR EXTRAMEDULLARY HEMATOPOIESIS IN THE SPLEEN

APPROVED BY SUPERVISORY COMMITTEE

Sean J. Morrison, Ph.D.

Diego H. Castrillon, M.D., Ph.D.

Michael Buszczak, Ph.D.

Ondine Cleaver, Ph.D.

DEDICATION

To my family, for their support and guidance.

THE NICHE FOR EXTRAMEDULLARY HEMATOPOIESIS IN THE SPLEEN

by

CHRISTOPHER N. INRA

DISSERTATION

Presented to the Faculty of the Graduate School of Biomedical Sciences

The University of Texas Southwestern Medical Center at Dallas

In Partial Fulfillment of the Requirements

For the Degree of

DOCTOR OF PHILOSOPHY

The University of Texas Southwestern Medical Center at Dallas

Dallas, Texas

May, 2017

Copyright

by

CHRISTOPHER N. INRA, 2015

All Rights Reserved

THE NICHE FOR EXTRAMEDULLARY HEMATOPOIESIS IN THE SPLEEN

CHRISTOPHER N. INRA

The University of Texas Southwestern Medical Center at Dallas, 2015

Supervising Professor: SEAN J. MORRISON, PH.D.

The ability to regenerate niches or to create new niches after injury is critical to accelerate tissue repair and may underlie the regenerative capacity of mammalian tissues. Despite its physiological importance, almost nothing is known about how mammalian tissues activate facultative niches after injury. The mouse hematopoietic system provides a dynamic example of new stem cell niche activation. After hematopoietic injury, hematopoietic stem cells (HSCs) mobilize from the bone marrow to the spleen and participate in extramedullary hematopoiesis (EMH), which supplements bone marrow hematopoiesis for as long as the hematopoietic stress persists. The induction of hematopoiesis in the spleen involves the creation or activation of a facultative niche in the spleen, yet no niche in this tissue has been

characterized. Understanding the nature of the extramedullary niche in the spleen will clarify how the hematopoietic microenvironment regulates HSC and other progenitor function to reestablish homeostasis after injury.

The work in this thesis identifies the cell types in the spleen that are physiologically important sources of the niche factors SCF and CXCL12 during extramedullary hematopoiesis. By using fluorescent reporter alleles for each niche factor, I have discovered that spleen endothelial and perivascular stromal cells secrete SCF, and a subset of spleen perivascular stromal cells secretes CXCL12. Conditional deletion of *Scf* from spleen endothelial or perivascular stromal cells impairs EMH after injury by depleting HSCs and myeloerythroid progenitors from the spleen. Conditional deletion of *Cxcl12* from spleen perivascular stromal cells impairs EMH by depleting myeloerythroid progenitors and mobilizing a minority of HSCs from the spleen.

This work conclusively demonstrates that spleen endothelial cells maintain EMH by secreting SCF, and spleen perivascular stromal cells maintain EMH by secreting both SCF and CXCL12. These cell types represent the first stromal populations in the spleen shown to maintain HSCs and EMH after injury. Further analyses of these cells during injury may reveal how hematopoietic niches are created.

TABLE OF CONTENTS

Title Fly.....	i
Dedication.....	ii
Title Page.....	iii
Copyright.....	iv
Abstract.....	v
Table of Contents.....	vii
Acknowledgements.....	ix
Prior Publications.....	xii
List of Figures and Tables.....	xiii
List of Abbreviations.....	xiv
CHAPTER 1: Background and Objective	
1.1 Introduction.....	1
1.2 The discovery of the HSC.....	1
1.3 Purification of HSCs.....	3
1.4 Genetic regulation of HSCs.....	5
1.5 The niche hypothesis.....	7
1.6 Early studies of niche factors.....	8
1.7 Early experimental investigation of the niche and the endosteal niche hypothesis....	10
1.8 The perivascular niche hypothesis.....	14
1.9 Other cell types in the niche.....	17
1.10 Circadian regulation of the niche.....	22
1.11 Extramedullary hematopoietic tissues.....	23

1.11.1 The fetal liver.....	23
1.11.2 The spleen.....	24
1.12 Extramedullary hematopoiesis in the spleen.....	25
1.13 The hematopoietic niche in the spleen.....	28
1.14 Statement of Purpose.....	29
1.15 Figures.....	31
 CHAPTER 2: The Niche for Extramedullary Hematopoiesis in the Spleen	
2.1 Summary.....	35
2.2 Results and Discussion.....	36
2.3 Methods.....	45
2.4 Author contributions.....	51
2.5 Figures, table, and video.....	52
 CHAPTER 3: Concluding Remarks	
3.1 Conclusions.....	74
3.2 Unanswered questions related to the hematopoietic niche in the spleen.....	75
3.2.1 What are the signals driving induction and resolution of EMH?.....	76
3.2.2 What are the signals that regulate niche cell division?.....	77
3.3 Future investigation of the HSC niche.....	77
3.3.1 The niche during development.....	78
3.3.2 Physiologic regulation of the niche.....	78
3.3.3 Discovery of novel niche factors.....	79
Bibliography.....	82

ACKNOWLEDGEMENTS

When I joined the Morrison Lab as a rotation student, I took on the project of identifying the hematopoietic stem cell niche in the spleen. I was assured it would be a quick, high-impact project that I'd be able to wrap up in around a year or so. It didn't take long for me to realize that things were not as easy as they initially seemed. I presented my experimental plan to my qualifying exam committee, and the universal response was that the project was too difficult, involved too many mouse models, would never be completed, and may not be technically feasible. One committee member was so appalled by the plan that he even asked if I'd ever spoken to Sean about the research topic. Later on in graduate school, a colleague told me that multiple post docs in the lab at the time believed the same. There were multiple difficult periods during the completion of this work when it seemed as though they may have been correct. Nothing in this project came easily. I had to earn everything. Every single development in this project was a battle. I generated and analyzed more than 20 different complex mouse models to complete this project. I received some help toward the end from Bo Zhou, Malea Murphy, and Melih Acar, three post docs in lab to whom I am eternally grateful.

Most of the experiments presented in this thesis should look familiar to my examination committee, as I outlined nearly this exact experimental plan in my qualifying proposal three years ago.

I've received a lot of help and guidance throughout my scientific career. First and foremost, Bo Zhou has been incredibly helpful to me during these last few months of grad school. The completion of this project and submission of this work would not have been possible without his willingness to take on extra experiments. I am truly grateful for his help. Malea

Murphy and Melih Acar also contributed directly to the completion of this project, and I thank them for their efforts on my behalf.

I've had a number of valuable mentors prior to grad school who helped me become the person I am today. Alison DeLong at Brown University was my first mentor who gave me an independent project. It was in her lab that I designed my first real experiment, gave my first presentation in front of an audience, and gained the confidence that I needed to succeed. Josh Blakeslee, a post doc in Alison's lab, was also instrumental in my early scientific development. I learned a lot in Alison's lab and am grateful for my time there. Chuck Inturrisi at Weill Cornell Medical College mentored me for a year after college. I thank him for his guidance and support.

Working under Sean has certainly been a unique experience. Thanks for having me in the lab.

I'd also like to thank the members of the Morrison Lab. Jeff Magee was something of a second PI to me for my first two years in the lab. Jeff's interest in my development and success kept me going through some difficult points in my project, and his keen intellect and clinical perspective contributed to how I think about science. Rob Signer was always willing to talk about my data with me, suggest experiments, and pull interesting papers that might be relevant to my project. Jeff and Rob were great bay mates.

Corbin Meacham, Michalis Agathocleous, and Elena Piskounova have been great friends to me. Their willingness to share a drink and occasionally commiserate made my years in the lab pass by a little quicker. John Mich was always fun to talk to and brought an interesting perspective to just about everything.

Of course, James Peyer has also been a great friend and graduate school compatriot during my time in the lab. James and I were the only two graduate students in the lab for much of

my tenure. James is truly one of the more interesting people I've ever met. I thank him for his camaraderie and friendship throughout grad school.

Thanks to Kristen Correll, Melissa Gross, and the Sarahs Manning and Mann for help with mouse management and genotyping. Thanks as well to the many mouse technicians who performed the everyday cage maintenance of my colony.

I'd also like to thank my thesis committee members, Diego Castrillon, Mike Buszczak, and Ondine Cleaver for their support and guidance. The MSTP administration, especially Andrew Zinn and Robin Downing, has been extremely helpful throughout grad school.

I'd also like to thank my friends who introduced me to rock climbing. I picked up rock climbing a little over a year ago and made some really great friends through the sport. Rachel, Kelly, Kenny, Anh, and Scott have been great climbing buddies and helped make some difficult periods a little easier.

Graduate school is not easy. My family gave me constant support and guidance through it all. Thanks for guiding me through this process.

PRIOR PUBLICATIONS

Acar, M., Kocherlakota, K.S., Murphy, M.M., Peyer, J.G., Oguro, H., **Inra, C.N.**, Jaiyeola, C., Zhao, Z., Luby-Phelps, K., and Morrison, S.J. (2015). Deep imaging of bone marrow shows non-dividing stem cells are perisinusoidal. *Nature Submitted*.

Gregus, A.M., **Inra, C.N.**, Giordano T.P. 3rd, Costa A.C., Rajadhyaksha A.M., and Inturrisi C.E. (2010). Spinal mediators that may contribute selectively to antinociceptive tolerance but not other effects of morphine as revealed by deletion of GluR5. *Neuroscience 169*, 475-487.

Inra, C.N., Zhou, B.O., Acar, M., Murphy, M.M., Zhao, Z., and Morrison, S.J. (2015). The niche for extramedullary hematopoiesis in the spleen. *Nature Submitted*.

LIST OF FIGURES AND TABLES

Figure 1.1. Hematopoiesis proceeds from HSCs through a series of more committed progenitors: p. 31

Figure 1.2. Nestin-GFP^{bright} cells express low levels of *Cxcl12* and *Scf*, and *NG2-CreER*-expressing cells do not maintain HSCs through CXCL12 or SCF secretion: p. 33

Table 2.1. Genes that are significantly (>8-fold and P<0.015) more highly expressed by *Scf*-GFP⁺ stromal cells in spleen as compared to the bone marrow: p. 52

Figure 2.1. Endothelial cells and perivascular stromal cells in the red pulp express *Scf* and *Cxcl12* in the spleen and proliferate upon induction of EMH: p. 55

Figure 2.2. During EMH most HSCs localize adjacent to *Tcf21*⁺ stromal cells in the red pulp: p. 57

Figure 2.3. *Tcf21*-expressing stromal cells are an important source of *Scf* and *Cxcl12* for EMH in the spleen: p. 59

Figure 2.4. Endothelial cells are an important source of *Scf* for EMH in the spleen: p. 61

Figure 2.5. Cy/G-CSF treatment induces EMH in the spleen: p. 63

Figure 2.6. Deletion of *Scf* from *LepR*⁺ cells significantly reduces the number of HSCs in the bone marrow and the spleen after induction of EMH: p. 65

Figure 2.7. Hematopoietic stem and progenitors reside perivascularly, adjacent to *Tcf21*-expressing stromal cells, in the red pulp before and after EMH induction: p. 67

Figure 2.8. Deletion of *Scf* or *Cxcl12* from *Tcf21*-expressing stromal cells in the spleen reduced peripheral blood cell counts but did not affect bone marrow hematopoiesis: p. 69

Figure 2.9. Deletion of *Scf*, but not *Cxcl12*, from endothelial cells in the spleen reduced peripheral blood cell counts but did not affect bone marrow hematopoiesis: p. 71

Video 1. HSCs are closely associated with *Tcf21*-CreER-expressing stromal cells in the red pulp of the spleen: p. 73

LIST OF ABBREVIATIONS

5FU	5-fluorouracil
BABB	Benzyl alcohol:benzyl benzoate
BrdU	5-bromo-2'-deoxyuridine
caPPR	Constitutively active parathyroid hormone receptor
CAR cells	CXCL12-abundant reticular stromal cells
CFU-S	Colony-forming unit-spleen
CLP	Common lymphoid progenitor
CMP	Common myeloid progenitor
Cy	Cyclophosphamide
DTR	Diphtheria toxin receptor
EBV	Epstein-Barr virus
EMH	Extramedullary hematopoiesis
FACS	Fluorescence activated cell sorting
G-CSF	Granulocyte-colony stimulating factor
G-CSFR	Granulocyte-colony stimulating factor receptor
GMP	Granulocyte-monocyte progenitor
H&E	Hematoxylin and eosin
HSC	Hematopoietic stem cell
LTMR	Long-term multilineage reconstituting
MEP	Megakaryocyte-erythroid progenitor
MPP	Multipotent progenitor
NT	Not treated

PLT	Platelet
PMF	Primary myelofibrosis
RBC	Red blood cell
RMA	Robust multi-array average
RP	Red pulp
sgRNA	Short guide RNA
siRNA	Short interfering RNA
WBC	White blood cell
WGA	Wheat germ agglutinin
WP	White pulp

1.1 Introduction

The hematopoietic stem cell (HSC) is the only cell type in the hematopoietic system with the capacity to generate all hematopoietic lineages, including more HSCs through self-renewal. Hematopoiesis in the bone marrow proceeds from HSCs through a series of committed progenitor cells to generate terminally differentiated red and white blood cells (Figure 1.1). Proper HSC function is maintained through both cell autonomous and non-cell autonomous factors produced by heterologous cell types in hematopoietic tissues. These heterologous cells that make up the HSC microenvironment and regulate HSC self-renewal are collectively termed the HSC niche. Recent work has elucidated major components of the HSC niche in the bone marrow, yet very little is known about hematopoietic niches in other tissues. An introduction to the history and biology of HSCs and the HSC niche is presented in this chapter.

1.2 The discovery of the HSC

The term “stem cell” (in German, “stammzelle”) was coined by Ernst Haeckel to describe the common unicellular organism from which all living species descended (Haeckel, 1868). The stem cell was first considered to be a phylogenetic entity. Haeckel was the first to use the term “stem cell” to describe primary cell of ontogeny, the fertilized egg (Haeckel, 1877). The hematopoietic system was the first tissue after the germline to be hypothesized as derived from a specific stem cell. Paul Ehrlich’s work on hematological staining revealed that the white blood cell pool was a heterogeneous mixture of cell types (Ehrlich, 1879). Some hematologists, notably

Artur Pappenheim and Alexander Maximow, began to use the term “stem cell” to refer to a progenitor cell for both red and white blood cells (Maximow, 1909; Pappenheim, 1896).

However, the idea of a common precursor cell for all hematopoietic lineages was controversial, and experimental techniques to test the stem cell hypothesis were only developed decades later.

The discovery of hematopoietic stem cells was ultimately dependent on bone marrow transplantation assays in lethally irradiated mice. Studies in the 1940’s and 1950’s demonstrated that restoration of the hematopoietic system by either protecting the spleen from irradiation with lead shielding or infusing bone marrow cells intravenously was sufficient to prevent death from the minimal lethal dose of irradiation (Jacobson et al., 1949; Lorenz et al., 1951). Transplanting donor bone marrow that was cytogenetically distinguishable from host cells definitively demonstrated that the reconstituted immune system in recipients was derived from donor hematopoietic cells (Ford et al., 1956). Reconstitution of the immune system by transplanted bone marrow cells provided evidence that cells within the bone marrow could regenerate the entire hematopoietic system. Still, it remained unclear if single cells in the bone marrow could differentiate into all hematopoietic lineages.

Ernest McCulloch and James Till were the first to experimentally demonstrate the existence of clonogenic bone marrow cells capable of generating all cell types of the hematopoietic system. While initially studying the radiation sensitivity of bone marrow cells, McCulloch and Till injected bone marrow into lethally irradiated recipient mice and examined hematopoietic colonies that formed in the spleen 11 days after transplantation. Single colonies in the spleen contained erythrocytes, myeloid cells, and megakaryocytes (Till and McCulloch, 1961). Introduction of radiation-induced genetic markers into transplanted cells helped to demonstrate that single, clonogenic bone marrow cells gave rise to multilineage hematopoietic

colonies (Becker et al., 1963; Wu et al., 1967). Donor cells from dissociated spleen colonies generated more spleen colonies when injected into lethally irradiated recipient mice, demonstrating that single spleen colony forming units (CFU-S) generated more CFU-S in addition to differentiated hematopoietic cells; CFU-S self-renewed (Siminovitch et al., 1963). Finally, CFU-S with radiation-induced genetic markers were discovered to produce cytogenetically indistinguishable thymic lymphocytes (Wu et al., 1968). CFU-S were thus self-renewing cells capable of generating all hematopoietic lineages. This series of experiments suggested the existence of a hematopoietic stem cell capable of multilineage differentiation and self-renewal but could not determine whether CFU-S were true stem cells with indefinite self-renewal potential or instead were multipotent progenitor cells with limited capacity for self-renewal.

1.3 Purification of HSCs

Efforts to isolate HSCs from the bone marrow proceeded from McCulloch and Till's seminal discoveries. Early HSC purification protocols relied on discrimination of CFU-S activity based on physical properties of bone marrow cells. The advent of multiparameter fluorescence activated cell sorting (FACS) greatly enhanced the ability to separate well-defined cell populations from complex mixtures and to isolate HSCs from bone marrow. Cell surface markers that identify HSCs with high sensitivity and specificity have since been discovered. These markers are essential to studying HSC biology. A brief history of HSC isolation and marker identification is reviewed in this section.

The first attempts to separate HSCs from heterogeneous bone marrow preparations relied on the physical properties of cells with CFU-S activity. McCulloch and Till's groups were the

first to demonstrate that CFU-S with different self-renewal capacity could be discriminated by velocity sedimentation (Worton et al., 1969). Further refinements to this technique allowed the discrimination of quiescent CFU-S from cycling CFU-S (Monette et al., 1974). The single parameter of cell size drastically limited the CFU-S purity of these physical preparations. Nonetheless, the ability to at least partially purify CFU-S activity by physical characteristics provided clear evidence that heterogeneity among CFU-S could not be entirely explained by environmental or stochastic processes.

A major advance in HSC isolation involved cell surface labeling with fluorescently conjugated lectins and monoclonal antibodies to separate cells by FACS. The first cell surface marker that differentially labeled cells with CFU-S activity was wheat germ agglutinin (WGA), a lectin that binds sialic acid (Visser and Bol, 1982). Electrophoretic mobility assays demonstrated that CFU-S could be separated from other bone marrow colony forming cells based on differences in electrical charge. Pre-treatment with neuraminidase, which cleaves negatively-charged sialic acid residues from cell surface glycoproteins, reduced the electrophoretic mobility of CFU-S more than other bone marrow populations, indicating that these cells had the highest number of cell surface sialic acid groups (Bol et al., 1981). Density centrifugation followed by cell surface labeling with FITC-conjugated WGA could isolate a population by FACS that had 80-fold enriched CFU-S activity (Visser and Bol, 1982). Additional labeling with a fluorescently conjugated monoclonal antibody against H2^k further purified CFU-S activity (Visser et al., 1984).

Irving Weissman's group was the first to discover cell surface markers that labeled a highly pure population of HSCs. Initially examining the early stages of B lineage differentiation, Weissman's group discovered that lineage marker-negative cells expressing low levels of Thy-1

(Lin⁻Thy-1^{lo}) representing approximately 0.2% of all bone marrow cells had enriched capacity to rescue and reconstitute all hematopoietic lineages in lethally irradiated recipient mice. A Thy-1⁺ cell preparation containing 200-400 Lin⁻Thy-1^{lo} cells rescued and reconstituted all irradiated recipient mice. Lin⁻Thy-1⁻ cells lacked the capacity to reconstitute all hematopoietic lineages (Muller-Sieburg et al., 1986). Lin⁻Thy-1^{lo} cells were later discovered to exhibit heterogeneous labeling with a monoclonal antibody against Sca-1. A minor population of Lin⁻Thy-1^{lo} cells representing 0.05% the bone marrow stained positive for Sca-1 and contained all bone marrow HSC activity, as defined by the ability to multilineage reconstitute lethally irradiated recipients. As few as 30 Lin⁻Thy-1^{lo}Sca-1⁺ cells could rescue lethally irradiated recipient mice, representing greater than 1000-fold purification of stem cell activity over whole bone marrow; Lin⁻Thy-1^{lo}Sca-1⁻ cells could not rescue irradiated recipients, although they had CFU-S activity (Spangrude et al., 1988).

The currently most widely used HSC markers can yield about a 50% pure population of HSCs. By comparing the gene expression profile of HSCs to more committed progenitors, Sean Morrison's group discovered that the SLAM family of cell surface proteins identified HSCs with high sensitivity and specificity. Single Lin⁻Sca-1⁺c-Kit⁺CD150⁺CD48⁻ cells could multilineage reconstitute lethally irradiated recipient mice, and approximately 1 in 2 Lin⁻Sca-1⁺c-Kit⁺CD150⁺CD48⁻ cells had HSC activity. HSC activity was not detected in CD150⁻ or CD48⁺ bone marrow populations. Identification of Lin⁻CD150⁺CD48⁻ HSCs was also performed in tissue sections (Kiel et al., 2005). Additional SLAM family proteins identified myeloid-biased and lymphoid-biased HSCs (Oguro et al., 2013). These simple, highly pure markers for HSCs have facilitated the study of HSC biology.

1.4 Genetic regulation of HSCs

High purity HSC markers combined with genetic mouse models has allowed for detailed studies of the genes that regulate HSC self-renewal. HSCs exhibit heterochronic regulatory programs, depend on metabolic sensing pathways, and are responsive to certain hormonal cues. While a complete review of HSC genetic programs is beyond the scope of this chapter, some representative examples are presented in this section.

HSCs are regulated by different genetic programs at different points during development. *Sox17* is highly expressed in fetal and neonatal, but not adult, HSCs. Genetic deletion of *Sox17* from fetal endothelial and hematopoietic cells causes a failure to generate or maintain fetal HSCs. Deletion of *Sox17* from neonatal hematopoietic cells depletes HSCs and causes lethality within 14 days, whereas deletion of *Sox17* from adult hematopoietic cells has no effect (Kim et al., 2007). Overexpression of *Sox17* in adult HSCs confers some properties of fetal HSCs to adult HSCs (He et al., 2011). Conversely, *Bmi-1* maintains adult, but not fetal, HSCs. *Bmi-1*^{-/-} mice exhibited normal fetal hematopoiesis but had reduced HSC numbers in adults. *Bmi-1* acted by suppressing *Ink4a* and *Arf* expression (Park et al., 2003).

Maintenance of HSC activity and self-renewal require multiple components of the PI3-kinase pathway. HSCs show a temporal dependence on *Pten*, in which adult HSCs require PTEN for their maintenance while fetal and neonatal HSCs do not (Magee et al., 2012). *Pten* deletion from adult HSCs rapidly depleted HSCs in the bone marrow and progressed to a fatal acute leukemia. Treatment of *Pten*-deficient mice with rapamycin rescued HSC depletion and delayed leukemia onset (Yilmaz et al., 2006). *Pten* deficiency increased the global protein translation rate in HSCs, and restoration of normal or sub-normal protein translation rates in *Pten*-deficient HSCs also rescued HSC depletion and delayed leukemogenesis (Signer et al., 2014). Other

components of the PI3-kinase pathway, such as *Lkb1*, are also necessary to maintain HSCs, although *Ampka1* and *Ampka2* are dispensable. Loss of *Lkb1* depleted HSCs, likely by causing large-scale chromosomal aberrations (Gan et al., 2010; Gurumurthy et al., 2010; Nakada et al., 2010). These PI3-kinase regulating pathways are critical to maintaining HSCs.

HSCs are sensitive to the hormonal status of the organism. Estrogen signaling has recently been shown to regulate cell cycle dynamics in HSCs. HSCs in female mice divide slightly more frequently than in male mice. Increased cycling in female HSCs was abolished when estrogen receptor- α was conditionally deleted from HSCs. Estradiol administration increased HSC cycling in both males and females, and HSC cycling increased during pregnancy (Nakada et al., 2014). Whether HSCs are responsive to physiological hormones other than estrogen is unknown.

1.5 The niche hypothesis

McCulloch and Till's work on CFU-S revolutionized the field of stem cell biology. However, it was clear that CFU-S and bone marrow HSCs differed significantly. Most importantly, CFU-S had impaired ability to reconstitute the hematopoietic systems of lethally irradiated mice relative to bone marrow HSCs. While it is now known that the CFU-S assay developed by McCulloch and Till measures predominantly multipotent progenitors, at the time of their discovery the discrepancies between CFU-S and bone marrow HSCs were mysterious. In 1978, Ray Schofield hypothesized that a stem cell niche in the bone marrow accounted for the different properties of CFU-S and HSCs (Schofield, 1978).

Schofield's niche hypothesis proposed that HSCs reside in the bone marrow "in association with other cells which determine [their] behavior" (Schofield, 1978). These resident

bone marrow cells prevent premature HSC differentiation, maintaining HSC proliferative potential and ability to reconstitute the hematopoietic systems of irradiated recipient mice. HSC progeny that do not occupy a niche lose the ability to proliferate as HSCs and are instead fated to differentiate. Thus, CFU-S are progeny of HSCs that have left the bone marrow niche and are on a path toward differentiation, unable to proliferate indefinitely and reconstitute irradiated recipients. Further, the niche hypothesis explains why irradiation is required for donor bone marrow engraftment. In an unirradiated mouse receiving a bone marrow transplant, donor HSCs fail to displace host HSCs from bone marrow niches; without support from niche cells, donor HSCs prematurely differentiate and fail to engraft long-term. By killing host HSCs, irradiation clears out bone marrow niche space, allowing donor HSCs to engraft in the niche and reconstitute the hematopoietic system long-term. Schofield's niche hypothesis had remarkable explanatory power for a variety of experimental observations. However, the identities of niche cells and niche factors remained unknown.

1.6 Early studies of niche factors

Spontaneous mutant mice from the Jackson Laboratory provided the first evidence that mutations in genes not expressed by hematopoietic cells could cause hematopoietic disorders. *Steel* (*Sl*, later discovered to encode *Scf*) and *white-spotting* (*W*, later discovered to encode *Kit*) mice both exhibit macrocytic anemia. However, bone marrow harboring mutations in the *Sl* locus did not transplant the anemia to irradiated recipient mice, whereas bone marrow harboring *W* mutations readily transplanted anemia to recipients (Russell, 1979). These observations along with the strikingly similar phenotypes of *W* and *Sl* mutant mice suggested a receptor-ligand

relationship between *W* and *Sl* genes, where the *Sl* gene product non-cell autonomously regulates HSCs through the *W* gene product.

If mice with *Sl* mutations truly have a compromised hematopoietic microenvironment, then wild-type hematopoietic tissue should rescue anemia in these mice. This hypothesis was tested in the 1970's through various spleen transplantation assays. The first such experiments were published by Seldon Bernstein in 1970, 8 years before the niche hypothesis was proposed. Bernstein transplanted *W* mutant spleens ectopically into the omental fat of *Sl/Sl^d* mice, which have one null *Sl* allele and one hypomorphic *Sl* allele. Although *W* mutant mice exhibit the same anemia as *Sl/Sl^d* mice, Bernstein observed that spleens from *W* mutants rescued the macrocytic anemia in *Sl/Sl^d* mice. This rescue was specific to hematopoietic tissue, as transplantation of non-hematopoietic tissues had no effect on anemia (Bernstein, 1970). These experiments demonstrated that a wild-type hematopoietic microenvironment could rescue hematopoietic defects in *Sl* mutant mice.

Further spleen transplantation experiments performed by Norman Wolf in 1978 demonstrated that the *Sl* gene product was a short-range factor. Wolf performed spleen transplants where he anastomosed a wild-type donor spleen directly to the endogenous spleen of a *Sl/Sl^d* mouse. By tissue histology, he observed that normal hematopoiesis occurred in the wild-type donor spleen but not in the mutant host spleen (Wolf, 1978). This observation suggested that the *Sl* gene product acts at short-range, and that hematopoietic cells must be in close contact with a functional hematopoietic microenvironment for normal hematopoiesis to occur. These spleen transplantation experiments in conjunction with the niche hypothesis established *Sl* as a likely niche factor. Moreover, they demonstrated that a hematopoietic niche exists in the spleen.

1.7 Early experimental investigation of the niche and the endosteal niche hypothesis

Early investigation into the bone marrow cell types that maintained HSCs in an undifferentiated state occurred in the 1970's and was thus limited to rather primitive techniques. Nonetheless, the experiments conducted in this era shaped the future of the HSC niche field. Early *in vitro* efforts to describe the cellular components of the HSC niche were performed by Michael Dexter and colleagues in 1977. They observed that a liquid culture system of heterogeneous bone marrow cells could support CFU-S proliferation *in vitro* for several months. The cultures contained both non-adherent hematopoietic cells and adherent cells comprised of mononuclear phagocytes, epithelial-like cells, and stromal cells referred to as “giant fat” cells. Hematopoietic clusters tended to form around adherent stromal cells, and culture conditions that promoted robust expansion of the adherent fraction also promoted greater CFU-S activity and cell density (Dexter et al., 1977). These findings supported the idea that stromal cells from the bone marrow comprise an important component of the HSC niche. As the stromal compartment in the bone marrow is complex, the precise identity of the stromal cells *in vivo* remained undefined.

A series of studies from Brian Lord and colleagues pointed to the bone as the nurturing component of the marrow. They separated bone marrow cells into “axial cells” that reside closest to the center of the bone marrow and “marginal cells” that reside closest to the bone surface. The separation technique they employed involved flushing the marrow using a needle to recover “axial cells” followed by vigorously washing the remaining cells from the bone surface to recover “marginal cells.” Variation of initial flushing pressure generated axial cores of different diameters and allowed the researchers to assay for CFU-S activity along a rough radial gradient of the bone marrow. Marginal zone bone marrow fractions demonstrated increased progenitor

activity relative to axial zone fractions (Lord and Hendry, 1972). Further work using the same experimental fractionation technique examined both CFU-S and more differentiated colony forming activity in the marginal zone and axial zone. This study found that CFU-S activity peaked at the bone surface whereas more differentiated colony forming activity peaked near the middle of the bone radius. The authors suggested that bone cells supported CFU-S, and differentiation of their progeny occurred in a spatial manner along the radius of the bone marrow (Lord et al., 1975). This was the first clear postulation that HSC niche cells *in vivo* were found close to the bone surface. Despite the imprecise experimental data supporting this hypothesis, the idea of an endosteal niche that supported HSCs formed the foundation for decades of future HSC niche research.

Further evidence that bone supports primitive hematopoietic cells came from *in vitro* co-culture assays of osteoblasts and hematopoietic cells. Taichman and Emerson tested whether human bone-derived osteoblasts could support hematopoiesis in culture. They found that osteoblasts in culture produced a number of hematopoietic cytokines and were capable of supporting cultured immature hematopoietic cells, assayed by morphology, for up to two weeks. Notably, osteoblasts in culture did not express *Scf* (Taichman and Emerson, 1994). This study further supported the idea of an endosteal niche for hematopoiesis and implicated osteoblasts as a likely niche cell type.

The advent of sophisticated mouse genetic tools allowed investigation of the HSC niche *in vivo* for the first time. Initial genetic evidence of an osteoblastic niche *in vivo* relied on mouse models that increased the number of osteoblasts in the bone marrow. Linheng Li's group used *Mx1-Cre* to delete the *Bmpr1a* gene from stromal cells in the bone marrow. This model caused an increase in both osteoblasts and HSCs in the bone marrow. The authors also localized putative

HSCs in sections using BrdU label retention as a marker and showed that BrdU-retaining cells that coexpressed some HSC markers associated closely with osteoblasts. They also proposed that close contact between osteoblasts and HSCs was mediated through homotypic N-cadherin interactions based on immunostaining in sections (Zhang et al., 2003). In concurrent studies, David Scadden's group generated mice expressing a constitutively active parathyroid hormone receptor (caPPR) in osteoblasts and observed that these mice had increased osteoblast and HSC numbers. Systemic administration of parathyroid hormone also expanded HSC number. Osteoblasts expressing caPPR were found to express higher levels of some cytokines and Notch ligand, which the authors argued was responsible for increased HSC number (Calvi et al., 2003). These studies suggested that osteoblasts were a component of the HSC niche *in vivo* but relied on indirect methodology and did not test necessity.

Subsequent studies did not support initial observations that osteoblast number correlated with HSC number in the bone marrow. If osteoblasts regulated HSCs directly, modulation of osteoblast number would exhibit acute effects on HSC number. Multiple studies either ablating or increasing the numbers of osteoblasts failed to detect acute effects on HSCs. Hector Aguila's group expressed the herpesvirus thymidine kinase gene in osteoblasts using the Col2.3 promoter, allowing them to conditionally ablate osteoblasts with ganciclovir. While osteoblast ablation caused progressive bone loss and loss of bone cellularity, it did not cause acute reductions in HSCs. Instead, osteoblast ablation acutely depleted lymphoid, myeloid, and erythroid lineages but only depleted HSCs after longer periods (Visnjic et al., 2004). Using the same model, Zhu and colleagues demonstrated acute depletion of B cell progenitors after osteoblast ablation that preceded any HSC depletion (Zhu et al., 2007). A different genetic model constitutively reduced osteoblast number through *biglycan* (*Bgn*) deficiency. While *Bgn*^{-/-} mice exhibited reduced

osteoblast numbers and less trabecular bone, they did not have any hematopoietic deficits and had normal HSC function (Kiel et al., 2007b). Finally, Lympéri and colleagues treated mice with strontium to increase osteoblast number in part by inhibiting osteoclast activity. They observed an increase in some hematopoietic progenitors but no effect on HSC number or function after strontium treatment (Lympéri et al., 2008). None of these studies supported direct regulation of HSCs by osteoblasts. Taken together, these studies indicated that while osteoblasts may directly regulate some hematopoietic progenitors, especially B cell progenitors, their regulation of HSCs was likely to be indirect.

The notion that HSCs reside in close contact with osteoblasts *in vivo* was also inconsistent with subsequent analyses. N-cadherin-mediated osteoblast and HSC contact was undermined by numerous studies showing lack of N-cadherin expression in HSCs and no dependence of HSC maintenance or hematopoiesis on N-cadherin expression in osteoblasts or HSCs (Foudi et al., 2009; Greenbaum et al., 2012; Kiel et al., 2009; Kiel et al., 2007b; Li and Zon, 2010; Morita et al., 2010). In their original study, Zhang and colleagues used BrdU label retention to identify HSCs in sections based on the assumption that HSCs divide less frequently than other hematopoietic populations (Zhang et al., 2003). However, this assumption was never explicitly tested, and the sensitivity and specificity of BrdU retention as a marker for HSCs was unknown. Kiel and colleagues found that most BrdU-retaining cells in the bone marrow were not HSCs and that most HSCs did not retain BrdU (Kiel et al., 2007a). Therefore, the label-retaining cells that Zhang and colleagues identified were most likely not HSCs, and the localization of label-retaining cells did not necessarily reflect the localization of HSCs. Finally, staining tissue sections with antibodies against SLAM markers allowed for localization of a relatively pure population of HSCs *in situ* for the first time. HSCs were found to localize near vasculature in the

bone marrow, with only a small fraction localizing near osteoblasts (Kiel et al., 2005). HSC localization studies suggested a perivascular, not endosteal, niche.

1.8 The perivascular niche hypothesis

The HSC niche is an anatomical structure associated with HSCs, and many studies support the existence of a perivascular HSC niche in the bone marrow. Visualizing HSCs in tissue sections provided the first evidence of a perivascular niche. Although HSCs could be flow cytometrically isolated for decades, the marker combinations used for FACS were too complex to identify HSCs in tissue sections and simpler combinations were essential to define the anatomical location of the niche. HSC localization experiments using simple, highly sensitive and specific SLAM markers were the first to propose that HSCs are located near blood vessels. Under steady-state conditions, most HSCs reside near endothelial cells in the bone marrow, with only a small fraction residing near bone (Kiel et al., 2005). Perivascular localization of HSCs has been observed by a number of labs (Casanova-Acebes et al., 2013; Kunisaki et al., 2013; Lo Celso et al., 2009; Nombela-Arrieta et al., 2013; Sipkins et al., 2005; Yamazaki et al., 2011).

While HSC localization studies in tissue sections supported the notion of a perivascular niche, HSCs are known to exit the bone marrow through sinusoids and mobilize to other tissues (Wright et al., 2001), and the possibility remained that HSC proximity to blood vessels merely reflected HSCs exiting or entering the bone marrow. Time-lapsed *in vivo* microscopy of HSCs and progenitors in the mouse calvarium revealed that HSCs and progenitors reside near distinct vascular microdomains that express high levels of CXCL12 and E-Selectin. HSCs and other progenitors remain in the same location for weeks at a time (Lo Celso et al., 2009; Sipkins et al., 2005). After irradiation, transplanted HSCs and progenitors homed near the endosteum (Lo

Celso et al., 2009; Xie et al., 2009), although this localization pattern may have reflected sinusoidal damage after irradiation (Hooper et al., 2009). Imaging studies of relatively pure populations of HSCs, both in tissue sections and in living animals, were consistent with a perivascular niche. However, imaging studies are merely associative, and the cell types that support HSCs could not be discovered through these methods. Functional studies were necessary to test the perivascular niche hypothesis directly.

Early functional evidence that cells near bone marrow vasculature produced niche factors necessary to maintain HSCs focused on the CXCL12-CXCR4 signaling axis. CXCL12 was first identified as a stimulating factor for B cell progenitors (Nagasawa et al., 1994). Analysis of mice harboring mutations in the receptor for CXCL12, CXCR4, indicated that CXCL12 had a more general role in maintaining hematopoiesis and proper homing of HSCs to the bone marrow during development (Ara et al., 2003; Nagasawa et al., 1996; Zou et al., 1998). Inhibition of CXCR4 in adult mice mobilized HSCs to the peripheral blood, supporting a role for CXCL12 in retaining HSCs in the bone marrow (Broxmeyer et al., 2005). Sugiyama and colleagues were the first to study the CXCL12-CXCR4 signaling axis in adult mice using conditional mouse models. Conditionally deleting *Cxcr4* from adult HSCs rapidly depleted HSCs and impaired hematopoiesis, demonstrating an essential role for CXCR4 signaling in maintaining functional HSCs. *Cxcl12-GFP* knock-in mice showed that CXCL12-abundant reticular stromal cells (CAR cells) around blood vessels comprised the predominant cellular source of CXCL12 in the bone marrow, with rare GFP expression near bone. Almost all HSCs identified in tissue sections were found in close proximity to *Cxcl12-GFP*⁺ cells (Sugiyama et al., 2006). This study was the first to identify the cellular source of a niche factor in the bone marrow, at least based on expression. A follow-up study demonstrated that short-term ablation of CAR cells reduced HSC numbers,

providing some evidence that CAR cells maintained HSCs (Omatsu et al., 2010). The data strongly suggested a perivascular source of niche factors for HSCs.

Ding and Morrison performed the first definitive experiments to determine the physiologically important sources of niche factors in the bone marrow. Their strategy involved generating a knock-in reporter allele for a known niche factor to identify its cellular expression pattern in the bone marrow and generating a floxed allele of the same niche factor to systematically delete this factor from different cell populations in the bone marrow. The first niche factor tested using this strategy was SCF, a known non-cell autonomous regulator of HSCs whose receptor is expressed on all immature hematopoietic progenitors (Ogawa et al., 1991). Analysis of *Scf*^{GFP} mice revealed that *Scf* was expressed at high levels in *Leptin receptor (Lepr)*-expressing perivascular stromal cells around sinusoids in the bone marrow. Low *Scf* expression was observed in sinusoidal endothelial cells, and no *Scf* expression was detected in any osteoblasts. Most HSCs identified in sections were found near *Scf*-GFP⁺ perivascular stromal cells (Ding et al., 2012). Conditional deletion of *Scf* from perivascular stromal cells using *Lepr*-Cre (DeFalco et al., 2001) or from endothelial cells using *Tie2*-Cre (Koni et al., 2001), but not from osteoblasts, hematopoietic cells, or *Nestin*-expressing cells depleted functional HSCs from the bone marrow (Ding et al., 2012). These results strongly emphasized that endothelial and perivascular stromal cells maintain HSCs in a perivascular niche around sinusoids. This work was the first to establish the functionally important cellular source of any niche factor *in vivo* and provided a generalizable strategy for future studies of the HSC niche.

Ding and Morrison and Daniel Link's group independently employed the same strategy to identify the physiologically relevant sources of CXCL12 in the bone marrow. While Nagasawa's group had previously demonstrated that perivascular stromal cells express high

levels of *Cxcl12* (Sugiyama et al., 2006) and that perivascular stromal cell ablation depleted HSCs (Omatsu et al., 2010), they did not test whether deletion of *Cxcl12* from these cells depleted HSCs from the bone marrow. Ding and Morrison found that *Cxcl12* was expressed abundantly in *Lepr*-expressing perivascular stromal cells and at low levels in endothelial cells and some osteoblasts. Interestingly, *Cxcl12* deletion from each of these populations perturbed different aspects of hematopoiesis. *Cxcl12* deletion from perivascular stromal cells using *Lepr*-Cre mobilized a minority of HSCs to the blood and spleen without appreciably depleting HSCs from the bone marrow, while *Cxcl12* deletion from endothelial cells using *Tie2*-Cre depleted HSCs from the bone marrow without any mobilization to the blood (Ding and Morrison, 2013). *Cxcl12* deletion from osteoblasts using *Col2.3*-Cre (Liu et al., 2004), by contrast, had no effect on HSCs but depleted lymphoid progenitors (Ding and Morrison, 2013). Daniel Link's group deleted *Cxcl12* from perivascular stromal cells and osteoblasts using *Prx-1*-Cre (Logan et al., 2002) and observed HSC depletion from the bone marrow, an effect also observed by Ding and Morrison (Ding and Morrison, 2013; Greenbaum et al., 2013). These studies reinforced the perivascular niche hypothesis and also revealed new insight into HSC niche biology. The same niche factor may have different effects on HSCs and other progenitors depending on its cellular source, and HSCs and other progenitors may occupy anatomically distinct niches.

1.9 Other cell types in the niche

Bone marrow cell types in addition to endothelial and perivascular stromal cells have been proposed to maintain HSCs. Most of the evidence to support a role for these cell types in maintaining HSCs comes from cell ablation models, either by genetic, surgical, or pharmacologic techniques. In any model that modulates cell number of a candidate niche

population, indirect effects on HSCs may confound interpretation of results, as occurred in early *in vivo* studies supporting the osteoblastic niche. Despite the checkered history of this experimental design, conclusions drawn from cell ablation studies still shape the niche field and will be reviewed here.

Nestin-expressing mesenchymal stromal cells have been proposed to be a component of the HSC niche. Paul Frenette's group used a *Nestin*-GFP transgene (Mignone et al., 2004) to identify rare bone marrow stromal cells that were located near HSCs in tissue sections. Flow cytometrically isolated *Nestin*-GFP⁺ cells expressed high levels of *Cxcl12* and *Scf* by qPCR (Mendez-Ferrer et al., 2010). They crossed a *Nestin*-CreER transgene (Balordi and Fishell, 2007) with a conditional diphtheria toxin receptor (DTR) allele and ablated *Nestin*-CreER-expressing cells by administering diphtheria toxin. HSCs were modestly depleted from bone marrow and increased in the spleen after cell ablation (Mendez-Ferrer et al., 2010). This study led to the popular acceptance that *Nestin*-expressing stromal cells in the bone marrow comprise the HSC niche. However, Ding and Morrison later demonstrated that the expression pattern of *Nestin* transgenes differs among different transgenes and that deletion of either *Scf* or *Cxcl12* using either *Nestin*-CreER or *Nestin*-Cre (Tronche et al., 1999) had no effect on HSCs or any other hematopoietic population (Ding and Morrison, 2013; Ding et al., 2012). Further, they showed that the *Nestin*-GFP transgene labels two distinct cell types in the bone marrow that can be discriminated by reporter fluorescence intensity, and that the cells reported to express high levels of *Cxcl12* and *Scf* were likely *Lepr*-expressing perivascular stromal cells, which do not express endogenous *Nestin* and do not recombine with either *Nestin*-CreER or *Nestin*-Cre (Ding et al., 2012).

A subsequent study from Frenette's group amended their prior conclusions about *Nestin* expression in the bone marrow. Frenette's group divided *Nestin*-GFP⁺ cells into *Nestin*-GFP^{bright} and *Nestin*-GFP^{dim} subsets and analyzed the bone marrow distribution of each population by three-dimensional microscopy. They reported that *Nestin*-GFP^{bright} cells were found surrounding arterioles, stained positive with an NG2 antibody, and did not overlap with *Lepr*-expressing perivascular stromal cells. *Nestin*-GFP^{dim} cells were found around sinusoids and largely overlapped with *Lepr*-expressing perivascular stromal cells. HSC localization experiments suggested that HSCs, especially non-cycling HSCs, showed a bias toward periarteriolar *Nestin*-GFP^{bright} cells. RNA-seq analyses on flow cytometrically sorted populations revealed 5-fold higher *Scf* and *Cxcl12* expression in *Nestin*-GFP^{bright} cells relative to *Nestin*-GFP^{dim} cells (Kunisaki et al., 2013). To test whether *Nestin*-GFP^{bright} cells maintained HSCs, they crossed *NG2*-CreER (Zhu et al., 2011) with a conditional DTR allele and ablated *NG2*-CreER-expressing cells by diphtheria toxin treatment. HSCs were depleted from the bone marrow and spleen after cell ablation (Kunisaki et al., 2013). These results suggested that *NG2*-expressing periarteriolar cells were part of the HSC niche.

The conclusions about *NG2*-expressing cells from Frenette's group have been inconsistent with subsequent studies. Their data indicating that *Nestin*-GFP^{bright} cells express higher levels of *Scf* and *Cxcl12* than *Nestin*-GFP^{dim} cells are inconsistent with data published in the same study. Microscopy and flow cytometry-based colocalization experiments indicated that *Nestin*-GFP^{bright} cells expressed *NG2* and *Nestin*-GFP^{dim} cells expressed *Lepr*. However, their RNA-seq data show the opposite expression pattern for *NG2* and *Lepr* and are consistent with *Lepr*-expressing perivascular stromal cells as the major source of *Scf* and *Cxcl12* in the bone marrow (Kunisaki et al., 2013). Further, quantitative PCR analyses of *Nestin*-GFP^{bright} cells and

Nestin-GFP^{dim} cells show that *Nestin*-GFP^{dim} cells express much higher levels of *Scf* and *Cxcl12* than *Nestin*-GFP^{bright} cells (Figure 1.2a). HSC localization studies using α -*catulin*-GFP to identify HSCs shows no bias of HSCs, regardless of cell cycle status, toward arterioles (Acar et al., 2015). Finally, deletion of *Cxcl12* or *Scf* using *NG2*-CreER had no effect on HSCs in the bone marrow or spleen (Figure 1.2b-1.2e). It is unlikely that *NG2*-expressing cells maintain HSCs through SCF or CXCL12 secretion. It remains possible that they regulate HSCs by other mechanisms, although there is minimal evidence to support this claim.

Non-myelinating Schwann cells may also comprise part of the bone marrow HSC niche. Hiromitsu Nakauchi's group conditionally deleted the TGF- β type II receptor, *Tgfr2*, from HSCs and discovered that *Tgfr2*-deficient mice had reduced bone marrow stem cell activity (Yamazaki et al., 2011). TGF- β is produced by many cell types in a latent form and requires interaction with integrin- β 8 (ITGB8) for full activity (Munger et al., 1999). Nakauchi's group observed that ITGB8 labeled bone marrow *Gfap*-GFP⁺ cells in tissue sections. *Gfap*-GFP⁺ cells were discovered to be non-myelinating Schwann cells that ensheathed bone marrow nerves and were not distributed perisinusoidally. A similar fraction of HSCs were found to localize near GFAP⁺ cells as with endothelial cells. Surgical denervation of the bone marrow resulted in loss of TGF- β expression, depletion of GFAP⁺ cells and depletion of HSCs in the bone marrow (Yamazaki et al., 2011). While bone marrow denervation profoundly depleted HSCs, it is unclear that loss of TGF- β activation by non-myelinating Schwann cells mediated this reduction. Nonetheless, non-myelinating Schwann cells may activate a ligand that maintains HSCs.

Some hematopoietic populations have been suggested as niche components. Frenette's group identified a subset of macrophages in the bone marrow expressing CD169 that maintain niche integrity. Pharmacological depletion of bone marrow macrophages or genetic ablation of

CD169⁺ macrophages using *Cd169*-DTR mice mobilizes HSCs from the bone marrow and modestly reduces CXCL12 produced by stromal cells in the bone marrow (Chow et al., 2011). Dan Link's group demonstrated that granulocyte-colony stimulating factor receptor (G-CSFR) expression restricted to CD68⁺ macrophages in otherwise G-CSFR-deficient mice is sufficient to promote G-CSF-induced HSC mobilization to the spleen (Christopher et al., 2011). These studies do not argue that macrophages maintain HSCs directly, but rather regulate the bone marrow microenvironment.

Finally, megakaryocytes have recently been suggested to maintain HSCs. Frenette's group found that genetically ablating megakaryocytes using the conditional DTR allele driven by *Cxcl4*-Cre (Tiedt et al., 2007) greatly increased bone marrow HSC number by driving HSCs into cycle. *Cxcl4*^{-/-} mice exhibited a similar effect (Bruns et al., 2014). However, this group defined HSCs as CD150⁺LSK cells, a cell population that also contains megakaryocyte progenitors (Oguro et al., 2013). It is not clear whether megakaryocyte ablation increases HSC numbers and cell cycle activity or merely increases megakaryocyte progenitors. Linheng Li's group also ablated megakaryocytes using the same DTR system and observed mainly increases in bone marrow ST-HSCs and MPPs and modestly increased HSC cycling activity. Deletion of *Tgfb1* from megakaryocytes showed similar effects, suggesting that megakaryocytes maintain HSC quiescence by secreting TGF- β (Zhao et al., 2014). Megakaryocytes may regulate HSCs in the niche, although these results may also reflect increased HSC and progenitor activity to restore homeostasis after gross perturbations of the hematopoietic system.

1.10 Circadian regulation of the niche

The activity of the HSC niche is regulated in a circadian pattern. HSCs periodically mobilize from the bone marrow to the blood during steady-state hematopoiesis. Mobilized HSCs eventually home back to the bone marrow or to other hematopoietic tissues (Wright et al., 2001). Paul Frenette's group has reported that physiologic HSC mobilization to the blood occurs in a circadian pattern. Circadian oscillation of HSC mobilization can be disrupted by perturbing the light-dark cycle in mice, by genetically disrupting the circadian clock, or by disrupting the sympathetic nervous system. CXCL12 protein level in the bone marrow is inversely correlated with circadian HSC mobilization and is also dependent on the central circadian clock and sympathetic tone (Mendez-Ferrer et al., 2008). Sympathetic nerves are proposed to act on bone marrow stromal cells to modulate the expression of cell adhesion molecules on bone marrow endothelial cells (Scheiermann et al., 2012). Pharmacologic HSC mobilization is most effective at the circadian peak of HSC mobilization (Lucas et al., 2008).

Circadian oscillation of HSC mobilization may also be governed by clearance of neutrophils in the bone marrow. Andrés Hidalgo's group demonstrated that aged circulating neutrophils are cleared by CD169⁺ macrophages in the bone marrow. Neutrophil production and clearance follow a circadian rhythm. Through a series of neutrophil transfer experiments and macrophage engulfment assays, they showed that neutrophil clearance by bone marrow macrophages reduces *Cxcl12* expression in bone marrow stromal cells and mobilizes HSCs and other progenitors to the blood (Casanova-Acebes et al., 2013). HSCs mobilize from the bone marrow in a circadian pattern dependent on both the sympathetic nervous system and bone marrow macrophage-mediated neutrophil clearance. The physiologic significance of this process

is unknown, as mice with disrupted circadian HSC mobilization patterns do not have any hematopoietic sequelae.

1.11 Extramedullary hematopoietic tissues

The HSC niche in the bone marrow has been intensively studied for decades, but niches in other hematopoietic tissues have received comparatively little attention. The hematopoietic system is unique among tissues in that its stem cells are mobile and home to different hematopoietic organs throughout the course of development and during injury in adult mammals. How HSCs adopt different niches during development and injury, the cellular components of hematopoietic niches in different organs, and the extent to which these niches are similar are currently unknown. The extramedullary tissues HSCs adopt during development and injury will be reviewed here.

1.11.1 The fetal liver

Mammalian hematopoiesis occurs in different organs throughout ontogeny. Primitive hematopoiesis, characterized by myelopoiesis and the production of nucleated erythrocytes, first occurs extraembryonically in the yolk sac around e7.5 in mice. Definitive hematopoiesis, producing all hematopoietic lineages, replaces primitive hematopoiesis beginning around e10.5 in mice. Definitive HSCs emerge from hemogenic endothelium in the aorta-gonad-mesonephros region to initiate definitive hematopoiesis (Bertrand et al., 2010; Boisset et al., 2010; Eilken et al., 2009), although lineage tracing studies suggest that some primitive yolk sac HSCs contribute to definitive hematopoiesis (Samokhvalov et al., 2007), and quantitative analysis suggests that the placenta produces some definitive HSCs (Gekas et al., 2005). By e11 in mice, definitive

HSCs are found in the fetal liver where they participate in hematopoiesis. The cellular nature of the hematopoietic niche in the fetal liver has not been studied, but it is clear that hematopoiesis in this tissue depends on CXCL12 and SCF secretion (Ding et al., 2012; Nagasawa et al., 1996).

The properties of fetal liver and adult bone marrow HSCs differ significantly. Whereas most bone marrow HSCs are quiescent, fetal liver HSCs cycle frequently and double in number every day until e14.5 (Morrison et al., 1995). Most HSCs contribute to hematopoiesis in the fetal liver, while only about one-third of adult bone marrow HSCs contribute to hematopoiesis throughout mouse adulthood (Busch et al., 2015). Fetal HSCs also give higher levels of reconstitution in lethally irradiated recipient mice (Morrison et al., 1995). The functional differences between fetal liver and bone marrow HSCs may reflect differences in their respective niches.

1.11.2 The spleen

The spleen is a site of hematopoiesis both during ontogeny and after injuries to the hematopoietic system. Beginning at e14 and persisting for a few weeks postnatally, the spleen is an active site of hematopoiesis. In adult mice, few HSCs remain in the spleen and hematopoiesis occurs mainly in the bone marrow. The remaining HSCs in the spleen are competent to reconstitute lethally irradiated recipient mice and are more likely to be in cycle than bone marrow HSCs (Morita et al., 2011). The physiologic significance of the few HSCs in the adult mouse spleen is not known. Increased hematopoiesis in the spleen supplements bone marrow hematopoiesis in a number of hematopoietic disorders and accelerates hematopoietic recovery after injury.

During steady-state hematopoiesis, the spleen normally functions as a secondary lymphatic tissue and as a filter for the blood. The spleen can be divided into two morphologically and functionally distinct regions, the white pulp and red pulp. Histologically, white pulp appears as white, circular regions surrounded by red pulp. B and T lymphocytes and antigen presenting cells comprise the major cell types of the white pulp. The adaptive immune response to blood-borne pathogens is initiated in white pulp germinal centers, where activated B cells proliferate. The red pulp primarily serves as a filter for the blood. Pathogens, other foreign material, and aged or damaged red blood cells and platelets are cleared from the bloodstream by resident red pulp phagocytic cells. Red pulp cell types include macrophages, plasma cells, reticular stromal cells, and myofibroblasts (Ross and Pawlina, 2006).

The vasculature of the spleen consists of a network of arteries, arterioles and sinusoids. The splenic artery enters through the spleen hilum and branches into central arterioles. White pulp organizes around the central arterioles, which further branch into radial arterioles and capillaries. The white pulp vasculature is thus mainly arterioles and capillaries. Red pulp vasculature is mainly an open circulation comprised of a large network of sinusoids. Sinusoids are a specialized blood vessel consisting of a single layer of endothelium with large fenestrations to allow for cell trafficking. Sinusoids are found in lymphatic tissue, liver, and bone marrow. Blood exits the red pulp through the splenic vein (Cesta, 2006).

1.12 Extramedullary hematopoiesis in the spleen

During injuries to the hematopoietic system, bone marrow may be insufficient to maintain homeostasis of the hematopoietic system. Increased hematopoiesis in hematopoietic tissues other than the bone marrow, a phenomenon termed extramedullary hematopoiesis

(EMH), supplements bone marrow hematopoiesis during injury. In mice, the spleen is a major site of EMH. During EMH, HSCs and other hematopoietic progenitors mobilize from the bone marrow to the spleen and undergo primarily myelopoiesis and erythropoiesis. EMH occurs in the red pulp of the spleen and can result in massive red pulp expansion and increased overall spleen size. EMH can persist for the duration of the hematopoietic insult, which may last months or years. Many injuries can cause EMH. The most relevant hematopoietic injuries resulting in EMH are reviewed in this section.

Primary myelofibrosis (PMF) is the prototypical bone marrow injury causing EMH. PMF is a clonal HSC disorder involving increased myelopoiesis and megakaryopoiesis (Ciurea et al., 2007). Most cases of PMF are caused by activating JAK2 mutations, MPL mutations, or calreticulin truncations in hematopoietic cells (Baxter et al., 2005; Klampfl et al., 2013; Kralovics et al., 2005; Levine et al., 2005; Nangalia et al., 2013; Pardanani et al., 2006). Bone marrow stromal cells do not harbor causal genetic mutations in PMF patients (Wang et al., 1992), although mouse models with stromal mutations can induce PMF (Walkley et al., 2007a; Walkley et al., 2007b). Imbalanced hematopoiesis in this disease, especially increased megakaryopoiesis, leads to overproduction of various cytokines, including TGF- β and platelet-derived growth factor, resulting in a pro-fibrotic bone marrow stromal reaction (Chagraoui et al., 2002; Reilly, 1992; Tefferi, 2005; Vannucchi et al., 2002). Secondary bone marrow fibrosis causes hematopoietic insufficiency and anemia, resulting in EMH in the spleen and other tissues; in some cases, EMH is the only source of hematopoiesis (Ferrant et al., 1982).

Anemia is also a general cause of extramedullary hematopoiesis in the spleen. Many diseases and injuries can lead to anemia and only representative examples of genetic and acquired anemia are presented here. Beta thalassemia is a congenital blood disorder caused by

ineffective hemoglobin production, resulting in defective erythropoiesis and increased peripheral erythrocyte destruction (Martin and Thompson, 2013). EMH, especially erythropoiesis, occurs in the spleen and liver of beta thalassemia patients. EMH is directly related to anemia, as blood transfusion restores normal hemoglobin levels and reverses hepatosplenomegaly associated with EMH (Rund and Rachmilewitz, 2005). Acquired anemia can also cause EMH. Chronic blood loss in mice causes mobilization of HSCs and other progenitors to the spleen and massively increased spleen erythropoiesis (Cheshier et al., 2007).

Pregnancy in mice increases hematopoiesis in the spleen. Blood volume increases substantially in the pregnant mouse, and erythropoiesis must similarly increase to maintain appropriate hematocrit levels. The pregnant mouse spleen approximately doubles in weight and exhibits 40-fold increased erythropoiesis (Fowler and Nash, 1968). EMH in the spleens of pregnant mice is dependent on estrogen signaling in HSCs, as deletion of the estrogen receptor from HSCs reduces the EMH response during pregnancy (Nakada et al., 2014). It is not known whether EMH occurs during pregnancy in humans, but there is evidence that spleen volume increases during human gestation (Maymon et al., 2006; Sheehan and Falkiner, 1948).

EMH also occurs during infection. In a mouse model of *Mycobacterium avium* infection, HSCs are driven into cycle by IFN γ and mobilize to the spleen. Other hematopoietic progenitors mobilize to the spleen as well (Baldrige et al., 2010). Infection with *Escherichia coli* similarly mobilizes HSCs and progenitors to the spleen. Mobilization in this context is dependent on TLR and NOD signaling (Burberry et al., 2014). EMH in the spleen during infection presumably creates granulocytes to fight the infectious agent.

Finally, myeloablative chemotherapy induces EMH. A number of chemotherapeutics can induce EMH in the spleen. One well-characterized myeloablative regimen involves a single

treatment with cyclophosphamide followed by daily injections of granulocyte-colony stimulating factor (G-CSF). Cyclophosphamide, an alkylating agent, kills dividing hematopoietic cells in the bone marrow, and G-CSF promotes subsequent hematopoietic recovery. This treatment regimen has a well-defined and reproducible time course in mice. After the second G-CSF injection, HSCs in the bone marrow divide symmetrically. By the third injection, HSCs mobilize to the blood and home to the spleen after the fourth injection. HSCs remain in the spleen for the duration of treatment (Morrison et al., 1997). EMH in the spleen has also been reported in a patient who received intermittent G-CSF following a chemotherapy regimen that included cyclophosphamide (Litam et al., 1993).

1.13 The hematopoietic niche in the spleen

Although EMH in the spleen supplements insufficient bone marrow hematopoiesis in a number of disease conditions and accelerates hematopoietic recovery after injury, almost nothing is known about the cellular components of the hematopoietic niche in the spleen. Early spleen transplantation studies suggest that *Scf* is necessary for EMH to occur in the spleen (Bernstein, 1970; Wolf, 1978). Localization of HSCs in the spleens of Cy+G-CSF treated mice using SLAM markers found that all HSCs localized in the red pulp and most were adjacent to sinusoidal endothelium (Kiel et al., 2005). This has led to the hypothesis that cells near sinusoids maintain HSCs during EMH. However, little work has been performed to identify the cellular components of the hematopoietic niche in the spleen. The current understanding of the hematopoietic niche in the spleen is reviewed below.

CD169⁺ macrophages, which have been suggested to regulate the HSC niche in the bone marrow, have also been implicated in supporting EMH. Using mice that expressed DTR under

control of the CD169 promoter, Paul Frenette's group discovered that CD169⁺ macrophages support erythropoiesis in the spleen after injury. Mice were depleted of CD169⁺ macrophages by diphtheria toxin administration and treated with 5-fluorouracil (5FU), a myeloablative chemotherapy that induces EMH in the spleen. Macrophage-depleted mice exhibited slowed erythropoietic recovery and reduced erythroblast numbers in the spleen after 5FU treatment. Further, mice depleted of macrophages exhibited reduced splenic erythropoiesis in a model of polycythemia vera (Chow et al., 2013). These experiments suggest that CD169⁺ macrophages support erythropoiesis in the spleen during recovery from at least some hematopoietic injuries.

Splenic CD169⁺ macrophages have recently been suggested to maintain HSCs in the spleen through VCAM-1. Matthias Nahrendorf's group used a model of atherosclerosis to induce EMH in the spleen (Dutta et al., 2012). They used this model in combination with short interfering RNA (siRNA) knockdown of VCAM-1 in macrophages. siRNA against VCAM-1 was delivered in liposomes, which preferentially target macrophages. Mice with VCAM-1 knockdown had fewer HSCs in the spleen and more HSCs in the peripheral blood than control mice after atherosclerosis (Dutta et al., 2015). These experiments suggest that VCAM-1 expression in splenic CD169⁺ macrophages retains HSCs in the spleen.

1.14 Statement of purpose

The activation of facultative niches during injury is a fundamental property of HSCs, yet very little is known about the cellular nature of any extramedullary hematopoietic niche. Indeed, the activation or creation of secondary niches after tissue injury is critical to accelerate repair and may underlie the regenerative capacity of mammalian tissues. As explained in previous sections, the mouse hematopoietic system provides a powerful model of dynamic niche activation. The

induction of hematopoiesis in the spleen involves activation or creation of a new niche in the spleen, yet very little work has been done to characterize this niche. I have used validated genetic tools and a well-characterized hematopoietic injury model to phenotypically and functionally identify the first stromal components of the hematopoietic niche in the spleen.

I began this project by using *Scf^{GFP}* and *Cxcl12^{dsRed}* mice to phenotypically identify the sources of these niche factors in the spleen. I discovered that endothelial and perivascular stromal cells express *Scf* and a subset of perivascular stromal cells express *Cxcl12*. I then characterized these cells during steady-state hematopoiesis and after various treatment time points with Cy+G-CSF. I performed gene expression profiling on the *Scf*-GFP⁺ cells in the spleen to find genes specifically expressed in spleen niche cells. Using this list of genes, I tested many Cre driver mice to find a Cre allele that deleted specifically in these cells. I discovered that *Tcf21-CreER* recombines specifically in spleen perivascular stromal cells and that *Vav1-Cre* recombines specifically in spleen endothelial cells. I used these Cre alleles to delete *Scf* or *Cxcl12* from endothelial and perivascular stromal cells to investigate whether endothelial or perivascular stromal cells maintained HSCs or other hematopoietic progenitors in the spleen after Cy+G-CSF treatment. I discovered that perivascular cells secrete both SCF and CXCL12 and that endothelial cells secrete SCF, but not CXCL12, to maintain hematopoiesis in the spleen after injury. These studies represent the first in depth genetic analysis of the hematopoietic niche in the spleen.

1.15 Figures

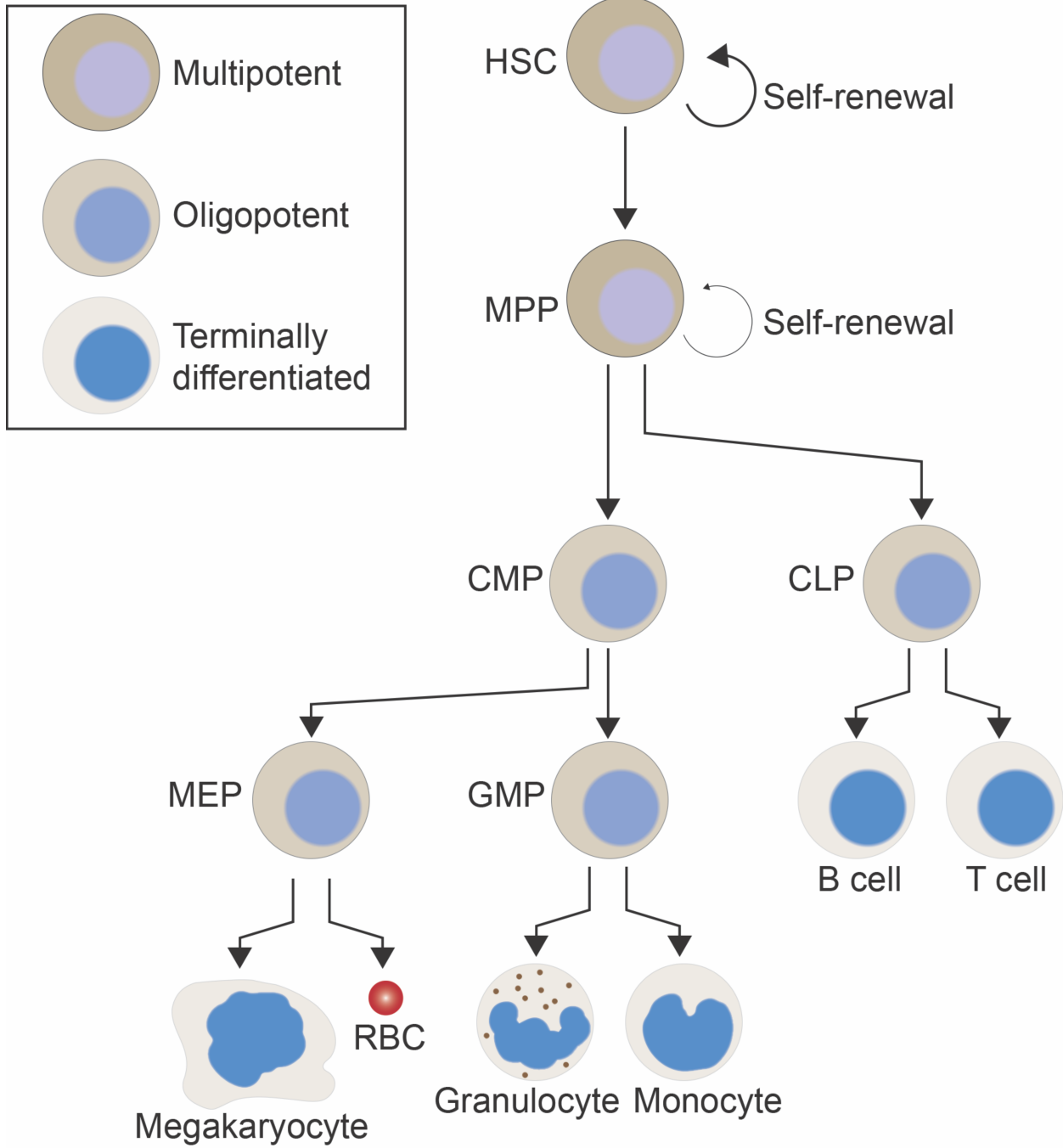


Figure 1.1. Hematopoiesis proceeds from HSCs through a series of more committed progenitors. HSCs reside at the top of the hematopoietic hierarchy. HSCs can divide asymmetrically to generate a more differentiated hematopoietic progenitor in addition to another HSC, or symmetrically to generate two new HSCs. HSCs have the greatest self-renewal potential. Generation of mature, terminally differentiated hematopoietic cells is achieved through a series of committed progenitor cells with limited self-renewal potential. HSC, hematopoietic stem cell; MPP, multipotent progenitor; CMP, common myeloid progenitor; CLP, common lymphoid progenitor; MEP, megakaryocyte-erythroid progenitor; GMP, granulocyte-monocyte progenitor; RBC, red blood cell. Adapted from (Oguro et al., 2013).

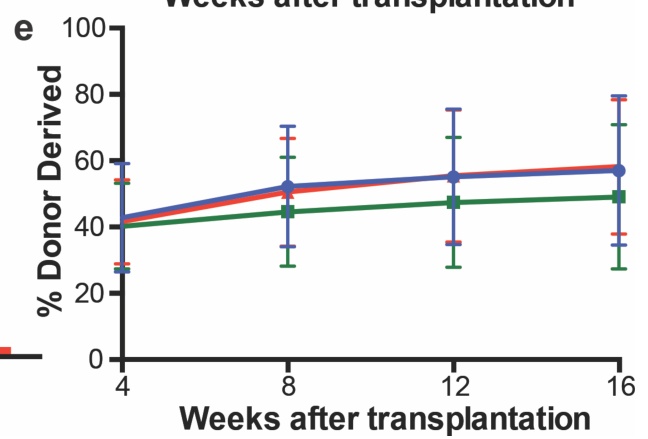
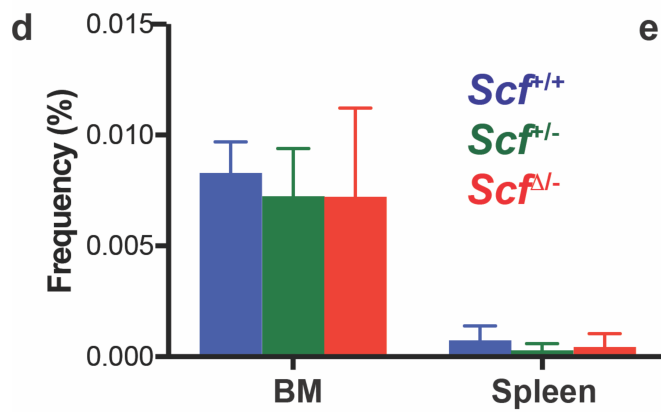
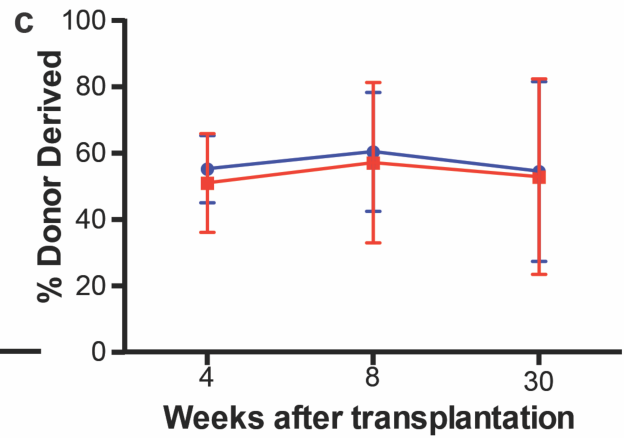
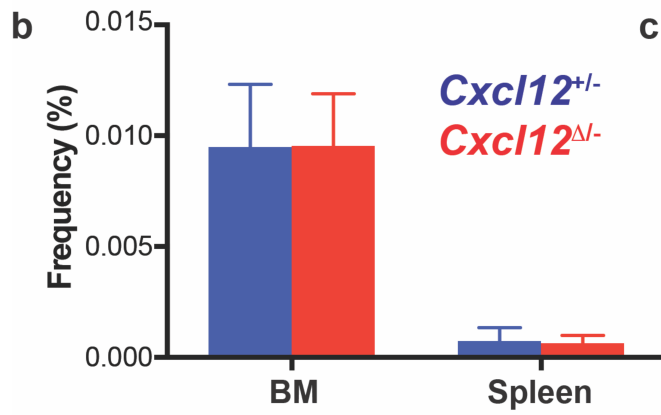
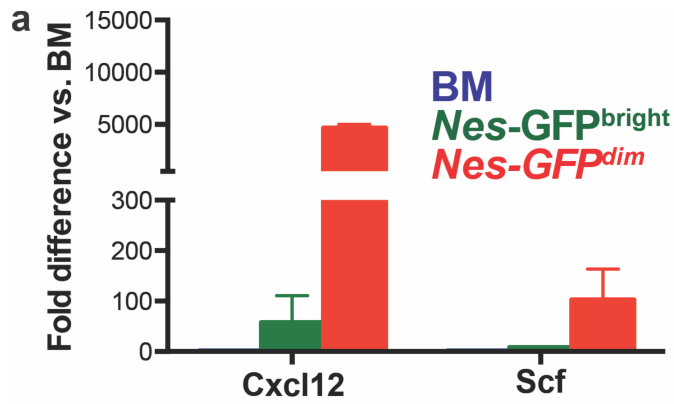


Figure 1.2. *Nestin*-GFP^{bright} cells express low levels of *Cxcl12* and *Scf*, and *NG2*-CreER-expressing cells do not maintain HSCs through CXCL12 or SCF secretion. **a**, Flow cytometrically sorted bone marrow *Nestin*-GFP^{bright} cells express much lower levels of *Cxcl12* and *Scf* mRNA than bone marrow *Nestin*-GFP^{dim} cells as measured by quantitative PCR (n=3-4 independent biological replicates for each population; transcript levels were normalized to β -*actin* mRNA and bars represent expression level relative to unfractionated bone marrow cells (BM)). **b-c**, Deletion of *Cxcl12* using *NG2*-CreER had no effect on bone marrow or spleen HSC frequency (**b**) and no effect on bone marrow long-term competitive reconstitution (**c**). **d-e**, Deletion of *Scf* using *NG2*-CreER had no effect on bone marrow or spleen HSC frequency (**d**) and no effect on bone marrow long-term competitive reconstitution (**e**). Mice aged 4-6 weeks were injected intraperitoneally with tamoxifen (100 mg/kg) once daily for 5 consecutive days. After 4 weeks, mice were killed and analyzed for HSC frequency by flow cytometry. 3×10^5 bone marrow cells and an equal number of wild-type competitor cells were transplanted into lethally irradiated recipients for long-term competitive reconstitution assays (n=5-7 mice per genotype in 5-7 independent experiments; +, wild-type or floxed allele; -, null allele; Δ , recombined floxed allele).

THE NICHE FOR EXTRAMEDULLARY HEMATOPOIESIS IN THE SPLEEN

2.1 Summary

Adult hematopoietic stem cells (HSCs) reside primarily in bone marrow (Morrison and Scadden, 2014). However, hematopoietic stresses such as myelofibrosis (Abdel-Wahab and Levine, 2009), anemia (Bennett et al., 1968; Cheshier et al., 2007), pregnancy (Fowler and Nash, 1968; Nakada et al., 2014), infection (Baldrige et al., 2010; Burberry et al., 2014) or myeloablation (Morrison et al., 1997) can mobilize HSCs to the spleen and induce extramedullary hematopoiesis (EMH). While the bone marrow HSC niche has been studied intensively, the EMH niche has received little attention. Here, we systematically assessed the physiological sources of the key niche factors, SCF (Wolf, 1978) and CXCL12 (Kollet et al., 2003), in normal spleen and after EMH induction by cyclophosphamide plus granulocyte colony-stimulating factor (Morrison et al., 1997). *Scf* was expressed by endothelial cells and *Tcf21*⁺ perivascular stromal cells, primarily around sinusoids in red pulp, while *Cxcl12* was expressed by a subset of *Tcf21*⁺ stromal cells. EMH induction markedly expanded the *Scf*-expressing endothelial cells and stromal cells by inducing their proliferation. Deep imaging and digital reconstruction of optically cleared spleen found more than 80% of HSCs within 5 μ m of a *Tcf21*⁺ stromal cell in red pulp. Conditional deletion of *Scf* from spleen endothelial cells did not affect bone marrow hematopoiesis but severely impaired EMH, depleting HSCs and myeloid progenitors from the spleen. Conditional deletion of *Scf* or *Cxcl12* using *Tcf21*-CreER also did not affect bone marrow hematopoiesis but severely impaired EMH. Endothelial cells and *Tcf21*-expressing perivascular stromal cells in red pulp thus create the splenic niche for EMH.

2.2 Results and discussion

The hematopoietic system differs from many other tissues by employing facultative niches that change in response to injury. Adult hematopoiesis occurs primarily in the bone marrow of mammals. However, a wide range of hematopoietic stresses induce extramedullary hematopoiesis (EMH) in which hematopoietic stem cells (HSCs) are mobilized to sites outside the bone marrow to expand hematopoiesis (Johns and Christopher, 2012). While the spleen is known mainly as a secondary lymphoid organ in which lymphocytes are activated in the white pulp (Mueller and Germain, 2009), the splenic red pulp is a prominent site of EMH in mice and humans (Freedman and Saunders, 1981; Johns and Christopher, 2012; Lowell et al., 1996; Tavassoli and Weiss, 1973). During EMH, HSCs are found mainly around sinusoids in the red pulp, raising the possibility of a perisinusoidal niche (Kiel et al., 2005). CXCL12 expression has been observed in sinusoidal endothelial cells in red pulp of the human spleen (Miwa et al., 2013) and macrophage ablation reduces splenic erythropoiesis after irradiation (Chow et al., 2013). However, little else is known about the expression patterns of niche factors in the spleen or the sources of factors that promote EMH. A fundamental but largely unexplored question concerns the nature of the EMH niche and the changes that enable EMH in adult spleen.

HSCs are rare in normal adult spleen (Morita et al., 2011) but myeloablation with cyclophosphamide followed by daily administration of granulocyte colony-stimulating factor (G-CSF) induces HSC mobilization from the bone marrow to the spleen and induction of EMH (Morrison et al., 1997). We used this model to identify the sources of key niche factors for EMH in the adult mouse spleen. We distinguished red pulp from white pulp in spleen sections based on morphology and anti-Laminin antibody staining. White pulp contains a dense network of small-

diameter radial arterioles branching off central arterioles, whereas red pulp contains a loose network of large-diameter sinusoids (Cesta, 2006). Laminin staining was bright and continuous around arterioles but dim and fenestrated around sinusoids (Figure 2.5a and 2.5b). CD3⁺ T cells clustered in white pulp within regions of dense Laminin staining whereas Ter119⁺ erythroid progenitors clustered in red pulp with less Laminin staining (Figure 2.5a and 2.5b). Upon EMH induction by cyclophosphamide plus 21 days of G-CSF (Cy+21d G-CSF), erythropoiesis and myelopoiesis increased in the red pulp, increasing spleen size, spleen cellularity, HSC number, and erythroid and myeloid progenitor numbers in the spleen (Figure 2.5c-2.5j). Spleen B and T cell numbers did not significantly change (Figure 2.5k).

To characterize the EMH niche we first examined the *Scf* and *Cxcl12* expression patterns in spleen sections from *Scf*^{GFP/+}; *Cxcl12*^{DsRed/+} mice (Ding and Morrison, 2013; Ding et al., 2012). In normal adult spleens and after EMH induction by Cy+21d G-CSF, *Scf*-GFP and *Cxcl12*-DsRed were primarily expressed throughout the spleen red pulp (Figure 2.1a, 2.1b and Figure 2.5n, 2.5o). Red pulp endothelial cells and perivascular stromal cells expressed high levels of *Scf*-GFP, irrespective of EMH induction (Figure 2.1a-2.1c and Figure 2.5n, 2.5o). In white pulp, *Scf*-GFP was expressed by many fewer stromal cells and central arteriolar endothelial cells (Figure 2.1a, 2.1b and Figure 2.5n, 2.5o). Radial arteriolar endothelial cells in white pulp rarely expressed *Scf*-GFP (Figure 1b and Figure 2.5o). *Cxcl12*-DsRed was not expressed by endothelial cells but was expressed by a subset of *Scf*-GFP⁺ perivascular stromal cells, primarily around red pulp sinusoids but to a lesser extent around white pulp central arterioles (Figure 2.1a-2.1c and Figure 2.5n, 2.5o).

In normal adult spleen, *Scf*-GFP⁺ cells represented 0.48±0.10% (Figure 2.1d) and *Cxcl12*-DsRed⁺ represented 0.031±0.011% (Figure 2.1f) of enzymatically dissociated spleen cells. Most

Scf-GFP⁺ cells (75±5.8%) were VE-Cadherin⁺CD45⁻Ter119⁻ endothelial cells (Figure 2.1 e). Indeed, 85±8.2% of all VE-Cadherin⁺CD45⁻Ter119⁻ spleen endothelial cells were *Scf*-GFP⁺ and none expressed *Cxcl12*-DsRed (Figure 2.1 e). Non-endothelial *Scf*-GFP⁺ cells were virtually all PDGFRβ⁺CD45⁻Ter119⁻ stromal cells (Figure 2.1 d). A minority of *Scf*-GFP⁺ stromal cells (22±3.8%) also expressed *Cxcl12*-DsRed (Figure 2.1 d) while virtually all *Cxcl12*-DsRed⁺ stromal cells expressed *Scf*-GFP (Figure 2.1 f). Therefore, in adult spleen *Scf* is expressed by VE-Cadherin⁺ endothelial cells and PDGFRβ⁺ stromal cells while *Cxcl12* is expressed by a minority of the *Scf*-expressing stromal cells, primarily around red pulp sinusoids.

EMH induction did not appear to alter spleen *Scf*-GFP or *Cxcl12*-DsRed expression patterns (see Figure 2.1 a versus Figure 2.5n). Flow cytometric analysis showed no change in GFP or DsRed fluorescence intensity of individual *Scf*-GFP or *Cxcl12*-DsRed expressing spleen cells after EMH induction (Figure 2.5l and 2.5m). However, the frequencies and absolute numbers of *Scf*-GFP and *Cxcl12*-DsRed cells increased significantly upon EMH induction (Figure 2.1 g-2.1l). *Scf*-GFP⁺ endothelial cells and perivascular stromal cell frequencies approximately doubled (Figure 2.1 k) and their absolute numbers increased at least 6-fold (Figure 2.1 l). *Scf*-GFP⁺VE-Cadherin⁺ endothelial cells, *Scf*-GFP⁺VE-Cadherin⁻ stromal cells, and *Cxcl12*-DsRed⁺ stromal cells rarely divided in normal adult spleen but all proliferated during the first 7 days of G-CSF administration when EMH was induced (Figure 2.1 m and 2.1n). This suggests that niche cell expansion facilitates increases in spleen HSC frequency (Figure 2.5g) and hematopoiesis (Figure 2.5h-2.5j) after EMH induction.

LepR⁺ stromal cells are the main sources of *Scf* and *Cxcl12* for HSC maintenance in the bone marrow (Ding and Morrison, 2013; Ding et al., 2012; Zhou et al., 2014). In the spleens of *Lepr-cre; tdTomato* mice, Tomato was expressed mainly in white pulp where HSCs are not

observed (Kiel et al., 2005). A few Tomato⁺ stromal cells were present around red pulp arteries and arterioles (Figure 2.6a). Only about 20% of *Scf*-GFP⁺ stromal cells expressed LepR (Figure 2.6b). LepR⁺ cells were VE-Cadherin⁻ (Figure 2.6b) and PDGFRβ⁺ (Figure 2.6c) stromal cells that accounted for 37±13% of the CFU-F formed by enzymatically dissociated spleen cells (Figure 2.6d).

Consistent with our prior study (Ding et al., 2012), young adult *Lepr-cre; Scf^{fl/-}* mice exhibited a significant decrease in the frequency of CD150⁺CD48⁻LSK HSCs in the bone marrow and a significant increase in spleen cellularity relative to *Scf^{+/-}* and *Scf^{+/+}* controls (Figure 2.6e and 2.6f). However, upon EMH induction by Cy+4d G-CSF, *Lepr-cre; Scf^{fl/-}* mice exhibited significant declines in spleen cellularity and spleen HSC number relative to *Scf^{+/-}* and *Scf^{+/+}* (Figure 2.6f and 2.6g). LepR⁺ perivascular stromal cells could, therefore, contribute to the EMH niche in adult spleen; however, this may also reflect the depletion of HSCs in the bone marrow (Figure 2.6e) prior to EMH induction.

To identify Cre alleles that recombine in spleen, but not bone marrow, stromal cells we assessed the gene expression profile of spleen *Scf*-GFP⁺VE-Cadherin⁻ stromal cells (Table 2.1). *Nestin*, *NG2* (*Cspg4*), and *Prx1* were expressed at low or undetectable levels (data not shown). *Nestin*-Cre (Tronche et al., 1999), *NG2*-Cre (Zhu et al., 2008), *NG2*-CreER (Zhu et al., 2011), and *Prx1*-Cre (Logan et al., 2002) did not recombine widely or specifically in *Scf*-GFP⁺ stromal cells in the spleen (data not shown). *Pdgfra* and *Pdgfrb* were both expressed by spleen *Scf*-GFP⁺ stromal cells but neither *Pdgfra*-CreER (Rivers et al., 2008) nor *Pdgfrb*-Cre (Cutler et al., 2011) recombined efficiently in these cells (data not shown). *Sm22* (*Tagln*), *Myh11*, *Sma* (*Acta2*), and *Tcf21* were significantly more highly expressed by spleen than bone marrow *Scf*-GFP⁺ stromal cells (Table 2.1). However, *Sm22*-Cre (Holtwick et al., 2002), *Myh11*-Cre (Xin et al., 2002), and

Sma-CreER (Wendling et al., 2009) recombined in few spleen *Scf*-GFP⁺ stromal cells (data not shown). None of these Cre alleles could be used to analyze the spleen EMH niche.

Tcf21-CreER (Acharya et al., 2011) recombined efficiently in spleen *Scf*-GFP⁺ stromal cells (Figure 2.2a) but not in bone marrow at all (Figure 2.2b and Figure 2.7a). *Tcf21-creER*; *tdTomato* mice that were gavaged with tamoxifen for 12 days at 4-6 weeks of age expressed Tomato in *Scf*-GFP⁺ stromal cells throughout red pulp (Figure 2.2a and 2.2c) but only in rare cells in white pulp (Figure 2.2a) and not in VE-Cadherin⁺ endothelial cells (Figure 2.2c and 2.2d). The *Tcf21*-CreER recombination pattern was similar after induction of EMH (Figure 2.7b). By flow cytometry, 85% of *Scf*-GFP⁺ stromal cells were positive for Tomato (Figure 2.2d). Tomato⁺CD45⁻Ter119⁻ stromal cells from enzymatically dissociated *Tcf21-creER*; *tdTomato* spleens accounted for 0.085±0.045% of spleen cells and 69±2% of spleen CFU-F (Figure 2.2e and 2.2f). These cells were uniformly positive for PDGFR α , PDGFR β , and Sca-1 but negative for LepR (Figure 2.2e).

We examined the localization of HSCs and c-kit⁺ hematopoietic progenitors in the spleen relative to *Tcf21*-CreER-expressing cells. c-kit⁺ hematopoietic progenitors were almost exclusively within red pulp in the normal spleen (Figure 2.7c) and after EMH induction (Figure 2.2j). We previously showed that CD150⁺CD48⁻Lineage⁻ HSCs localized adjacent to red pulp sinusoids in spleens with EMH (Kiel et al., 2005). A limitation of imaging rare HSCs in tissue sections is that only small numbers of HSCs can be localized. To assess larger numbers of HSCs, we used a new technique that permits deep-imaging of α -catulin-GFP⁺c-kit⁺ HSCs in optically cleared hematopoietic tissues (Acar et al., 2015). α -catulin is highly restricted in its expression to HSCs in the bone marrow, where 1 in 3 α -catulin-GFP⁺c-kit⁺ cells give long-term multilineage reconstitution of irradiated mice (Acar et al., 2015). In the spleens of mice treated with Cy+4d G-

CSF, only $0.011 \pm 0.002\%$ of splenocytes were α -catulin-GFP⁺c-kit⁺ (Figure 2.2g). In competitive reconstitution assays, all long-term multilineage reconstituting cells in the spleen were α -catulin-GFP⁺, and 1 in 3.6 α -catulin-GFP⁺c-kit⁺ spleen cells gave long-term multilineage reconstitution (Figure 2.2h). These cells also gave long-term multilineage reconstitution in secondary recipient mice (data not shown). This level of purity is similar to the best markers available.

After antibody staining of a large segment of *Tcf21-creER; tdTomato; a-catulin*^{GFP/+} spleen, we cleared the tissue (Figure 2.7d) then used confocal microscopy to acquire tiled, Z-stacked optical sections to a depth of 300 μ m and digitally reconstructed the tissue (Video 1). *a-catulin*-GFP⁺c-kit⁺ HSCs were found exclusively within the red pulp, where 49% were immediately adjacent to Tomato⁺ stromal cells and 81% were within 5 μ m (Figure 2.2i and 2.2j). By comparison, only 12% and 44% of random spots were immediately adjacent to Tomato⁺ stromal cells or within 5 μ m, respectively (Figure 2.2i). HSCs thus localize adjacent to *Tcf21*-CreER-expressing stromal cells associated with sinusoids in the red pulp of the spleen.

To test if *Tcf21*-CreER-expressing perivascular cells are an important source of SCF for EMH, we treated *Tcf21-creER; Scf*^{f/f} and littermate control mice with tamoxifen for 12 days at 4-6 weeks of age. A month later, bone marrow and spleen cellularity, blood cell counts, and bone marrow hematopoiesis were normal in *Tcf21-creER; Scf*^{f/f} mice relative to littermate controls (Figure 2.3a-2.3g and Figure 2.8a-2.8f). Then we treated *Tcf21-creER; Scf*^{f/f} mice and littermate controls with cyclophosphamide followed by 4, 8, or 21 days of G-CSF. Relative to littermate controls, *Tcf21-creER; Scf*^{f/f} mice had significantly reduced spleen cellularity (Figure 2.3a) and significantly reduced numbers of spleen CD150⁺CD48⁻Lineage⁻Sca-1⁺c-kit⁺ HSCs (Figure 2.3b), common myeloid progenitors (CMPs (Akashi et al., 2000); Figure 2.3c), granulocyte-monocyte progenitors (GMPs (Akashi et al., 2000); Figure 2.3d) and megakaryocyte-erythroid progenitors

(MEPs (Akashi et al., 2000); Figure 2.3e) after 8 to 21 days of G-CSF treatment. *Tcf21-creER*; *Scf^{fl/fl}* mice did not differ from controls with respect to bone marrow cellularity or the numbers of HSCs, CMPs, GMPs, or MEPs in the bone marrow, irrespective of Cy+G-CSF treatment (Figure 2.3f and 2.3g and Figure 2.8d-2.8f). Consistent with the reduced spleen EMH, *Tcf21-creER*; *Scf^{fl/fl}* mice had significantly reduced white blood cell, red blood cell, and platelet counts after 8 to 21 days of G-CSF treatment (Figure 2.8a-2.8c). Conditional deletion of *Scf* in *Tcf21-CreER*-expressing stromal cells thus depletes HSCs and reduces EMH in the spleen without affecting bone marrow HSC number or hematopoiesis.

We also conditionally deleted *Cxcl12* from *Tcf21-CreER*-expressing cells. Bone marrow and spleen cellularity, blood cell counts, and bone marrow hematopoiesis were normal in *Tcf21-creER*; *Cxcl12^{fl/-}* mice relative to littermate controls (Figure 2.3h-2.3n and Figure 2.8j-2.8l). Then we treated *Tcf21-creER*; *Cxcl12^{fl/-}* mice and littermate controls with Cy+G-CSF. Relative to *Cxcl12^{+/-}* or *Cxcl12^{fl/-}* controls, *Tcf21-creER*; *Cxcl12^{fl/-}* mice exhibited significantly reduced spleen cellularity (Figure 2.3h) and significantly reduced numbers of spleen CMPs (Figure 2.3j), GMPs (Figure 2.3k), and MEPs (Figure 2.3l) after 8 to 21 days of G-CSF treatment. In bone marrow, *Tcf21-creER*; *Cxcl12^{fl/-}* mice had normal cellularity and normal numbers of CMPs, GMPs, and MEPs (Figure 2.8m, 2.8j-2.8l). Although the number of HSCs in the spleens of *Tcf21-creER*; *Cxcl12^{fl/-}* mice did not significantly differ from littermate controls (Figure 2.3i), HSC numbers were significantly elevated in the blood and in the bone marrow of *Tcf21-creER*; *Cxcl12^{fl/-}* mice after 21 days of G-CSF treatment (Figure 2.3n and 2.3o). This suggests that some HSCs were mobilized from the spleens of *Tcf21-creER*; *Cxcl12^{fl/-}* mice. *Tcf21-creER*; *Cxcl12^{fl/-}* mice also had significantly reduced red blood cell counts after 21 days of G-CSF treatment

(Figure 2.8g-2.8i). *Tcf21*-CreER-expressing stromal cells are thus an important source of CXCL12 for EMH in the spleen without reducing bone marrow HSC number or hematopoiesis.

To test the significance of SCF expression by spleen endothelial cells we sought a Cre allele that would recombine in spleen but not bone marrow endothelium. Although *Vav1*-Cre is best known for its ability to recombine in hematopoietic cells (de Boer et al., 2003), we discovered it also recombines efficiently in spleen but not bone marrow endothelial cells. *Vav1-cre; tdTomato* mice exhibited Tomato expression throughout the red pulp that overlapped with VE-Cadherin staining and rare recombined cells in the white pulp (Figure 2.4a and 2.4b). Tomato⁺CD45⁻Ter119⁻ cells from *Vav1-cre; tdTomato* spleens accounted for 0.35±0.05% of enzymatically dissociated spleen cells and were uniformly positive for VE-Cadherin but uniformly negative for PDGFRβ (Figure 2.4c). 70±5% of VE-Cadherin⁺ spleen endothelial cells were Tomato⁺ in *Vav1-cre; tdTomato* mice but only 8.4±0.5% were Tomato⁺ in the bone marrow (Figure 2.4d). *Vav1*-Cre thus recombined efficiently in spleen endothelial cells but not spleen stromal cells or bone marrow endothelial cells.

Cxcl12 was not expressed by spleen endothelial cells (Figure 2.1e). Consistent with this, *Vav1-cre; Cxcl12^{fl/-}* mice had normal blood counts, cellularity, and numbers of HSCs, CMPs, GMPs, and MEPs in bone marrow and spleen after Cy+G-CSF (Figure 2.9a-2.9m).

Although *Vav1*-Cre recombines in hematopoietic cells (de Boer et al., 2003), hematopoietic cells do not express *Scf* and *Vav1-cre; Scf^{fl/-}* mice have normal HSC frequency, HSC function, and hematopoiesis in bone marrow (Ding and Morrison, 2013; Ding et al., 2012). *Scf* transcript levels in spleen endothelial cells from *Vav1-cre; Scf^{fl/-}* mice were only at 14±6% of control levels (Figure 2.4e). Prior to EMH induction with Cy+G-CSF, *Vav1-cre; Scf^{fl/-}* mice did not significantly differ from *Scf^{fl/-}* controls with respect to bone marrow or spleen cellularity, or

the numbers of HSCs, CMPs, GMPs, or MEPs in the bone marrow or spleen (Figure 2.4f-2.4l and Figure 2.9q-2.9s). However, when we induced EMH we observed significant declines in spleen cellularity and the numbers of spleen HSCs, CMPs, GMPs, and MEPs in *Vav1-cre; Scf^{fl/-}* mice relative to littermate controls after 4 to 21 days of G-CSF treatment (Figure 2.4f-2.4j). *Vav1-cre; Scf^{fl/-}* mice did not significantly differ from *Scf^{fl/-}* controls with respect to bone marrow cellularity or the numbers of bone marrow HSCs, CMPs, GMPs, or MEPs irrespective of Cy+G-CSF treatment (Figure 2.4k, 2.4l and Figure 2.9q-2.9s). Consistent with reduced spleen EMH, *Vav1-cre; Scf^{fl/-}* mice had significantly reduced red blood cell counts relative to *Scf^{fl/-}* controls (Figure 2.9n-2.9p). Conditional deletion of *Scf* from spleen endothelial cells thus depletes HSCs and reduces EMH in the spleen without significantly affecting bone marrow HSC number or hematopoiesis.

Our data demonstrate that the EMH niche in mouse spleen is created by endothelial cells and *Tcf21*-expressing stromal cells associated with red pulp sinusoids, providing an explanation for the long-standing observation that EMH occurs around red pulp sinusoids. These SCF and CXCL12-expressing cells are present in normal adult spleen but are largely quiescent. Upon induction of EMH by cyclophosphamide/G-CSF, both niche cell types are induced to proliferate and markedly expand in number. The companion study from Grunewald et al. (submitted) demonstrates that VEGF over-expression in adult liver is sufficient to induce EMH in the liver and spleen, partly by expanding mesenchymal stromal cells in the spleen - likely the *Tcf21*-expressing cells we identified. Grunewald et al. further demonstrate that G-CSF-induced EMH depends upon VEGF expression, suggesting that VEGF is a key physiological signal for EMH induction and splenic niche cell expansion. Together these studies characterize both the nature of the EMH niche and the molecular signals that induce EMH in adult mammals.

2.3 Methods

Mice

All mice were maintained on a C57BL/6 background, including *Scf*^{GFP/+} (Ding et al., 2012), *Scf*^{fl/+} (Ding et al., 2012), *Cxcl12*^{DsRed/+} (Ding and Morrison, 2013), *Cxcl12*^{fl/+} (Ding and Morrison, 2013), *Rosa26-tdTomato* (Madisen et al., 2010), *Vav1-cre* (de Boer et al., 2003), *Lepr-cre* (DeFalco et al., 2001), *Tcf21-creER* (Acharya et al., 2011) and *α-catulin*^{GFP/+}. To induce CreER activity in *Tcf21-creER* mice, 4-6-week-old mice were administered 2 mg tamoxifen (Sigma) daily by oral gavage for 12 consecutive days. For induction of EMH, mice were injected at day 0 with a single dose of 4 mg cyclophosphamide followed by daily injections of 5 μg G-CSF for 4 to 21 days. Both male and female mice were used in these studies. All mice were housed in the Animal Resource Center at the University of Texas Southwestern Medical Center (UTSW). All procedures were approved by the UTSW Institutional Animal Care and Use Committee.

Flow cytometric analysis of hematopoietic cells

Bone marrow cells were isolated by flushing the femur or tibia with Ca²⁺ and Mg²⁺ free HBSS with 2% heat-inactivated bovine serum using a 3 ml syringe fitted with a 25-gauge needle. Spleen cells were obtained by crushing the spleen between two frosted slides. The cells were dissociated to a single cell suspension by gently passing through the needle several times and then filtering through a 40 μm nylon mesh. Blood was collected by cardiac puncture, and white blood cells were isolated by ficoll centrifugation according to the manufacturer's instructions (GE Healthcare). The following antibodies were used to isolate HSCs: anti-CD150 (TC15-

12F12.2), anti-CD48 (HM48-1), anti-Sca-1 (E13-161.7), anti-c-kit (2B8) and the following antibodies against lineage markers (anti-Ter119, anti-B220 (6B2), anti-Gr1 (8C5), anti-CD2 (RM2-5), anti-CD3 (17A2), anti-CD5 (53-7.3) and anti-CD8 (53-6.7)). Hematopoietic progenitors were identified by flow cytometry using the following antibodies: anti-Sca-1 (E13-161.7), anti-c-kit (2B8) and the following antibodies against lineage markers (anti-Ter119, anti-B220 (6B2), anti-Gr1 (8C5), anti-CD2 (RM2-5), anti-CD3 (17A2), anti-CD5 (53-7.3) and anti-CD8 (53-6.7)), anti-CD34 (RAM34), anti-CD135 (Flt3) (A2F10), anti-CD16/32 (FcγR) (93), anti-CD127 (IL7Rα) (A7R34), anti-CD24 (M1/69), anti-CD43 (1B11), anti-B220 (6B2), anti-IgM (II/41), anti-CD3 (17A2), anti-Gr-1 (8C5), anti-Mac-1 (M1/70), anti-CD41 (MWRReg30), anti-CD71 (C2) and anti-Ter119. DAPI was used to exclude dead cells. Antibodies were obtained from eBioscience or BD Bioscience.

Flow cytometric analysis of stromal cells

To isolate bone marrow stromal cells the marrow was gently flushed out of the bone marrow cavity with a 3-ml syringe fitted with a 23-gauge needle and then transferred into 1 ml pre-warmed bone marrow digestion solution (200 U/ml DNase I (Sigma), 250 µg/ml Liberase^{DL} (Roche) in HBSS plus Ca²⁺ and Mg²⁺) and incubated at 37°C for 30 minutes with gentle shaking. To isolate splenic stromal cells, the spleen capsule was cut into ~1 mm³ fragments using scissors and then digested as above in spleen digestion solution (200 U/ml DNase I, 250 µg/ml Liberase^{DL}, 1 mg/ml Collagenase, type 4 (Roche) and 500 µg/ml Collagenase D (Roche) in HBSS plus Ca²⁺ and Mg²⁺). After a brief vortex, the spleen fragments were allowed to sediment for ~3 minutes and the supernatant was transferred to another tube on ice. The sedimented (undigested) spleen fragments were subjected to a second round of digestion. The two fractions

of digested cells were pooled and filtered through a 100 µm nylon mesh. Anti-PDGFR α (APA5), anti-PDGFR β (APB5), anti-LepR (R&D), anti-CD45 (30F-11) and anti-Ter119 antibodies were used to isolate stromal cells. For analysis of endothelial cells, mice were injected intravenously into the retro-orbital venous sinus with 10 µg Alexa Fluor 660 conjugated anti-VE-Cadherin antibody (BV13) 10 minutes before sacrifice. Samples were analyzed using a FACS Aria or FACSCanto II flow cytometer (BD Biosciences).

5-bromo-2'-deoxyuridine (BrdU) incorporation assay

To assess BrdU incorporation into spleen cells after EMH induction, mice were intraperitoneally injected with a single dose of BrdU (2mg BrdU/per mouse) then maintained on 0.5mg BrdU/ml drinking water for seven days. Endothelial cells were labeled by intravenous injection of an anti-VE-Cadherin antibody (eBioscience). Enzymatically dissociated spleen cells were stained with antibodies against surface markers and the target cell populations were sorted then resorted to ensure purity. The sorted cells were then fixed, and stained with an anti-BrdU antibody using the BrdU APC Flow Kit (BD Biosciences) according to the manufacturer's instructions.

Long-term competitive reconstitution assay

Adult recipient mice were irradiated using an XRAD 320 x-ray irradiator (Precision X-Ray Inc.) with two doses of 540 rad (total 1080 rad) delivered at least 2 hours apart. Cells were injected into the retro-orbital venous sinus of anesthetized mice. Sorted doses of splenocytes from donor mice with EMH were transplanted along with 3×10^5 recipient bone marrow cells. Recipient mice were bled every 4 weeks to assess the level of donor-derived blood cells, including myeloid, B and T cells for at least 16 weeks. Blood was subjected to ammonium chloride/potassium red cell

lysis before antibody staining. Antibodies including anti-CD45.2 (104), anti-CD45.1 (A20), anti-Gr1 (8C5), anti-Mac-1 (M1/70), anti-B220 (6B2), and anti-CD3 (KT31.1) were used for flow cytometric analysis.

Tissue sectioning and confocal imaging

For bone marrow sections, freshly dissected bones were fixed in 4% paraformaldehyde overnight followed by 3 days of decalcification in 10% EDTA dissolved in PBS. Bones were sectioned using the CryoJane tape-transfer system (Instrumedics). For spleen sections, freshly dissected spleens were fixed in 4% paraformaldehyde for 1 hour followed by 1 day incubation in 10% Sucrose in PBS. Frozen spleens were sectioned with a cryostat (Leica). For whole mount imaging, spleens were sectioned into ~2 mm pieces. Spleen sections were blocked in PBS with 10% horse serum for 1 hour and then stained overnight with chicken-anti-GFP (Aves), and/or rabbit-anti-Laminin (Abcam) antibodies. Donkey-anti-chicken Alexa Fluor 488 and/or Donkey-anti-rabbit Alexa Fluor 647 were used as secondary antibodies (Invitrogen). Specimens were mounted with anti-fade prolong gold (Invitrogen) and images were acquired with either a Zeiss LSM780 confocal microscope or a Leica SP8 confocal microscope equipped with a resonant scanner. Three dimensional images were achieved using Bitplane Imaris v7.7.1 software.

Deep imaging of spleens

Spleens were harvested and fixed for 4 hours in 4% PFA at 4°C. Since the Spleen capsule is highly autofluorescent, spleens were sectioned perpendicular to the long axis into 300 µm thick sections using a Leica VT100S vibrotome. These 300 µm sections were fixed for an additional 2 hours in 4% PFA and blocked overnight in staining solution (10% DMSO, 0.5% IgePal630

(Sigma), and 5% donkey serum (Jackson ImmunoResearch) in PBS). All staining steps were performed in staining solution on a rotator at room temperature. Spleen sections were stained for three days in primary antibodies, washed overnight in several changes of PBS then stained for three days in secondary antibodies. The stained sections were dehydrated in a methanol dehydration series then incubated for 3 hours in 100% methanol with several changes. The methanol was then exchanged with benzyl alcohol:benzyl benzoate 1:2 mix (BABB clearing (Becker et al., 2013)). The tissues were incubated in BABB for 3 hours to overnight with several exchanges of fresh BABB. Spleen sections were mounted in BABB between two cover slips and sealed with silicone (Premium waterproof silicone II clear, General Electric). We found it necessary to clean the BABB of peroxides (which can accumulate as a result of exposure to air and light) by adding 10 g of activated aluminum oxide (Sigma) to 40ml of BABB and rotating for at least 1 hour, then centrifuging at 2000xg for 10 minutes to remove the suspended aluminum oxide particles. Images were acquired using a Zeiss LSM780 confocal microscope with a Zeiss LD LCI Plan-Apo 25x/0.8 multi-immersion objective lens, which has a 570 μm working distance. Images were taken at 512x512 pixel resolution with 2 μm Z-steps, pinhole for the internal detector at 47.7 μm . Random spots were inserted into images by generating randomized X, Y, and Z coordinates using the random integer generator at www.random.org.

Quantitative real-time PCR

Cells were sorted directly into Trizol (Life Technologies). Total RNA was extracted according to the manufacturer's instructions. Total RNA was reverse transcribed using SuperScript III Reverse Transcriptase (Life Technologies). Quantitative real-time PCR was performed using SYBR green on a LightCycler 480 (Roche). *β -actin* was used to normalize the RNA content of

samples. Primers used in this study were *Scf*: 5'-GCCAGAACTAGATCCTTTACTCCTGA-3' and 5'-CATAAATGGTTTTGTGACACTGACTCTG-3'; *β -actin*: 5'-GCTCTTTTCCAGCCTTCCTT-3'; and 5'-CTTCTGCATCCTGTCAGCAA-3'.

Gene expression profiling

Three independent samples of 5,000 spleen *Scf*-GFP⁺VE-Cadherin⁻ spleen stromal cells and two independent samples of 5,000 unfractionated spleen cells were flow cytometrically sorted into Trizol. Total RNA was extracted, amplified, and sense strand cDNA was generated using the Ovation Pico WTA System V2 (NuGEN) according to the manufacturer's instructions. cDNA was fragmented and biotinylated using the Encore Biotin Module (NuGEN) according to the manufacturer's instructions. Labeled cDNA was hybridized to Affymetrix Mouse Gene ST 1.0 chips according to the manufacturer's instructions. Expression values for all probes were normalized and determined using the robust multi-array average (RMA) method (Irizarry et al., 2003).

Statistical methods

Panels in all figures represented multiple independent experiments performed on different days with different mice. Sample sizes were not based on power calculations. No randomization or blinding was performed. No animals were excluded from analysis. Variation is always indicated using standard deviation. For analysis of the statistical significance of differences between two groups we generally performed two-tailed Student's *t*-tests. For analysis of the statistical significance of differences among three groups, we performed Repeated Measures one-way

ANOVAs with Greenhouse-Geisser correction (variances between groups were not equal) and Tukey's multiple comparison tests with individual variances computed for each comparison.

2.4 Author contributions

I initiated the project, designed experiments, characterized spleen niche factor expression patterns, tested and discovered Cre recombination patterns, and performed most experiments, including all functional analyses of *Scf* and *Cxcl12*. Bo Zhou characterized marker expression of spleen stromal cells and spleen stromal cell dynamics during EMH. Melih Acar generated and characterized the α -catulin^{GFP/+} mice. Malea Murphy analyzed HSC localization in the spleen. Zhiyu Zhao performed statistical analyses. I wrote this section with Bo Zhou and Sean Morrison. This section was submitted to *Nature* in modified form as:

Inra, C.N., Zhou, B.O., Acar, M., Murphy, M.M., Zhao, Z., and Morrison, S.J. (2015). The niche for extramedullary hematopoiesis in the spleen. *Nature Submitted*.

2.5 Figures, table, and video

Table 2.1. Genes that are significantly (>8-fold and P<0.015) more highly expressed by *Scf*-GFP⁺ stromal cells in spleen as compared to the bone marrow. Data show mean±s.d. for log₂ transformed expression values (n=3 independent samples/cell population). Maximal background expression was considered to be 6.6 (log₂(100)); all expression values below this threshold were set to 6.6 for purposes of calculating fold-change. Two-tailed Student's t-tests were used to assess statistical significance. Data for bone marrow *Scf*-GFP⁺ stromal cells are from (Ding et al., 2012).

Gene	Gene name	Unigene	Spleen <i>Scf</i> - GFP ⁺	BM <i>Scf</i> - GFP ⁺	Fold change
<i>Coch</i>	Coagulation factor C homolog	Mm.21325	12.1±0.3	6.6±0.0	45.4
<i>Ccl21a</i>	Chemokine (C-C motif) ligand 21A	Mm.45881 5	12.5±0.1	7.1±0.4	41.1
<i>Acta2</i>	Actin, alpha 2, smooth muscle, aorta	Mm.21302 5	11.9±0.3	6.7±0.1	35.2
<i>Cxcl13</i>	Chemokine (C-X-C motif) ligand 13	Mm.10116	11.8±0.3	6.8±0.2	30.3
<i>Tcf21</i>	Transcription factor 21	Mm.16497	11.3±0.6	6.6±0.0	25.9
<i>Clca1</i>	Chloride channel calcium activated 1	Mm.45455 3	11.1±0.3	6.6±0.0	22.5
<i>Ifi2712a</i>	Interferon, alpha-inducible protein 27 like 2A	Mm.27127 5	11.3±0.2	7.2±0.4	16.6
<i>Pln</i>	Phospholamban	Mm.34145	10.7±0.1	6.6±0.0	16.3
<i>Parm1</i>	Prostate androgen-regulated mucin-like 1	Mm.5002	10.8±0.3	6.8±0.1	16.0
<i>Fn1</i>	Fibronectin 1	Mm.19309	10.7±0.4	6.8±0.2	14.9

		9				
<i>Col14a1</i>	Collagen, type XIV, alpha 1	Mm.29785	9	10.4±0.2	6.7±0.1	12.6
<i>Nr4a1</i>	Nuclear receptor subfamily 4, group A, 1	Mm.119		10.5±0.6	7.0±0.3	11.2
<i>Agtr1a</i>	Angiotensin II receptor, type 1a	Mm.35062		10.7±0.7	7.3±0.6	11.0
<i>Fos</i>	FBJ osteosarcoma oncogene	Mm.24651	3	11.4±0.4	8.0±0.4	10.7
<i>Atp1b2</i>	ATPase, Na ⁺ /K ⁺ transporter, beta 2	Mm.23520	4	10.6±0.2	7.2±0.2	10.6
<i>Tnxb</i>	Tenascin XB	Mm.29052	7	9.9±0.5	6.6±0.0	9.5
<i>Myh11</i>	Myosin, heavy polypeptide 11, smooth muscle	Mm.25070	5	10.7±0.7	7.5±0.2	9.4
<i>Hspb1</i>	Heat shock protein 1	Mm.13849		10.8±0.7	7.6±0.2	9.3
<i>Clca2</i>	Chloride channel calcium activated 2	Mm.20897		9.8±0.4	6.6±0.0	8.8
<i>Tagln</i>	Transgelin	Mm.28328	3	10.4±0.5	7.3±0.9	8.6
<i>Nr2f2</i>	Nuclear receptor subfamily 2, group F, 2	Mm.15814	3	10.7±0.3	7.6±0.3	8.5
<i>Mustn1</i>	Musculoskeletal, embryonic nuclear protein 1	Mm.22089	5	10.8±0.5	7.7±0.7	8.2
<i>Aspn</i>	Asporin	Mm.38321	6	9.7±0.6	6.6±0.0	8.2

<i>Sparcl1</i>	SPARC-like 1	Mm.29027	12.1±0.1	9.1±0.4	8.1
----------------	--------------	----------	----------	---------	-----

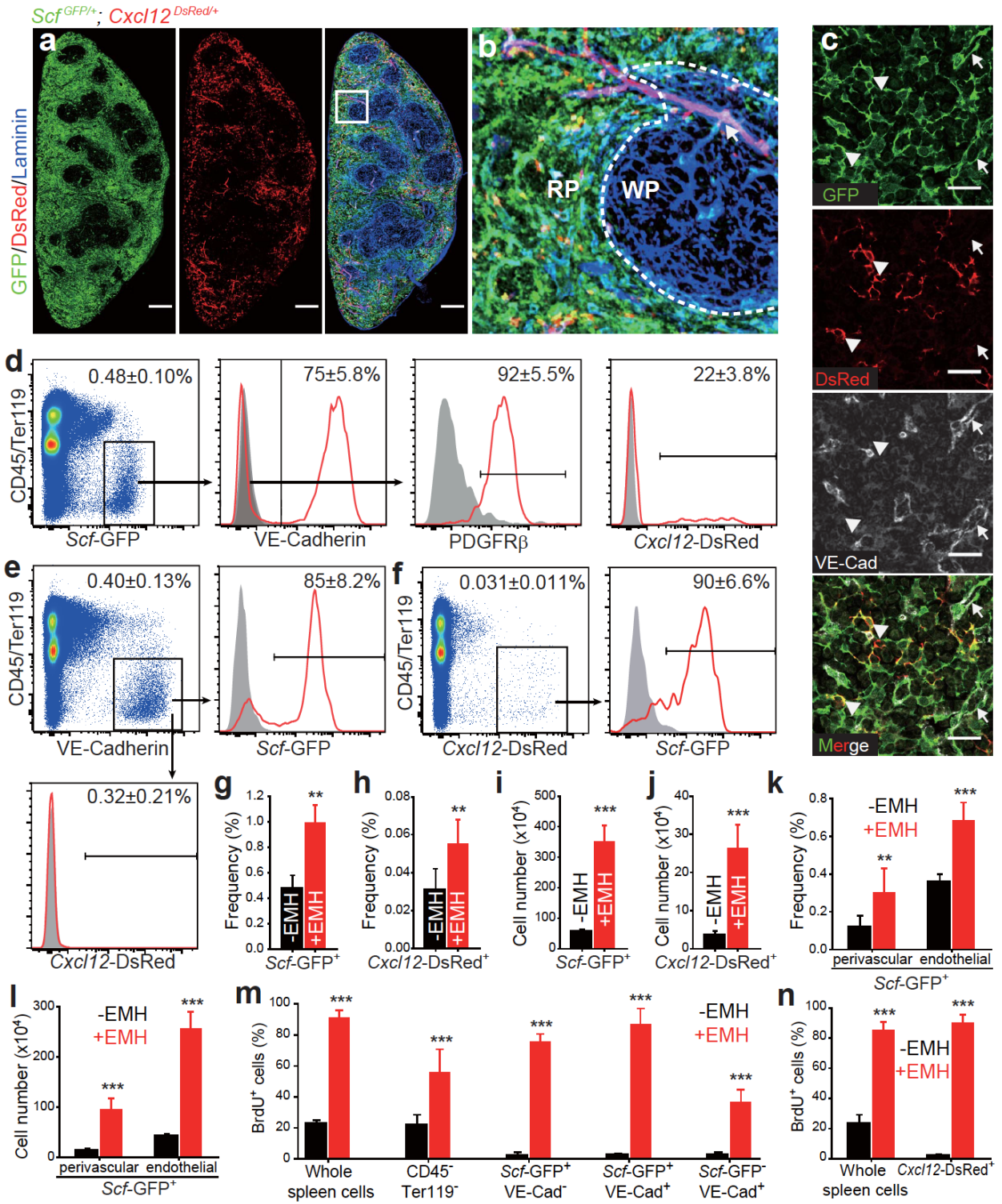


Figure 2.1. Endothelial cells and perivascular stromal cells in the red pulp express *Scf* and *Cxcl12* in the spleen and proliferate upon induction of EMH. a, b, *Scf*-GFP and *Cxcl12*-DsRed were mainly expressed by stromal cells in the red pulp of normal spleens. (b) High-magnification view of the boxed area in (a). Dashed lines depict the boundary between white pulp and red pulp. Arrow indicates central arteriole in the white pulp, around which rare stromal cells expressed *Cxcl12*-DsRed. Scale bar=400 μ m. c, Confocal imaging of red pulp in spleen from *Scf*^{GFP/+}; *Cxcl12*^{DsRed/+} mice showed that VE-Cadherin⁺ endothelial cells (arrows) expressed *Scf*-GFP while VE-Cadherin⁻ stromal cells (arrowheads) expressed *Scf*-GFP and sometimes *Cxcl12*-DsRed. Scale bar=25 μ m (representative images from 3 mice in 3 independent experiments). d-f, Flow cytometric analysis of enzymatically dissociated normal spleen cells from *Scf*^{GFP/+}; *Cxcl12*^{DsRed/+} mice. *Scf*-GFP was expressed by VE-Cadherin⁺ endothelial cells and PDGFR β ⁺ stromal cells, a subset of which also expressed *Cxcl12*-DsRed (d). Most VE-Cadherin⁺ endothelial cells were positive for *Scf*-GFP but negative for *Cxcl12*-DsRed (e). Most *Cxcl12*-DsRed⁺ cells were positive for *Scf*-GFP (f). Data represent mean \pm s.d. from 3 mice from 3 independent experiments. g-l, The frequencies (g,i, and k) and absolute numbers (h,j, and l) of *Scf*-GFP⁺ cells (g, h), *Cxcl12*-DsRed⁺ cells (i, j), *Scf*-GFP⁺VE-Cadherin⁺ endothelial cells and *Scf*-GFP⁺VE-Cadherin⁻ stromal cells (k, l) all significantly increased upon induction of EMH by Cy+21d G-CSF (+EMH) (n=5 *Scf*^{GFP/+} mice and 4 *Cxcl12*^{DsRed/+} mice from 3 independent experiments). m, n, BrdU was co-administered to *Scf*^{GFP/+} mice (m) or *Cxcl12*^{DsRed/+} mice (n) along with G-CSF for 7 days after cyclophosphamide treatment. Endothelial and stromal cells in normal adult spleen were largely quiescent but proliferated after cyclophosphamide/G-CSF treatment. Data represent 3 mice/genotype/condition from 2 independent experiments. Two-tailed student's t-tests were used to assess statistical significance (P<0.01, ***P<0.001).**

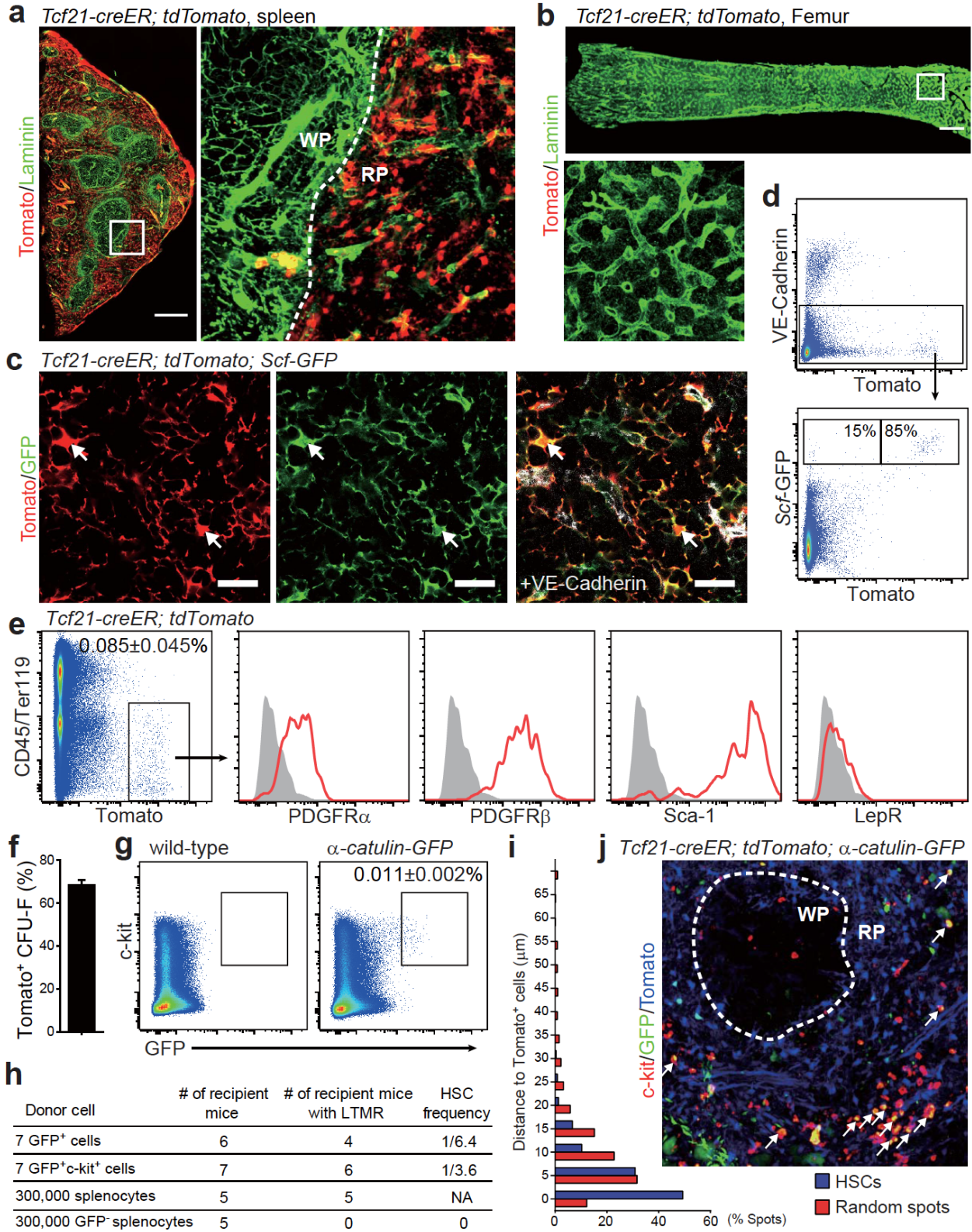


Figure 2.2. During EMH most HSCs localize adjacent to *Tcf21*⁺ stromal cells in the red pulp. **a**, Tamoxifen-treated adult *Tcf21-creER; tdTomato* mice exhibited widespread Tomato expression by perivascular stromal cells in the red pulp of the spleen. The dashed line depicts the boundary between white pulp (WP) and red pulp (RP). Scale bar=400 μ m (n=4 mice from 4 independent experiments). **b**, No Tomato expression was detected in whole mount images of bone marrow in femurs, or femur sections, from tamoxifen-treated adult *Tcf21-creER; tdTomato* mice (similar results were obtained in tibias, pelvises, vertebrae and calvaria, data not shown, scale bar=500 μ m, n=3 mice from 3 independent experiments). **c, d**, Most *Scf*-GFP⁺VE-Cadherin⁻ stromal cells were Tomato⁺ (arrows) by confocal imaging (**c**; scale bar=25 μ m) and flow cytometry (**d**). **e**, Tomato⁺CD45⁻Ter119⁻ stromal cells from enzymatically dissociated spleen were uniformly positive for PDGFR α , PDGFR β , and Sca-1 but negative for LepR (n=3 mice from 3 independent experiments). **f**, Percentage of all CFU-F colonies formed by enzymatically dissociated *Tcf21-creER; tdTomato* spleen cells that were Tomato⁺. Macrophage colonies were excluded by staining with anti-CD45 antibody (n=3 mice from 3 independent experiments). **g**, *α -catulin*-GFP⁺c-kit⁺ HSCs represented 0.011 \pm 0.002% of dissociated spleen cells in *α -catulin*^{GFP/+} mice with EMH (n=3-4 mice/genotype from 3 independent experiments). **h**, Competitive reconstitution assays in irradiated mice showed that *α -catulin*-GFP⁺c-kit⁺ splenocytes were highly enriched for long-term multilineage reconstituting (LTMR) HSCs (n=5-7 recipient mice/donor from one experiment). **i, j**, Deep imaging of *α -catulin*-GFP⁺c-kit⁺ HSCs (arrows in **j**) in optically cleared spleen from a *Tcf21-creER; tdTomato; α -catulin*^{GFP/+} mouse with EMH. The distance from *α -catulin*-GFP⁺c-kit⁺ HSCs or random spots to Tomato⁺ stromal cells (**i**; data represent 223 *α -catulin*-GFP⁺c-kit⁺ cells and 2273 random spots). *α -catulin*-GFP⁺c-kit⁺ HSCs were exclusively in the red pulp (**j**). A few megakaryocytes and endothelial cells also expressed *α -catulin*-GFP but were easily distinguished from *α -catulin*-GFP⁺c-kit⁺ cells based on morphology and c-kit expression. See Extended Data Fig. 3e for a low magnification view.

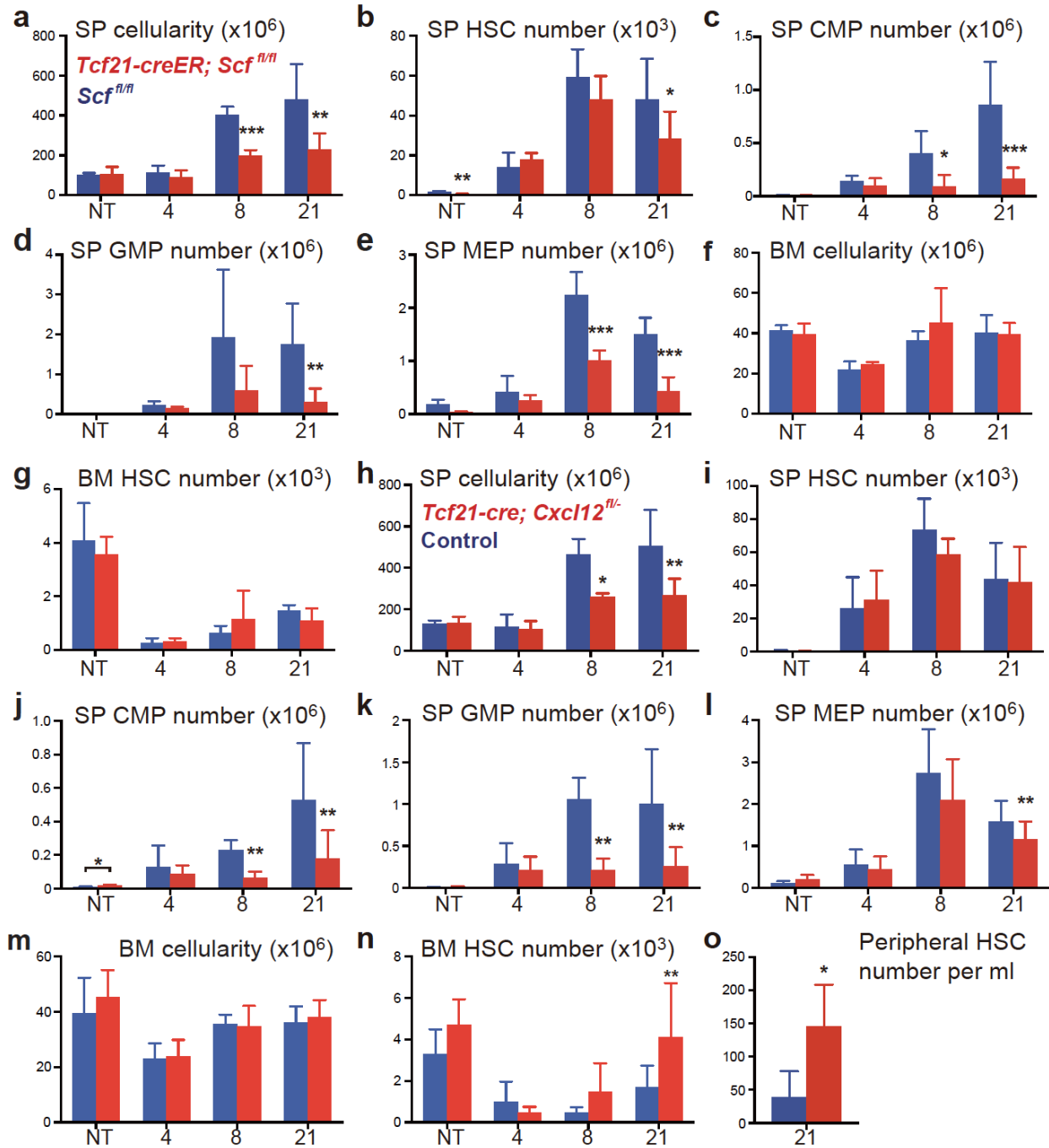


Figure 2.3. *Tcf21*-expressing stromal cells are an important source of *Scf* and *Cxcl12* for EMH in the spleen. **a-g,** *Tcf21-creER*; *Scf^{fl/fl}* and *Scf^{fl/fl}* control mice were treated with tamoxifen then examined a month later either under normal conditions (not treated, NT) or after treatment with cyclophosphamide plus 4, 8, or 21 days of G-CSF to induce EMH. Data show spleen cellularity (**a**), and numbers of CD150⁺CD48⁻LSK HSCs (**b**), CD34⁺FcγR⁻Lineage⁻Sca-1⁻c-kit⁺ common myeloid progenitors (CMPs) (**c**), CD34⁺FcγR⁺Lineage⁻Sca-1⁻c-kit⁺ granulocyte/macrophage progenitors (GMPs) (**d**) and CD34⁻FcγR⁻Lineage⁻Sca-1⁻c-kit⁺ megakaryocyte/erythroid progenitors (MEPs) (**e**) in the spleen as well as cellularity (femur+tibia, **f**) and number of HSCs (**g**) in bone marrow (mean±s.d. from 3-6 independent experiments, the number of mice per genotype is shown in panel **a**). **h-n,** *Tcf21-creER*; *Cxcl12^{fl/-}* and *Cxcl12^{+/-}* or *Cxcl12^{fl/-}* control mice were treated with tamoxifen then examined a month later either under normal conditions (NT) or after treatment with cyclophosphamide plus 4, 8, or 21 days of G-CSF to induce EMH. Data show spleen cellularity (**h**), and numbers of HSCs (**i**), CMPs (**j**), GMPs (**k**) and MEPs (**l**) in the spleen, as well as cellularity (femur+tibia, **m**) and HSC number in bone marrow (**n**; mean±s.d. from 3 independent experiments, the number of mice per genotype is shown in panel **h**). **o,** Number of CD150⁺CD48⁻LSK HSCs per ml of blood in tamoxifen-treated control and *Tcf21-creER*; *Cxcl12^{fl/-}* mice after Cy+21d G-CSF (n=4 *Cxcl12^{fl/-}* and 3 *Tcf21-creER*; *Cxcl12^{fl/-}* mice from 3 independent experiments). Two-tailed student's t-tests were used to assess statistical significance (*P<0.05, **P<0.01, ***P<0.001).

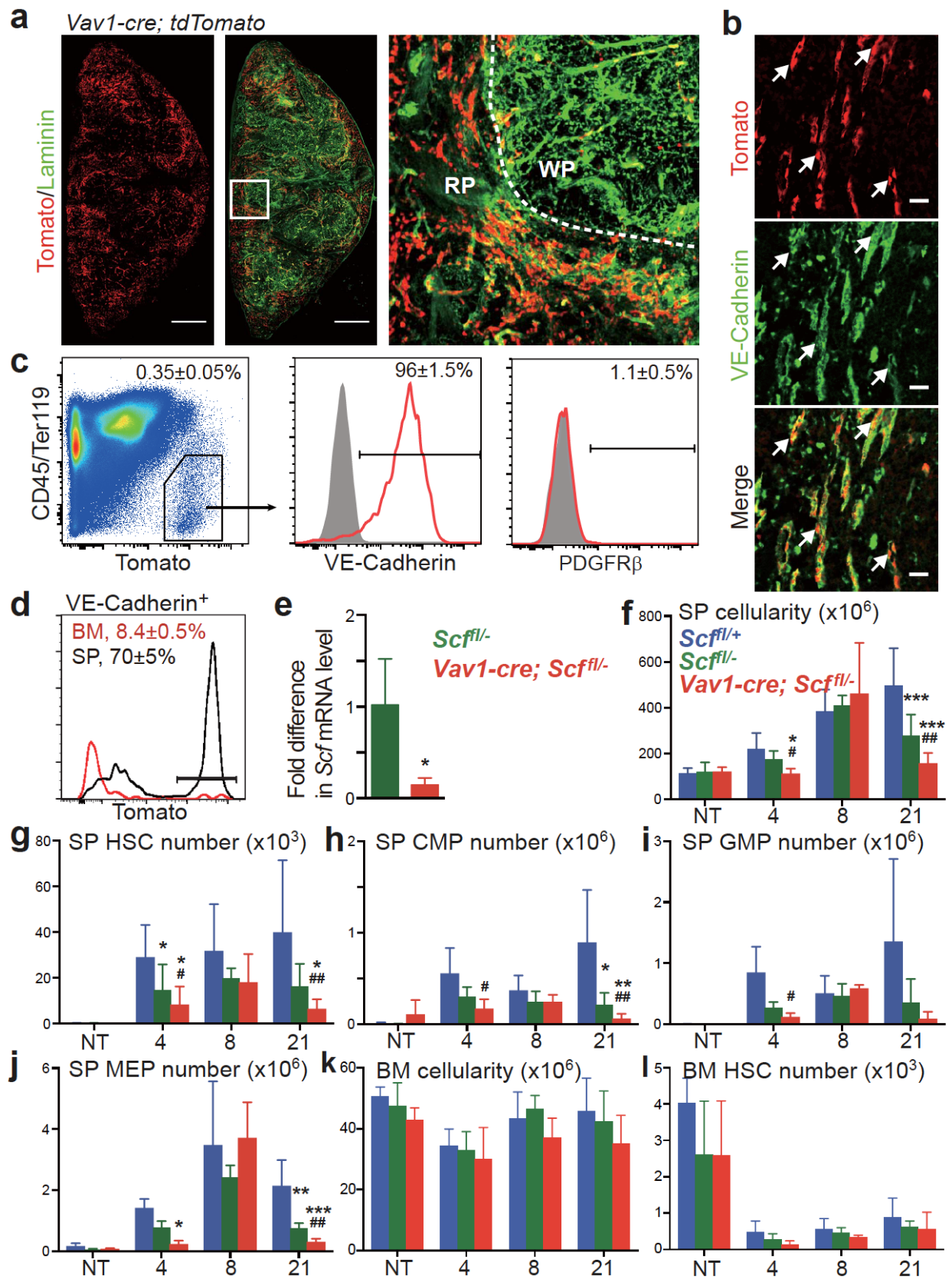


Figure 2.4. Endothelial cells are an important source of *Scf* for EMH in the spleen. **a, b,** *Vav1-cre; tdTomato* mice exhibited perivascular Tomato expression that co-localized with VE-Cadherin (arrows in **b**) in endothelial cells in the red pulp (RP) of the spleen. Note that Tomato was also expressed by hematopoietic cells in these mice but levels of Tomato expression in endothelial cells were ~10-100 fold higher than in hematopoietic cells. Therefore short-exposure images showed mainly Tomato fluorescence in endothelial cells. Scale bar=400 μ m (n=3 mice from 3 independent experiments). **c,** Tomato^{high}CD45^{Ter119}⁻ cells in *Vav1-cre; tdTomato* mice were uniformly positive for VE-Cadherin and negative for PDGFR β . (n=3 mice from 3 independent experiments) **d,** Flow cytometric analysis of VE-Cadherin⁺ cells in *Vav1-cre; tdTomato* mice showed that *Vav1-Cre* recombined in most spleen endothelial cells but in very few bone marrow endothelial cells (n=4 mice from 3 independent experiments). **e,** *Scf* transcripts in VE-Cadherin⁺ endothelial cells from *Vav1-cre; Scf^{f/f-}* mice and *Scf^{f/+}* controls (*Scf* was normalized to β -actin; n=4 mice from 3 independent experiments). **f-l,** *Vav1-cre; Scf^{f/f-}* mice and *Scf^{f/+}*, *Scf^{f/f-}* controls were not treated (NT) or treated with cyclophosphamide plus 4, 8, or 21 days of G-CSF to induce EMH. Data show spleen cellularity (**f**), and numbers of HSCs (**g**), CMPs (**h**), GMPs (**i**) and MEPs (**j**) in the spleen as well as cellularity (femur+tibia, **k**) and number of HSCs in bone marrow (**l**; mean \pm s.d. from 3-8 independent experiments, the number of mice per genotype is indicated in each panel). Statistical significance of differences among genotypes was assessed using a Repeated Measures one-way ANOVA with Greenhouse-Geisser correction along with Tukey's multiple comparison tests with individual variances. * indicates statistical significance relative to *Scf^{f/+}* mice while # indicates statistical significance between *Scf^{f/f-}* and *Vav1-cre; Scf^{f/f-}* mice (* or # P<0.05, ** or ## P<0.01, *** P<0.001).

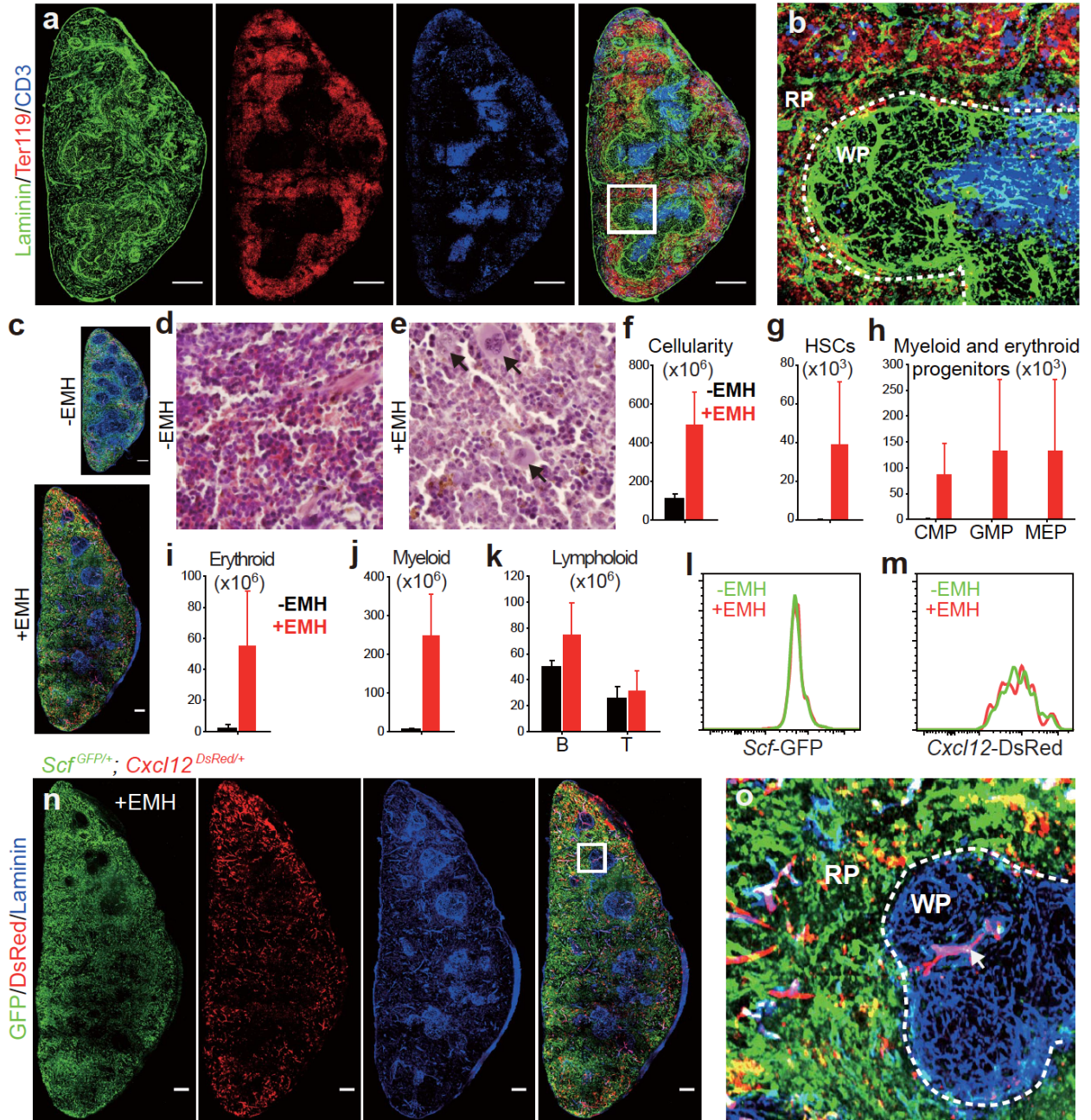


Figure 2.5. Cy/G-CSF treatment induces EMH in the spleen. **a, b**, Staining with anti-Laminin antibody distinguished the vasculature of red pulp (RP) and white pulp (WP). The red pulp and white pulp were definitively marked by clusters of Ter119⁺ cells (red) and CD3⁺ cells (blue), respectively. Dashed line depicts the boundary between red pulp and white pulp. Scale bar=400 μm (representative images from 3 mice in 3 independent experiments). **c**, Spleen sections of the same magnification show the enlargement of the spleen after induction of EMH by Cy+21day G-CSF. These are the same images as in Fig. 1a and Extended Fig. 1n, adjusted to reflect the same magnification. **d, e**, Hematoxylin and Eosin (H&E) staining showing the increase in hematopoiesis in the spleen after induction of EMH using Cy/G-CSF (+EMH, **e**) as evidenced by the presence of megakaryocytes (arrows; n=3 mice/condition from 3 independent experiments). **f-k**, Cy/G-CSF treatment significantly increased spleen cellularity (**f**), as well as the numbers of HSCs (**g**), myeloid and erythroid progenitors (**h**), erythroid cells (**i**) and myeloid cells (**j**) in the spleen but not the number of lymphoid cells (**k**). **l, m**, The intensity of *Scf*-GFP (**l**) and *Cxcl12*-DsRed (**m**) fluorescence among spleen stromal cells that expressed these genes did not significantly differ before (-EMH) and after induction of EMH (+EMH) using Cy/G-CSF. **n, o**, Whole-mount imaging of thick spleen sections from *Scf*^{GFP/+}; *Cxcl12*^{DsRed/+} mice after the induction of EMH by Cy+21d G-CSF. **o**, High-magnification view of the boxed area in (**n**). Dashed lines depict the boundaries between white pulp and red pulp. Arrow indicates the central arteriole in white pulp, around which stromal cells expressed *Cxcl12*-DsRed. Scale bar=400 μm (representative images from 3 mice from 3 independent experiments).

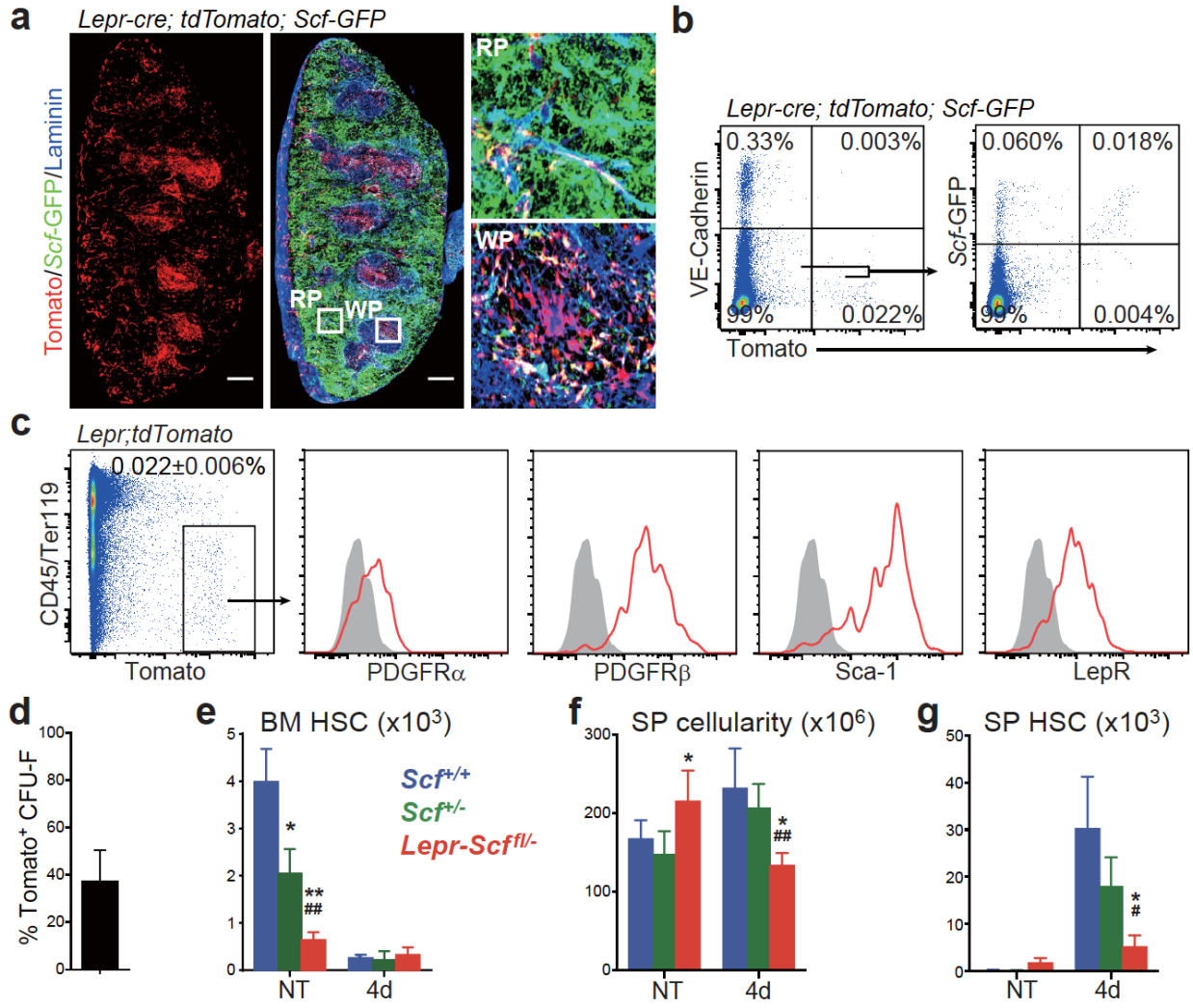


Figure 2.6. Deletion of *Scf* from *LepR*⁺ cells significantly reduces the number of HSCs in the bone marrow and the spleen after induction of EMH. **a**, Whole mount images of spleens from *Lepr-cre; tdTomato; Scf*^{GFP/+} mice showed Tomato expression was primarily in the stromal cells of the white pulp. Although most *Scf*-GFP expression was in endothelial cells and perivascular stromal cells of the red pulp (Fig. 1a-d), some *Scf*-GFP⁺ stromal cells were in the white pulp, most of which appeared to express *LepR*. Dashed line depicts the boundary between red pulp (RP) and white pulp (WP). Scale bar=400 μm (images of representative of 6 mice from 4 independent experiments). **b**, Flow cytometric analysis of enzymatically dissociated spleen cells from *Lepr-cre; tdTomato; Scf*^{GFP/+} mice showed that only a small minority of non-endothelial *Scf*-GFP⁺ cells were positive for Tomato (n=3 mice from 3 independent experiments). **c**, Tomato⁺CD45⁻Ter119⁻ stromal cells in the spleens of *Lepr-cre; tdTomato* mice expressed PDGFRα, PDGFRβ, Sca-1 and *LepR* (n=3 mice from 3 independent experiments). **d**, Percentage of all CFU-F colonies formed by enzymatically dissociated whole spleen cells from *Lepr-cre; tdTomato* mice that expressed Tomato. Macrophage colonies were excluded by staining with anti-CD45 antibody (n=4 mice from 3 independent experiments). **e**, *Lepr-cre; Scf*^{f/f-} mice had significantly fewer HSCs in the bone marrow than wild-type and *Scf*^{f/f-} controls before induction of EMH (n=4 mice/genotype/time point mice from 4 independent experiments). **f, g**, *Lepr-cre; Scf*^{f/f-} mice displayed significantly lower spleen cellularity (**f**) and HSC number (**g**) in the spleen than wild-type and *Scf*^{f/f-} controls after induction of EMH with cyclophosphamide plus 4 days of G-CSF (n=4 mice/genotype/time point from 4 independent experiments). The statistical significance of differences between genotypes was assessed using Repeated Measures one-way ANOVAs with Greenhouse-Geisser correction and Tukey's multiple comparison tests with individual variances computed for each comparison. * indicates statistical significance relative to wild-type (*Scf*^{+/+}). # indicates statistical significance between *Scf*^{+/-} and *Lepr-cre; Scf*^{f/f-} (* or # P<0.05, ** or ## P<0.01).

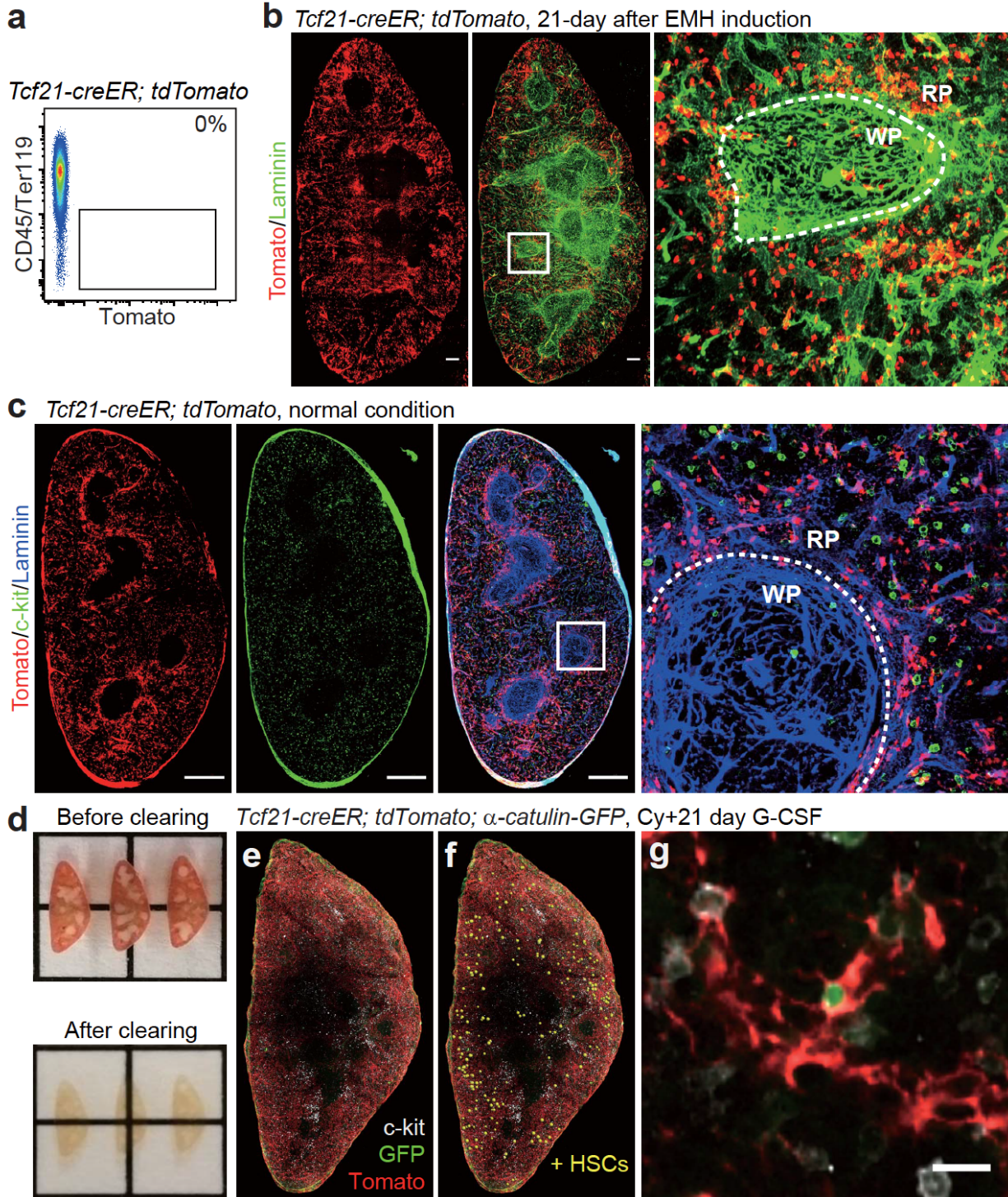


Figure 2.7. Hematopoietic stem and progenitors reside perivascularly, adjacent to *Tcf21*-expressing stromal cells, in the red pulp before and after EMH induction. **a**, Tomato was not expressed by enzymatically dissociated bone marrow cells from *Tcf21-creER; tdTomato* mice that had been administered tamoxifen for 12 days (n=3 mice from 3 independent experiments). **b**, EMH induction by Cy+21d G-CSF did not alter the general expression pattern of Tomato in the spleens of tamoxifen-treated *Tcf21-creER; tdTomato* mice (like in normal spleens it was expressed mainly in red pulp). Dashed line depicts the boundary between red pulp (RP) and white pulp (WP). Scale bar=400 μ m (n=2 mice from 2 independent experiments). **c**, The vast majority of c-kit⁺ hematopoietic progenitors localized adjacent to *Tcf21*-expressing stromal cells in the red pulp of the normal spleen. Scale bar=400 μ m (n=3 mice from 3 independent experiments). **d**, 300 μ m thick sections of spleen before and after optical clearing using BABB. **e-g**, Deep imaging of α -catulin-GFP⁺c-kit⁺ HSCs in a cleared spleen segment from *Tcf21-creER; tdTomato; α -catulin* mice. **e**, Low magnification view and **(f)** same view as in **(e)** except that α -Catulin-GFP⁺c-kit⁺ HSCs were manually identified and annotated with yellow spheres using the Imaris spot function. **g**, A representative high magnification image showing an α -Catulin-GFP⁺c-kit⁺ HSC surrounded by Tomato⁺ stromal cells. Scale bar=10 μ m.

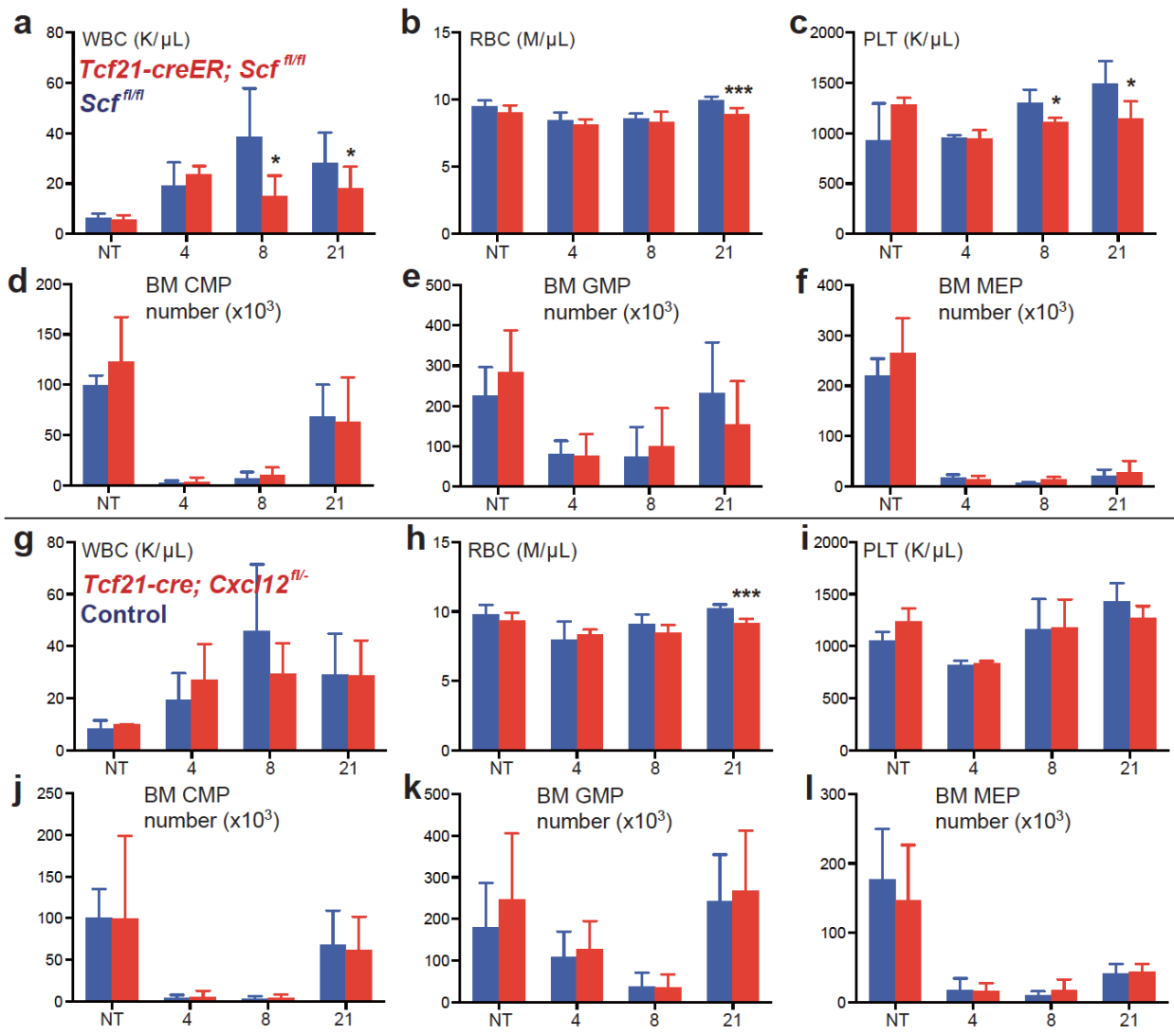


Figure 2.8. Deletion of *Scf* or *Cxcl12* from *Tcf21*-expressing stromal cells in the spleen reduced peripheral blood cell counts but did not affect bone marrow hematopoiesis. **a-f**, *Tcf21-creER*; *Scf^{fl/fl}* and *Scf^{fl/fl}* control mice were treated with tamoxifen then examined a month later without further treatment (not treated, NT) or after treatment with cyclophosphamide plus 4, 8, or 21 days of G-CSF to induce EMH. Data show white blood cell (WBC) (**a**), red blood cell (RBC) (**b**), and platelet (PLT) counts (**c**) as well as numbers of CMPs (**d**), GMPs (**e**) and MEPs (**f**) in the bone marrow (mean±s.d. from 3 (NT), 3 (4d), 5 (8d), and 7 (21d) mice/genotype from 3 (NT), 3 (4d), 4 (8d), and 6 (21d) independent experiments). **g-l**, *Tcf21-cre*; *Cxcl12^{fl/fl}* mice and littermate controls (*Cxcl12^{fl/fl}* or *Cxcl12^{+/-}*) were treated with tamoxifen then examined a month later without further treatment (NT) or after treatment with cyclophosphamide plus 4, 8, or 21 days of G-CSF to induce EMH. Data show WBC (**g**), RBC (**h**), and PLT counts (**i**), as well as numbers of CMPs (**j**), GMPs (**k**) and MEPs (**l**) in the bone marrow (mean±s.d. from 3 (NT), 4 (4d), 3 (8d), and 10 (21d) mice/genotype from 3 (NT), 4 (4d), 3 (8d) and 7 (21d) independent experiments). Two-tailed student's t-tests were used to assess statistical significance (*P<0.05, ***P<0.001).

Figure 2.9. Deletion of *Scf*, but not *Cxcl12*, from endothelial cells in the spleen reduced peripheral blood cell counts but did not affect bone marrow hematopoiesis. **a-m**, *Vav1-cre*; *Cxcl12^{fl/fl}* mice and *Cxcl12^{fl/-}* controls were treated with Cy+4-21d G-CSF to induce EMH. Data show WBC (**a**), RBC (**b**), and platelet (**c**) counts, spleen cellularity (**d**) and numbers of HSCs (**e**), CMPs (**f**), GMPs (**g**) and MEPs (**h**) in the spleen as well as bone marrow cellularity (**i**), and numbers of HSCs (**j**), CMPs (**k**), GMPs (**l**) and MEPs (**m**) in the bone marrow (mean±s.d. from 3 (4d) and 5 (21d) mice/genotype from 3 (4d) and 5 (21d) independent experiments). Two-tailed student's t-tests were used to assess statistical significance. **n-s**, *Vav1-cre*; *Scf^{fl/-}* mice and *Scf^{fl/+}*, *Scf^{fl/-}* controls were treated with Cy+4-21d G-CSF to induce EMH. Data show WBC (**n**), RBC (**o**), and platelet (PLT) (**p**) counts as well as numbers of CMPs (**q**), GMPs (**r**) and MEPs (**s**) in the bone marrow (mean±s.d. from 3 (NT), 3 (4d), 3 (8d), and 8 (21d) mice/genotype from 3 (NT), 3 (4d), 3 (8d), and 8 (21d) independent experiments). The statistical significance of differences among genotypes was assessed using Repeated Measures one-way ANOVAs with Greenhouse-Geisser correction and Tukey's multiple comparison tests with individual variances computed for each comparison. * indicates statistical significance relative to *Scf^{fl/+}* controls. # indicates statistical significance between *Scf^{fl/-}* and *Vav1-cre*; *Scf^{fl/-}* (* or # P<0.05, ** or ## P<0.01).

Video 1. HSCs are closely associated with *Tcf21*-CreER-expressing stromal cells in the red pulp of the spleen. The video shows a 300 μ m section of spleen from a *Tcf21-creER; tdTomato; α -catulin-GFP* mouse in which EMH was induced by treatment with Cy+21d G-CSF. The spleen section was stained with antibodies against c-kit (white), α -Catulin-GFP (green), and DsRed (red), then cleared, imaged, and digitally reconstructed. HSCs are α -Catulin-GFP⁺c-kit⁺ and are sometimes represented with yellow spheres to clearly mark their position during parts of the video. To show the spatial relationship between α -Catulin-GFP⁺c-kit⁺ HSCs and Tomato⁺ cells all channels 20-30 μ m beyond the spot of interest were occasionally masked. Note that the capsule on the margin of the spleen section is highly autofluorescent.

3.1 Conclusions

The experiments presented in this thesis identify a perivascular niche for EMH in the spleen. The major sources of SCF and CXCL12 in the mouse spleen during hematopoietic injury are found primarily near red pulp sinusoids, explaining the longstanding observations that EMH occurs predominantly in the red pulp and that HSCs are located near sinusoids after Cy/G-CSF treatment (Kiel et al., 2005). *Tcf21*-expressing perivascular stromal cells in the spleen red pulp maintain EMH through secretion of both SCF and CXCL12. Spleen endothelial cells maintain EMH through secretion of SCF but not CXCL12. Both *Tcf21*-expressing stromal cells and endothelial cells expand in number during the course of EMH. This cell expansion follows recruitment of HSCs and progenitors to the spleen and likely accounts for how the splenic hematopoietic niche accommodates EMH during hematopoietic stress. Notably, the per-cell expression levels of *Scf* and *Cxcl12* do not increase during EMH, suggesting that the hematopoietic niche in the spleen constitutively secretes SCF and CXCL12, though whether it is constitutively competent to support hematopoiesis is unknown. The identity of the signal that induces EMH or how it changes the spleen remains unknown.

There are several differences between the splenic niche and the bone marrow niche that this study has revealed. Most notably, HSCs are disproportionately depleted relative to other cell types from bone marrow after conditional deletion of *Scf* from perivascular cells. In contrast, HSCs in spleens lacking perivascular SCF secretion are depleted equally relative to total spleen cellularity. By contrast, immature progenitors of the myeloerythroid lineage are

disproportionately depleted from spleens lacking perivascular SCF secretion. Similarly, HSCs are depleted from bone marrow lacking CXCL12, while CXCL12 loss from spleen depletes myeloid and erythroid progenitors. The reason for these differences is unknown. Nonetheless, spleen HSCs do depend to some extent upon CXCL12 for their maintenance in the spleen as conditional deletion of *Cxcl12* from spleen stromal cells does increase HSC frequency in the blood.

Another distinction between the niche in the bone marrow and in the spleen is the expression pattern of SCF and CXCL12. Perivascular stromal cells in the bone marrow uniformly express high levels of both CXCL12 and SCF (Ding and Morrison, 2013). In the spleen, however, *Tcf21*-expressing stromal cells uniformly express high levels of SCF but only a subset expresses CXCL12. This heterogeneity of niche factor expression raises the intriguing possibility that *Tcf21*⁺ cells exhibit functional heterogeneity. Some *Tcf21*-expressing cells may have a greater capacity to support HSCs and progenitors than others. Whether bone marrow or spleen perivascular stromal cells exhibit heterogeneous expression of other niche factors is currently unknown. Further, endothelial cells in the spleen express much higher levels of SCF than endothelial cells in the bone marrow. Bone marrow endothelial cells express very low levels of SCF (Ding et al., 2012). The physiological basis for this difference in SCF expression is unknown.

3.2 Unanswered questions related to the hematopoietic niche in the spleen

While the work presented in this thesis is a significant step toward understanding how the EMH niche is regulated in response to injury, many important questions lay beyond the scope of these studies. Questions concerning the onset and resolution of EMH and the signals driving

niche cell proliferation are areas of future study. Perspectives and future experiments to address these questions are presented in this section.

3.2.1 What are the signals driving induction and resolution of EMH?

One important question that remains unanswered concerns the signals that drive the onset and resolution of EMH. This study did not seek to address this topic, instead focusing on identifying the cells that maintained EMH. It is unknown whether different injuries that induce EMH rely on the same extracellular signals to induce HSC mobilization or whether different injuries release different cytokines to induce EMH. However, most models that induce extramedullary hematopoiesis drive HSCs into cycle prior to mobilization. For instance, *Pten* deletion from HSCs drives HSCs into cycle and mobilizes them to the spleen; rapamycin administration blocks these effects (Magee et al., 2012; Yilmaz et al., 2006). Interestingly, rapamycin administration also prevents Cy/G-CSF-mediated HSC mobilization, indicating that PI3K signaling is necessary to mobilize HSCs during recovery from myeloablation (Magee et al., 2012). Different injuries that mobilize HSCs to the spleen to induce EMH may converge on activation of the PI3K pathway in HSCs. Perturbations in hematopoietic homeostasis may lead to the production of signals that activate the PI3K pathway in HSCs that dissipate after homeostasis is restored. These signals may originate from the bone marrow perivascular stromal cells and endothelial cells that make up the bone marrow HSC niche or could be produced by cells types in peripheral tissues.

3.2.2 What are the signals that regulate niche cell division?

My work indicates that niche cells in the spleen divide and expand in number after the onset of EMH. The signals regulating this response and whether this response is dependent upon the presence of hematopoietic progenitors in the spleen remain unknown. The cells that make up the niche, endothelial cells and perivascular stromal cells, are also major components of the spleen tissue architecture, ensuring adequate blood supply and supporting tissue integrity in addition to maintaining hematopoietic stem and progenitor cells. Physical expansion of spleen size may cause niche cell division to maintain tissue integrity, regardless of whether EMH is induced in the spleen. One way to test this hypothesis would be to induce splenomegaly without concomitant EMH and test whether niche cells undergo expansion. Infection with Epstein-Barr virus (EBV) causes splenomegaly via increased lymphocyte infiltration in the red pulp but does not induce EMH (O'Malley, 2013). Niche cell expansion in the context of EBV infection would suggest that niche cell division is dependent on splenomegaly, whereas lack of division would suggest dependence on EMH and potentially signals derived from hematopoietic progenitors.

3.3 Future investigation of the HSC niche

There are many questions regarding general HSC niche biology that will likely be addressed in future studies. The HSC niche during ontogeny has not been characterized. Which physiologic signals meaningfully regulate HSC niches during development? Finally, most of the niche studies from our lab have relied upon previously validated niche factors to discover new niche cell types. A more complete repertoire of niche factors would facilitate the study of HSC niche biology. These questions and how they may be experimentally tested are addressed in this section.

3.3.1 The niche during development

HSCs during development are primarily located in the fetal liver. In contrast to adult HSCs, fetal liver HSCs divide frequently and symmetrically, doubling their numbers every day (Morrison et al., 1995). The cells in the fetal liver that maintain fetal HSCs are unknown. The most straightforward way to identify the fetal liver niche is to take an analogous approach as in (Ding et al., 2012). The *Scf*^{GFP} and *Cxcl12*^{DsRed} alleles could be used to identify the expression pattern of known niche factors in the fetal liver. Sorting these cells and testing candidate Cre drivers would allow for functional testing of niche cell types in the fetal liver. Identifying the HSC niche in the fetal liver would offer profound insight into a niche that expands HSCs during development. The differences between the fetal liver HSC niche and the adult bone marrow HSC niche may underlie the biological differences between fetal and adult HSCs.

3.3.2 Physiologic regulation of the niche

It is currently unknown whether the bone marrow HSC niche is meaningfully regulated by the physiologic status of the host. While physiologic HSC mobilization from the bone marrow exhibits circadian oscillations (Casanova-Acebes et al., 2013; Mendez-Ferrer et al., 2008), no physiologic function of circadian HSC mobilization has been discovered. Genetic disruption of the circadian clock has been shown to have no effect the hematopoietic system (Ieyasu et al., 2014). It is unclear if circadian regulation of HSC mobilization has any function. What physiologic cues regulate hematopoiesis, and do they act through the niche or directly on HSCs and progenitors? Answering this question will reveal how tissue stem cell activity is determined by host physiology.

3.3.3 Discovery of novel niche factors

A major goal of HSC niche research is to discover novel cell non-autonomous factors that regulate HSCs. One approach to this problem centers on identifying secreted gene products that are expressed specifically in bone marrow perivascular stromal cells relative to other bone marrow populations. Mice with conditional loss of these gene products from bone marrow stromal populations are then assessed for hematopoietic abnormalities, especially HSC depletion.

This approach has a number of shortcomings. First, it assumes that niche factors will be expressed specifically in perivascular stromal cells. However, *Cxcl12*, a validated niche factor, is expressed by multiple bone marrow cell types (Ding and Morrison, 2013). Analyses focusing exclusively on genes specifically expressed by perivascular stromal cells could inappropriately exclude niche factors. Moreover, the approach assumes that perivascular stromal cells will be the major source of additional niche factors. While *Scf* and *Cxcl12* are highly expressed by this cell type, other cells may be responsible for factors regulating HSCs and hematopoiesis.

Thrombopoietin, which is known to regulate HSCs cell non-autonomously (Murone et al., 1998), is produced in large amounts by the liver as well as bone marrow stromal cells, and

erythropoietin is produced by the kidney. Perivascular stromal cells thus may not be the sole source of all HSC niche factors. The approach is also labor, time, and resource intensive. For each gene tested, a reporter allele, null allele, and conditional allele must be generated.

Conditional alleles must be crossed with multiple Cre drivers, and each new study claiming to discover a new niche component results in at least one more Cre driver to be tested. Finally, there may be non-protein niche factors. Small metabolites may regulate HSC function.

Another way to identify new cell non-autonomous regulators of HSCs and hematopoiesis would be through cell autonomous studies of HSCs, namely to identify the receptors on HSCs that regulate their function. Many cell non-autonomous regulators of HSCs will act on a receptor. Discovering which receptors are necessary for HSC maintenance will open new pathways for niche factor discovery.

The ability to isolate HSCs, introduce genetic elements in culture and transplant them into irradiated recipients makes them suitable for a focused CRISPR-Cas9 screen. Genome-wide screens using CRISPR-Cas9 technology have been successfully performed *in vitro* (Shalem et al., 2015) and can likely be adapted to *in vivo* systems. Ideally, HSCs from mice expressing a Tet-repressible Cas9 gene would be isolated by flow cytometry, transduced with short guide RNAs (sgRNAs) directed against known mammalian receptors or receptor families, and transplanted into recipient mice. Recipient mice will be placed on doxycycline water to prevent Cas9 expression. After allowing 6-8 weeks for HSCs to engraft, recipient mice will be bled, and DNA from peripheral blood granulocytes will be sequenced to determine initial representation of sgRNAs in HSCs contributing to hematopoiesis. Recipient mice will then be placed on normal water to allow Cas9 activation and gene targeting. Mice will be bled periodically, and DNA from peripheral blood granulocytes will be sequenced to determine representation of sgRNAs at different time points after doxycycline withdrawal. sgRNAs targeting receptors that are necessary for HSCs to contribute to hematopoiesis will be depleted after doxycycline withdrawal. While this approach may miss some functional receptors due to inefficient genetic targeting and may generate some false positives due to off-target effects, it is high-throughput, allowing many receptors to be tested at once, functional, and unbiased, and would obviate many of the shortcomings of current strategies. Further, some receptors identified through this

approach may be orphan receptors with no known ligand or transmembrane proteins that are not regulated by ligand binding. Nonetheless, this screen would generate many targets for further biological or pharmacological studies.

BIBLIOGRAPHY

- Abdel-Wahab, O.I., and Levine, R.L. (2009). Primary myelofibrosis: update on definition, pathogenesis, and treatment. *Annual review of medicine* *60*, 233-245.
- Acar, M., Kocherlakota, K.S., Murphy, M.M., Peyer, J.G., Oguro, H., Inra, C.N., Jaiyeola, C., Zhao, Z., Luby-Phelps, K., and Morrison, S.J. (2015). Deep imaging of bone marrow shows non-dividing stem cells are perisinusoidal. *Nature Submitted*.
- Acharya, A., Baek, S.T., Banfi, S., Eskiocak, B., and Tallquist, M.D. (2011). Efficient inducible Cre-mediated recombination in Tcf21 cell lineages in the heart and kidney. *Genesis* *49*, 870-877.
- Akashi, K., Traver, D., Miyamoto, T., and Weissman, I.L. (2000). A clonogenic common myeloid progenitor that gives rise to all myeloid lineages. *Nature* *404*, 193-197.
- Ara, T., Tokoyoda, K., Sugiyama, T., Egawa, T., Kawabata, K., and Nagasawa, T. (2003). Long-term hematopoietic stem cells require stromal cell-derived factor-1 for colonizing bone marrow during ontogeny. *Immunity* *19*, 257-267.
- Baldrige, M.T., King, K.Y., Boles, N.C., Weksberg, D.C., and Goodell, M.A. (2010). Quiescent haematopoietic stem cells are activated by IFN-gamma in response to chronic infection. *Nature* *465*, 793-797.
- Balordi, F., and Fishell, G. (2007). Mosaic removal of hedgehog signaling in the adult SVZ reveals that the residual wild-type stem cells have a limited capacity for self-renewal. *The Journal of neuroscience : the official journal of the Society for Neuroscience* *27*, 14248-14259.
- Baxter, E.J., Scott, L.M., Campbell, P.J., East, C., Fourouclas, N., Swanton, S., Vassiliou, G.S., Bench, A.J., Boyd, E.M., Curtin, N., *et al.* (2005). Acquired mutation of the tyrosine kinase JAK2 in human myeloproliferative disorders. *Lancet* *365*, 1054-1061.
- Becker, A.J., Mc, C.E., and Till, J.E. (1963). Cytological demonstration of the clonal nature of spleen colonies derived from transplanted mouse marrow cells. *Nature* *197*, 452-454.
- Becker, K., Jahrling, N., Saghafi, S., and Dodt, H.U. (2013). Immunostaining, dehydration, and clearing of mouse embryos for ultramicroscopy. *Cold Spring Harbor protocols* *2013*, 743-744.

Bennett, M., Pinkerton, P.H., Cudkowicz, G., and Bannerman, R.M. (1968). Hemopoietic progenitor cells in marrow and spleen of mice with hereditary iron deficiency anemia. *Blood* 32, 908-921.

Bernstein, S.E. (1970). Tissue transplantation as an analytic and therapeutic tool in hereditary anemias. *Am J Surg* 119, 448-451.

Bertrand, J.Y., Chi, N.C., Santoso, B., Teng, S., Stainier, D.Y., and Traver, D. (2010). Haematopoietic stem cells derive directly from aortic endothelium during development. *Nature* 464, 108-111.

Boisset, J.C., van Cappellen, W., Andrieu-Soler, C., Galjart, N., Dzierzak, E., and Robin, C. (2010). In vivo imaging of haematopoietic cells emerging from the mouse aortic endothelium. *Nature* 464, 116-120.

Bol, S., van Vliet, M., and van Slingerland, V. (1981). Electrophoretic mobility properties of murine hemopoietic cells in different stages of development. *Experimental hematology* 9, 431-443.

Broxmeyer, H.E., Orschell, C.M., Clapp, D.W., Hangoc, G., Cooper, S., Plett, P.A., Liles, W.C., Li, X., Graham-Evans, B., Campbell, T.B., *et al.* (2005). Rapid mobilization of murine and human hematopoietic stem and progenitor cells with AMD3100, a CXCR4 antagonist. *The Journal of experimental medicine* 201, 1307-1318.

Bruns, I., Lucas, D., Pinho, S., Ahmed, J., Lambert, M.P., Kunisaki, Y., Scheiermann, C., Schiff, L., Poncz, M., Bergman, A., *et al.* (2014). Megakaryocytes regulate hematopoietic stem cell quiescence through CXCL4 secretion. *Nature medicine* 20, 1315-1320.

Burberry, A., Zeng, M.Y., Ding, L., Wicks, I., Inohara, N., Morrison, S.J., and Nunez, G. (2014). Infection mobilizes hematopoietic stem cells through cooperative NOD-like receptor and Toll-like receptor signaling. *Cell host & microbe* 15, 779-791.

Busch, K., Klapproth, K., Barile, M., Flossdorf, M., Holland-Letz, T., Schlenner, S.M., Reth, M., Hofer, T., and Rodewald, H.R. (2015). Fundamental properties of unperturbed haematopoiesis from stem cells in vivo. *Nature* 518, 542-546.

Calvi, L.M., Adams, G.B., Weibrecht, K.W., Weber, J.M., Olson, D.P., Knight, M.C., Martin, R.P., Schipani, E., Divieti, P., Bringhurst, F.R., *et al.* (2003). Osteoblastic cells regulate the haematopoietic stem cell niche. *Nature* 425, 841-846.

Casanova-Acebes, M., Pitaval, C., Weiss, L.A., Nombela-Arrieta, C., Chevre, R., N, A.G., Kunisaki, Y., Zhang, D., van Rooijen, N., Silberstein, L.E., *et al.* (2013). Rhythmic modulation of the hematopoietic niche through neutrophil clearance. *Cell* *153*, 1025-1035.

Cesta, M.F. (2006). Normal structure, function, and histology of mucosa-associated lymphoid tissue. *Toxicologic pathology* *34*, 599-608.

Chagraoui, H., Komura, E., Tulliez, M., Giraudier, S., Vainchenker, W., and Wendling, F. (2002). Prominent role of TGF-beta 1 in thrombopoietin-induced myelofibrosis in mice. *Blood* *100*, 3495-3503.

Cheshier, S.H., Prohaska, S.S., and Weissman, I.L. (2007). The effect of bleeding on hematopoietic stem cell cycling and self-renewal. *Stem cells and development* *16*, 707-717.

Chow, A., Huggins, M., Ahmed, J., Hashimoto, D., Lucas, D., Kunisaki, Y., Pinho, S., Leboeuf, M., Noizat, C., van Rooijen, N., *et al.* (2013). CD169(+) macrophages provide a niche promoting erythropoiesis under homeostasis and stress. *Nature medicine* *19*, 429-436.

Chow, A., Lucas, D., Hidalgo, A., Mendez-Ferrer, S., Hashimoto, D., Scheiermann, C., Battista, M., Leboeuf, M., Prophete, C., van Rooijen, N., *et al.* (2011). Bone marrow CD169+ macrophages promote the retention of hematopoietic stem and progenitor cells in the mesenchymal stem cell niche. *The Journal of experimental medicine* *208*, 261-271.

Christopher, M.J., Rao, M., Liu, F., Woloszynek, J.R., and Link, D.C. (2011). Expression of the G-CSF receptor in monocytic cells is sufficient to mediate hematopoietic progenitor mobilization by G-CSF in mice. *The Journal of experimental medicine* *208*, 251-260.

Ciurea, S.O., Merchant, D., Mahmud, N., Ishii, T., Zhao, Y., Hu, W., Bruno, E., Barosi, G., Xu, M., and Hoffman, R. (2007). Pivotal contributions of megakaryocytes to the biology of idiopathic myelofibrosis. *Blood* *110*, 986-993.

Cuttler, A.S., LeClair, R.J., Stohn, J.P., Wang, Q., Sorenson, C.M., Liaw, L., and Lindner, V. (2011). Characterization of Pdgfrb-Cre transgenic mice reveals reduction of ROSA26 reporter activity in remodeling arteries. *Genesis* *49*, 673-680.

de Boer, J., Williams, A., Skavdis, G., Harker, N., Coles, M., Tolaini, M., Norton, T., Williams, K., Roderick, K., Potocnik, A.J., *et al.* (2003). Transgenic mice with hematopoietic and lymphoid specific expression of Cre. *European journal of immunology* *33*, 314-325.

DeFalco, J., Tomishima, M., Liu, H., Zhao, C., Cai, X., Marth, J.D., Enquist, L., and Friedman, J.M. (2001). Virus-assisted mapping of neural inputs to a feeding center in the hypothalamus. *Science* 291, 2608-2613.

Dexter, T.M., Allen, T.D., and Lajtha, L.G. (1977). Conditions controlling the proliferation of haemopoietic stem cells in vitro. *Journal of cellular physiology* 91, 335-344.

Ding, L., and Morrison, S.J. (2013). Haematopoietic stem cells and early lymphoid progenitors occupy distinct bone marrow niches. *Nature* 495, 231-235.

Ding, L., Saunders, T.L., Enikolopov, G., and Morrison, S.J. (2012). Endothelial and perivascular cells maintain haematopoietic stem cells. *Nature* 481, 457-462.

Dutta, P., Courties, G., Wei, Y., Leuschner, F., Gorbатов, R., Robbins, C.S., Iwamoto, Y., Thompson, B., Carlson, A.L., Heidt, T., *et al.* (2012). Myocardial infarction accelerates atherosclerosis. *Nature* 487, 325-329.

Dutta, P., Hoyer, F.F., Grigoryeva, L.S., Sager, H.B., Leuschner, F., Courties, G., Borodovsky, A., Novobrantseva, T., Ruda, V.M., Fitzgerald, K., *et al.* (2015). Macrophages retain hematopoietic stem cells in the spleen via VCAM-1. *The Journal of experimental medicine* 212, 497-512.

Ehrlich, P. (1879). Ueber die spezifischen Granulationen des Blutes. *Archiv fuer Anatomie und Physiologie*, 571-579.

Eilken, H.M., Nishikawa, S., and Schroeder, T. (2009). Continuous single-cell imaging of blood generation from haemogenic endothelium. *Nature* 457, 896-900.

Ferrant, A., Rodhain, J., Cauwe, F., Cogneau, M., Beckers, C., Michaux, J.L., Verwilghen, R., and Sokal, G. (1982). Assessment of bone marrow and splenic erythropoiesis in myelofibrosis. *Scandinavian journal of haematology* 29, 373-380.

Ford, C.E., Hamerton, J.L., Barnes, D.W., and Loutit, J.F. (1956). Cytological identification of radiation-chimaeras. *Nature* 177, 452-454.

Foudi, A., Hochedlinger, K., Van Buren, D., Schindler, J.W., Jaenisch, R., Carey, V., and Hock, H. (2009). Analysis of histone 2B-GFP retention reveals slowly cycling hematopoietic stem cells. *Nat Biotechnol* 27, 84-90.

Fowler, J.H., and Nash, D.J. (1968). Erythropoiesis in the spleen and bone marrow of the pregnant mouse. *Developmental biology* 18, 331-353.

Freedman, M.H., and Saunders, E.F. (1981). Hematopoiesis in the human spleen. *American journal of hematology* 11, 271-275.

Gan, B., Hu, J., Jiang, S., Liu, Y., Sahin, E., Zhuang, L., Fletcher-Sananikone, E., Colla, S., Wang, Y.A., Chin, L., *et al.* (2010). Lkb1 regulates quiescence and metabolic homeostasis of haematopoietic stem cells. *Nature* 468, 701-704.

Gekas, C., Dieterlen-Lievre, F., Orkin, S.H., and Mikkola, H.K. (2005). The placenta is a niche for hematopoietic stem cells. *Developmental cell* 8, 365-375.

Greenbaum, A., Hsu, Y.M., Day, R.B., Schuettpelz, L.G., Christopher, M.J., Borgerding, J.N., Nagasawa, T., and Link, D.C. (2013). CXCL12 in early mesenchymal progenitors is required for haematopoietic stem-cell maintenance. *Nature* 495, 227-230.

Greenbaum, A.M., Revollo, L.D., Woloszynek, J.R., Civitelli, R., and Link, D.C. (2012). N-cadherin in osteolineage cells is not required for maintenance of hematopoietic stem cells. *Blood* 120, 295-302.

Gurumurthy, S., Xie, S.Z., Alagesan, B., Kim, J., Yusuf, R.Z., Saez, B., Tzatsos, A., Oszolak, F., Milos, P., Ferrari, F., *et al.* (2010). The Lkb1 metabolic sensor maintains haematopoietic stem cell survival. *Nature* 468, 659-663.

Haeckel, E. (1868). *Natürliche Schöpfungsgeschichte* (Berlin: Georg Reimer).

Haeckel, E. (1877). *Anthropogenie*, 3rd edn (Leipzig: Wilhelm Engelmann).

He, S., Kim, I., Lim, M.S., and Morrison, S.J. (2011). Sox17 expression confers self-renewal potential and fetal stem cell characteristics upon adult hematopoietic progenitors. *Genes & development* 25, 1613-1627.

Holtwick, R., Gotthardt, M., Skryabin, B., Steinmetz, M., Potthast, R., Zetsche, B., Hammer, R.E., Herz, J., and Kuhn, M. (2002). Smooth muscle-selective deletion of guanylyl cyclase-A prevents the acute but not chronic effects of ANP on blood pressure. *Proceedings of the National Academy of Sciences of the United States of America* 99, 7142-7147.

Hooper, A.T., Butler, J.M., Nolan, D.J., Kranz, A., Iida, K., Kobayashi, M., Kopp, H.G., Shido, K., Petit, I., Yanger, K., *et al.* (2009). Engraftment and reconstitution of hematopoiesis is dependent on VEGFR2-mediated regeneration of sinusoidal endothelial cells. *Cell stem cell* 4, 263-274.

Ieyasu, A., Tajima, Y., Shimba, S., Nakauchi, H., and Yamazaki, S. (2014). Clock gene *Bmal1* is dispensable for intrinsic properties of murine hematopoietic stem cells. *Journal of negative results in biomedicine* 13, 4.

Irizarry, R.A., Hobbs, B., Collin, F., Beazer-Barclay, Y.D., Antonellis, K.J., Scherf, U., and Speed, T.P. (2003). Exploration, normalization, and summaries of high density oligonucleotide array probe level data. *Biostatistics* 4, 249-264.

Jacobson, L.O., Marks, E.K., and *et al.* (1949). The role of the spleen in radiation injury. *Proceedings of the Society for Experimental Biology and Medicine Society for Experimental Biology and Medicine* 70, 740-742.

Johns, J.L., and Christopher, M.M. (2012). Extramedullary hematopoiesis: a new look at the underlying stem cell niche, theories of development, and occurrence in animals. *Veterinary pathology* 49, 508-523.

Kiel, M.J., Acar, M., Radice, G.L., and Morrison, S.J. (2009). Hematopoietic stem cells do not depend on N-cadherin to regulate their maintenance. *Cell stem cell* 4, 170-179.

Kiel, M.J., He, S., Ashkenazi, R., Gentry, S.N., Teta, M., Kushner, J.A., Jackson, T.L., and Morrison, S.J. (2007a). Haematopoietic stem cells do not asymmetrically segregate chromosomes or retain BrdU. *Nature* 449, 238-242.

Kiel, M.J., Radice, G.L., and Morrison, S.J. (2007b). Lack of evidence that hematopoietic stem cells depend on N-cadherin-mediated adhesion to osteoblasts for their maintenance. *Cell stem cell* 1, 204-217.

Kiel, M.J., Yilmaz, O.H., Iwashita, T., Terhorst, C., and Morrison, S.J. (2005). SLAM family receptors distinguish hematopoietic stem and progenitor cells and reveal endothelial niches for stem cells. *Cell* 121, 1109-1121.

Kim, I., Saunders, T.L., and Morrison, S.J. (2007). Sox17 dependence distinguishes the transcriptional regulation of fetal from adult hematopoietic stem cells. *Cell* 130, 470-483.

Klampfl, T., Gisslinger, H., Harutyunyan, A.S., Nivarthi, H., Rumi, E., Milosevic, J.D., Them, N.C., Berg, T., Gisslinger, B., Pietra, D., *et al.* (2013). Somatic mutations of calreticulin in myeloproliferative neoplasms. *The New England journal of medicine* 369, 2379-2390.

Kollet, O., Shivtiel, S., Chen, Y.Q., Suriawinata, J., Thung, S.N., Dabeva, M.D., Kahn, J., Spiegel, A., Dar, A., Samira, S., *et al.* (2003). HGF, SDF-1, and MMP-9 are involved in stress-induced human CD34+ stem cell recruitment to the liver. *The Journal of clinical investigation* 112, 160-169.

Koni, P.A., Joshi, S.K., Temann, U.A., Olson, D., Burkly, L., and Flavell, R.A. (2001). Conditional vascular cell adhesion molecule 1 deletion in mice: impaired lymphocyte migration to bone marrow. *The Journal of experimental medicine* 193, 741-754.

Kralovics, R., Passamonti, F., Buser, A.S., Teo, S.S., Tiedt, R., Passweg, J.R., Tichelli, A., Cazzola, M., and Skoda, R.C. (2005). A gain-of-function mutation of JAK2 in myeloproliferative disorders. *The New England journal of medicine* 352, 1779-1790.

Kunisaki, Y., Bruns, I., Scheiermann, C., Ahmed, J., Pinho, S., Zhang, D., Mizoguchi, T., Wei, Q., Lucas, D., Ito, K., *et al.* (2013). Arteriolar niches maintain haematopoietic stem cell quiescence. *Nature* 502, 637-643.

Levine, R.L., Wadleigh, M., Cools, J., Ebert, B.L., Wernig, G., Huntly, B.J., Boggon, T.J., Wlodarska, I., Clark, J.J., Moore, S., *et al.* (2005). Activating mutation in the tyrosine kinase JAK2 in polycythemia vera, essential thrombocythemia, and myeloid metaplasia with myelofibrosis. *Cancer cell* 7, 387-397.

Li, P., and Zon, L.I. (2010). Resolving the controversy about N-cadherin and hematopoietic stem cells. *Cell stem cell* 6, 199-202.

Litam, P.P., Friedman, H.D., and Loughran, T.P., Jr. (1993). Splenic extramedullary hematopoiesis in a patient receiving intermittently administered granulocyte colony-stimulating factor. *Annals of internal medicine* 118, 954-955.

Liu, F., Voitge, H.W., Braut, A., Kronenberg, M.S., Lichtler, A.C., Mina, M., and Kream, B.E. (2004). Expression and activity of osteoblast-targeted Cre recombinase transgenes in murine skeletal tissues. *The International journal of developmental biology* 48, 645-653.

Lo Celso, C., Fleming, H.E., Wu, J.W., Zhao, C.X., Miake-Lye, S., Fujisaki, J., Cote, D., Rowe, D.W., Lin, C.P., and Scadden, D.T. (2009). Live-animal tracking of individual haematopoietic stem/progenitor cells in their niche. *Nature* 457, 92-96.

Logan, M., Martin, J.F., Nagy, A., Lobe, C., Olson, E.N., and Tabin, C.J. (2002). Expression of Cre Recombinase in the developing mouse limb bud driven by a Prxl enhancer. *Genesis* 33, 77-80.

Lord, B.I., and Hendry, J.H. (1972). The distribution of haemopoietic colony-forming units in the mouse femur, and its modification by x rays. *The British journal of radiology* 45, 110-115.

Lord, B.I., Testa, N.G., and Hendry, J.H. (1975). The relative spatial distributions of CFUs and CFUc in the normal mouse femur. *Blood* 46, 65-72.

Lorenz, E., Uphoff, D., Reid, T.R., and Shelton, E. (1951). Modification of irradiation injury in mice and guinea pigs by bone marrow injections. *Journal of the National Cancer Institute* 12, 197-201.

Lowell, C.A., Niwa, M., Soriano, P., and Varmus, H.E. (1996). Deficiency of the Hck and Src tyrosine kinases results in extreme levels of extramedullary hematopoiesis. *Blood* 87, 1780-1792.

Lucas, D., Battista, M., Shi, P.A., Isola, L., and Frenette, P.S. (2008). Mobilized hematopoietic stem cell yield depends on species-specific circadian timing. *Cell stem cell* 3, 364-366.

Lymperi, S., Horwood, N., Marley, S., Gordon, M.Y., Cope, A.P., and Dazzi, F. (2008). Strontium can increase some osteoblasts without increasing hematopoietic stem cells. *Blood* 111, 1173-1181.

Madisen, L., Zwingman, T.A., Sunkin, S.M., Oh, S.W., Zariwala, H.A., Gu, H., Ng, L.L., Palmiter, R.D., Hawrylycz, M.J., Jones, A.R., *et al.* (2010). A robust and high-throughput Cre reporting and characterization system for the whole mouse brain. *Nature neuroscience* 13, 133-140.

Magee, J.A., Ikenoue, T., Nakada, D., Lee, J.Y., Guan, K.L., and Morrison, S.J. (2012). Temporal changes in PTEN and mTORC2 regulation of hematopoietic stem cell self-renewal and leukemia suppression. *Cell stem cell* 11, 415-428.

Martin, A., and Thompson, A.A. (2013). Thalassemias. *Pediatric clinics of North America* 60, 1383-1391.

Maximow, A. (1909). Der Lymphozyt als gemeinsame Stammzelle der verschiedenen Blutelemente in der embryonalen Entwicklung und im postfetalen Leben der Säugetiere. *Fol Haematol* 8, 125-134.

Maymon, R., Strauss, S., Vaknin, Z., Weinraub, Z., Herman, A., and Gayer, G. (2006). Normal sonographic values of maternal spleen size throughout pregnancy. *Ultrasound in medicine & biology* 32, 1827-1831.

Mendez-Ferrer, S., Lucas, D., Battista, M., and Frenette, P.S. (2008). Haematopoietic stem cell release is regulated by circadian oscillations. *Nature* 452, 442-447.

Mendez-Ferrer, S., Michurina, T.V., Ferraro, F., Mazloom, A.R., Macarthur, B.D., Lira, S.A., Scadden, D.T., Ma'ayan, A., Enikolopov, G.N., and Frenette, P.S. (2010). Mesenchymal and haematopoietic stem cells form a unique bone marrow niche. *Nature* 466, 829-834.

Mignone, J.L., Kukekov, V., Chiang, A.S., Steindler, D., and Enikolopov, G. (2004). Neural stem and progenitor cells in nestin-GFP transgenic mice. *The Journal of comparative neurology* 469, 311-324.

Miwa, Y., Hayashi, T., Suzuki, S., Abe, S., Onishi, I., Kirimura, S., Kitagawa, M., and Kurata, M. (2013). Up-regulated expression of CXCL12 in human spleens with extramedullary haematopoiesis. *Pathology* 45, 408-416.

Monette, F.C., Gilio, M.J., and Chalifoux, P. (1974). Separation of proliferating CFU from Go cells of murine bone marrow. *Cell and tissue kinetics* 7, 443-450.

Morita, Y., Ema, H., and Nakauchi, H. (2010). Heterogeneity and hierarchy within the most primitive hematopoietic stem cell compartment. *The Journal of experimental medicine* 207, 1173-1182.

Morita, Y., Iseki, A., Okamura, S., Suzuki, S., Nakauchi, H., and Ema, H. (2011). Functional characterization of hematopoietic stem cells in the spleen. *Experimental hematology* 39, 351-359 e353.

Morrison, S.J., Hemmati, H.D., Wandycz, A.M., and Weissman, I.L. (1995). The purification and characterization of fetal liver hematopoietic stem cells. *Proceedings of the National Academy of Sciences of the United States of America* 92, 10302-10306.

Morrison, S.J., and Scadden, D.T. (2014). The bone marrow niche for haematopoietic stem cells. *Nature* 505, 327-334.

Morrison, S.J., Wright, D.E., and Weissman, I.L. (1997). Cyclophosphamide/granulocyte colony-stimulating factor induces hematopoietic stem cells to proliferate prior to mobilization.

Proceedings of the National Academy of Sciences of the United States of America *94*, 1908-1913.

Mueller, S.N., and Germain, R.N. (2009). Stromal cell contributions to the homeostasis and functionality of the immune system. *Nature reviews Immunology* *9*, 618-629.

Muller-Sieburg, C.E., Whitlock, C.A., and Weissman, I.L. (1986). Isolation of two early B lymphocyte progenitors from mouse marrow: a committed pre-pre-B cell and a clonogenic Thy-1-lo hematopoietic stem cell. *Cell* *44*, 653-662.

Munger, J.S., Huang, X., Kawakatsu, H., Griffiths, M.J., Dalton, S.L., Wu, J., Pittet, J.F., Kaminski, N., Garat, C., Matthay, M.A., *et al.* (1999). The integrin alpha v beta 6 binds and activates latent TGF beta 1: a mechanism for regulating pulmonary inflammation and fibrosis. *Cell* *96*, 319-328.

Murone, M., Carpenter, D.A., and de Sauvage, F.J. (1998). Hematopoietic deficiencies in c-mpl and TPO knockout mice. *Stem cells* *16*, 1-6.

Nagasawa, T., Hirota, S., Tachibana, K., Takakura, N., Nishikawa, S., Kitamura, Y., Yoshida, N., Kikutani, H., and Kishimoto, T. (1996). Defects of B-cell lymphopoiesis and bone-marrow myelopoiesis in mice lacking the CXC chemokine PBSF/SDF-1. *Nature* *382*, 635-638.

Nagasawa, T., Kikutani, H., and Kishimoto, T. (1994). Molecular cloning and structure of a pre-B-cell growth-stimulating factor. *Proceedings of the National Academy of Sciences of the United States of America* *91*, 2305-2309.

Nakada, D., Oguro, H., Levi, B.P., Ryan, N., Kitano, A., Saitoh, Y., Takeichi, M., Wendt, G.R., and Morrison, S.J. (2014). Oestrogen increases haematopoietic stem-cell self-renewal in females and during pregnancy. *Nature* *505*, 555-558.

Nakada, D., Saunders, T.L., and Morrison, S.J. (2010). Lkb1 regulates cell cycle and energy metabolism in haematopoietic stem cells. *Nature* *468*, 653-658.

Nangalia, J., Massie, C.E., Baxter, E.J., Nice, F.L., Gundem, G., Wedge, D.C., Avezov, E., Li, J., Kollmann, K., Kent, D.G., *et al.* (2013). Somatic CALR mutations in myeloproliferative neoplasms with nonmutated JAK2. *The New England journal of medicine* *369*, 2391-2405.

Nombela-Arrieta, C., Pivarnik, G., Winkel, B., Canty, K.J., Harley, B., Mahoney, J.E., Park, S.Y., Lu, J., Protopopov, A., and Silberstein, L.E. (2013). Quantitative imaging of

haematopoietic stem and progenitor cell localization and hypoxic status in the bone marrow microenvironment. *Nature cell biology* 15, 533-543.

O'Malley, D.P. (2013). *Atlas of Spleen Pathology*, 2013 edn (New York: Springer).

Ogawa, M., Matsuzaki, Y., Nishikawa, S., Hayashi, S., Kunisada, T., Sudo, T., Kina, T., and Nakauchi, H. (1991). Expression and function of c-kit in hemopoietic progenitor cells. *The Journal of experimental medicine* 174, 63-71.

Oguro, H., Ding, L., and Morrison, S.J. (2013). SLAM family markers resolve functionally distinct subpopulations of hematopoietic stem cells and multipotent progenitors. *Cell stem cell* 13, 102-116.

Omatsu, Y., Sugiyama, T., Kohara, H., Kondoh, G., Fujii, N., Kohno, K., and Nagasawa, T. (2010). The essential functions of adipo-osteogenic progenitors as the hematopoietic stem and progenitor cell niche. *Immunity* 33, 387-399.

Pappenheim, A. (1896). Ueber Entwicklung und Ausbildung der Erythroblasten. *Virchows Arch* 145, 587-643.

Pardanani, A.D., Levine, R.L., Lasho, T., Pikman, Y., Mesa, R.A., Wadleigh, M., Steensma, D.P., Elliott, M.A., Wolanskyj, A.P., Hogan, W.J., *et al.* (2006). MPL515 mutations in myeloproliferative and other myeloid disorders: a study of 1182 patients. *Blood* 108, 3472-3476.

Park, I.K., Qian, D., Kiel, M., Becker, M.W., Pihalja, M., Weissman, I.L., Morrison, S.J., and Clarke, M.F. (2003). Bmi-1 is required for maintenance of adult self-renewing haematopoietic stem cells. *Nature* 423, 302-305.

Reilly, J.T. (1992). Pathogenesis of idiopathic myelofibrosis: role of growth factors. *Journal of clinical pathology* 45, 461-464.

Rivers, L.E., Young, K.M., Rizzi, M., Jamen, F., Psachoulia, K., Wade, A., Kessaris, N., and Richardson, W.D. (2008). PDGFRA/NG2 glia generate myelinating oligodendrocytes and piriform projection neurons in adult mice. *Nature neuroscience* 11, 1392-1401.

Ross, M.H., and Pawlina, W. (2006). *Histology: A Text and Atlas*, 5th edn (Baltimore, MD: Lippincott Williams & Wilkins).

Rund, D., and Rachmilewitz, E. (2005). Beta-thalassemia. *The New England journal of medicine* 353, 1135-1146.

Russell, E.S. (1979). Hereditary anemias of the mouse: a review for geneticists. *Adv Genet* 20, 357-459.

Samokhvalov, I.M., Samokhvalova, N.I., and Nishikawa, S. (2007). Cell tracing shows the contribution of the yolk sac to adult haematopoiesis. *Nature* 446, 1056-1061.

Scheiermann, C., Kunisaki, Y., Lucas, D., Chow, A., Jang, J.E., Zhang, D., Hashimoto, D., Merad, M., and Frenette, P.S. (2012). Adrenergic nerves govern circadian leukocyte recruitment to tissues. *Immunity* 37, 290-301.

Schofield, R. (1978). The relationship between the spleen colony-forming cell and the haemopoietic stem cell. *Blood Cells* 4, 7-25.

Shalem, O., Sanjana, N.E., and Zhang, F. (2015). High-throughput functional genomics using CRISPR-Cas9. *Nature reviews Genetics* 16, 299-311.

Sheehan, H.L., and Falkiner, N.M. (1948). Splenic aneurysm and splenic enlargement in pregnancy. *British medical journal* 2, 1105.

Signer, R.A., Magee, J.A., Salic, A., and Morrison, S.J. (2014). Haematopoietic stem cells require a highly regulated protein synthesis rate. *Nature* 509, 49-54.

Siminovitch, L., McCulloch, E.A., and Till, J.E. (1963). The Distribution of Colony-Forming Cells among Spleen Colonies. *Journal of cellular physiology* 62, 327-336.

Sipkins, D.A., Wei, X., Wu, J.W., Runnels, J.M., Cote, D., Means, T.K., Luster, A.D., Scadden, D.T., and Lin, C.P. (2005). In vivo imaging of specialized bone marrow endothelial microdomains for tumour engraftment. *Nature* 435, 969-973.

Spangrude, G.J., Heimfeld, S., and Weissman, I.L. (1988). Purification and characterization of mouse hematopoietic stem cells. *Science* 241, 58-62.

Sugiyama, T., Kohara, H., Noda, M., and Nagasawa, T. (2006). Maintenance of the hematopoietic stem cell pool by CXCL12-CXCR4 chemokine signaling in bone marrow stromal cell niches. *Immunity* 25, 977-988.

Taichman, R.S., and Emerson, S.G. (1994). Human osteoblasts support hematopoiesis through the production of granulocyte colony-stimulating factor. *The Journal of experimental medicine* *179*, 1677-1682.

Tavassoli, M., and Weiss, L. (1973). An electron microscopic study of spleen in myelofibrosis with myeloid metaplasia. *Blood* *42*, 267-279.

Tefferi, A. (2005). Pathogenesis of myelofibrosis with myeloid metaplasia. *Journal of clinical oncology : official journal of the American Society of Clinical Oncology* *23*, 8520-8530.

Tiedt, R., Schomber, T., Hao-Shen, H., and Skoda, R.C. (2007). Pf4-Cre transgenic mice allow the generation of lineage-restricted gene knockouts for studying megakaryocyte and platelet function in vivo. *Blood* *109*, 1503-1506.

Till, J.E., and McCulloch, E.A. (1961). A direct measurement of the radiation sensitivity of normal mouse bone marrow cells. *Radiation research* *14*, 213-222.

Tronche, F., Kellendonk, C., Kretz, O., Gass, P., Anlag, K., Orban, P.C., Bock, R., Klein, R., and Schutz, G. (1999). Disruption of the glucocorticoid receptor gene in the nervous system results in reduced anxiety. *Nature genetics* *23*, 99-103.

Vannucchi, A.M., Bianchi, L., Cellai, C., Paoletti, F., Rana, R.A., Lorenzini, R., Migliaccio, G., and Migliaccio, A.R. (2002). Development of myelofibrosis in mice genetically impaired for GATA-1 expression (GATA-1(low) mice). *Blood* *100*, 1123-1132.

Visnjic, D., Kalajzic, Z., Rowe, D.W., Katavic, V., Lorenzo, J., and Aguila, H.L. (2004). Hematopoiesis is severely altered in mice with an induced osteoblast deficiency. *Blood* *103*, 3258-3264.

Visser, J.W., Bauman, J.G., Mulder, A.H., Eliason, J.F., and de Leeuw, A.M. (1984). Isolation of murine pluripotent hemopoietic stem cells. *The Journal of experimental medicine* *159*, 1576-1590.

Visser, J.W., and Bol, S.J. (1982). A two-step procedure for obtaining 80-fold enriched suspensions of murine pluripotent hemopoietic stem cells. *Stem cells* *1*, 240-249.

Walkley, C.R., Olsen, G.H., Dworkin, S., Fabb, S.A., Swann, J., McArthur, G.A., Westmoreland, S.V., Chambon, P., Scadden, D.T., and Purton, L.E. (2007a). A

microenvironment-induced myeloproliferative syndrome caused by retinoic acid receptor gamma deficiency. *Cell* 129, 1097-1110.

Walkley, C.R., Shea, J.M., Sims, N.A., Purton, L.E., and Orkin, S.H. (2007b). Rb regulates interactions between hematopoietic stem cells and their bone marrow microenvironment. *Cell* 129, 1081-1095.

Wang, J.C., Lang, H.D., Lichter, S., Weinstein, M., and Benn, P. (1992). Cytogenetic studies of bone marrow fibroblasts cultured from patients with myelofibrosis and myeloid metaplasia. *British journal of haematology* 80, 184-188.

Wendling, O., Bornert, J.M., Chambon, P., and Metzger, D. (2009). Efficient temporally-controlled targeted mutagenesis in smooth muscle cells of the adult mouse. *Genesis* 47, 14-18.

Wolf, N.S. (1978). Dissecting the hematopoietic microenvironment. III. Evidence for a positive short range stimulus for cellular proliferation. *Cell and tissue kinetics* 11, 335-345.

Worton, R.G., McCulloch, E.A., and Till, J.E. (1969). Physical separation of hemopoietic stem cells differing in their capacity for self-renewal. *The Journal of experimental medicine* 130, 91-103.

Wright, D.E., Wagers, A.J., Gulati, A.P., Johnson, F.L., and Weissman, I.L. (2001). Physiological migration of hematopoietic stem and progenitor cells. *Science* 294, 1933-1936.

Wu, A.M., Till, J.E., Siminovitch, L., and McCulloch, E.A. (1967). A cytological study of the capacity for differentiation of normal hemopoietic colony-forming cells. *Journal of cellular physiology* 69, 177-184.

Wu, A.M., Till, J.E., Siminovitch, L., and McCulloch, E.A. (1968). Cytological evidence for a relationship between normal hemopoietic colony-forming cells and cells of the lymphoid system. *The Journal of experimental medicine* 127, 455-464.

Xie, Y., Yin, T., Wiegraeb, W., He, X.C., Miller, D., Stark, D., Perko, K., Alexander, R., Schwartz, J., Grindley, J.C., *et al.* (2009). Detection of functional haematopoietic stem cell niche using real-time imaging. *Nature* 457, 97-101.

Xin, H.B., Deng, K.Y., Rishniw, M., Ji, G., and Kotlikoff, M.I. (2002). Smooth muscle expression of Cre recombinase and eGFP in transgenic mice. *Physiological genomics* 10, 211-215.

Yamazaki, S., Ema, H., Karlsson, G., Yamaguchi, T., Miyoshi, H., Shioda, S., Taketo, M.M., Karlsson, S., Iwama, A., and Nakauchi, H. (2011). Nonmyelinating Schwann cells maintain hematopoietic stem cell hibernation in the bone marrow niche. *Cell* *147*, 1146-1158.

Yilmaz, O.H., Valdez, R., Theisen, B.K., Guo, W., Ferguson, D.O., Wu, H., and Morrison, S.J. (2006). Pten dependence distinguishes haematopoietic stem cells from leukaemia-initiating cells. *Nature* *441*, 475-482.

Zhang, J., Niu, C., Ye, L., Huang, H., He, X., Tong, W.G., Ross, J., Haug, J., Johnson, T., Feng, J.Q., *et al.* (2003). Identification of the haematopoietic stem cell niche and control of the niche size. *Nature* *425*, 836-841.

Zhao, M., Perry, J.M., Marshall, H., Venkatraman, A., Qian, P., He, X.C., Ahamed, J., and Li, L. (2014). Megakaryocytes maintain homeostatic quiescence and promote post-injury regeneration of hematopoietic stem cells. *Nature medicine* *20*, 1321-1326.

Zhou, B.O., Yue, R., Murphy, M.M., Peyer, J.G., and Morrison, S.J. (2014). Leptin-receptor-expressing mesenchymal stromal cells represent the main source of bone formed by adult bone marrow. *Cell stem cell* *15*, 154-168.

Zhu, J., Garrett, R., Jung, Y., Zhang, Y., Kim, N., Wang, J., Joe, G.J., Hexner, E., Choi, Y., Taichman, R.S., *et al.* (2007). Osteoblasts support B-lymphocyte commitment and differentiation from hematopoietic stem cells. *Blood* *109*, 3706-3712.

Zhu, X., Bergles, D.E., and Nishiyama, A. (2008). NG2 cells generate both oligodendrocytes and gray matter astrocytes. *Development* *135*, 145-157.

Zhu, X., Hill, R.A., Dietrich, D., Komitova, M., Suzuki, R., and Nishiyama, A. (2011). Age-dependent fate and lineage restriction of single NG2 cells. *Development* *138*, 745-753.

Zou, Y.R., Kottmann, A.H., Kuroda, M., Taniuchi, I., and Littman, D.R. (1998). Function of the chemokine receptor CXCR4 in haematopoiesis and in cerebellar development. *Nature* *393*, 595-599.